NOTE TO USERS

This reproduction is the best copy available.

UMI®

LIQUID DISTRIBUTION AND ITS EFFECT ON THE ORGANIC REMOVAL IN A TRICKLE BED BIOREACTOR

By

Maryam Jedari Eyvazi

Bachelor of Chemical Engineering

Azad University, Tehran, Iran, 1999

A thesis

Presented to Ryerson University

in partial fulfillment of the

requirements for the degree of

Master of Applied Science

in the Program of

Chemical Engineering

Toronto, Ontario, Canada, 2005

Copyright © 2005 by Maryam Jedari Eyvazi

UMI Number: EC53020

UMI®

Authors Declaration

I hereby declare that I am the solo author of this thesis.

I authorize Ryerson University to lend this thesis to other institutions or individuals for the purpose of scholarly research.

I further authorize Ryerson University to reproduce this thesis by photocopying or by other means, in total or in part, at the request of other institutions or individuals for the purpose of scholarly research.

Borrower's page

Ryerson University requires the signature of all persons using or photocopying this thesis. Please sign below and give address and date.

NAME	SIGNITURE
Md. Akbar Hossain MASc in EnvSciMo	Jan. 08

Abstract

Liquid Distribution and its Effect of the Organic Removal in a Trickling Bed Filter

Maryam Jedari Eyvazi

MASc, Chemical Engineering Program

Ryerson University

Toronto, 2005

Propylene glycol methyl ether was removed from wastewater in a trickling bed bioreactor under different liquid distribution conditions. A 0.3 m diameter column filled with two heights of 0.7 m and 1.4 m with 2 cm plastic spheres with were used. The wastewater flow rate varied from 0.184 to 0.918 $kg/m^2.s$. The effect of the initial liquid distribution was examined using two types of liquid distributors: a multipoint liquid distributor and a central single point liquid distributor. Over 96 hours of treatment period, the BOD_5 was reduced by 85% and 65% under the most uniform liquid distribution condition and the poor liquid distribution condition, respectively, achieved in this study. Increasing the liquid flow rate from 0.184 to 0.918 $kg/m^2.s$, it increased the dynamic liquid holdup by 53 % and the apparent BOD_5 removal rate constant by 23 % at 1.4 m bed height using the multipoint liquid distributor.

Moreover, with the use of the multipoint liquid distributor, the apparent reaction when the liquid flow rate was increased from 0.184 $kg/m^2.s$ to 0.918 $kg/m^2.s$. In addition, it was found that the effect of an increase in the bed height on the percentage BOD_5 removal was not significant when initial liquid distribution was uniform. Under the uniform initial condition, only 4% increase in the percentage BOD_5 removal was observed when the bed height increased from 0.7 to 1.4 m whereas when the initial distribution was extremely non-uniform, the percentage of BOD_5 removal was increased by 20% with increasing the bed height. The local distribution of the BOD_5 removal was not uniform across the bed cross-section and it was affected by the liquid flow distribution across the bed cross-section.

Acknowledgment

Table of Content

List of Figures

Figure A.6: Effect of the liquid flow rate on the apparent BOD removal rate constant. The data is obtained after 96 hours of treatment with [PGME] o=300ppm using multipoint delivery distributor.

List of Tables

Nomenclature

Symbol	Description
a	Total surface area per unit packed column [m^2/m^3]
a_h	Hydraulic area of packing per unit packed volume [m^2/m^3]
A_m	Surface area per unit weight of dried cell for mass transfer [cm^2/g]
B	Constant at equation (4.9)
B_1	Initial dissolved oxygen of seed control [mg/l]
B_2	Final dissolved oxygen of seed control [mg/l]
BOD$_5$	5-day biochemical oxygen demand [mg/l]
C	Organic matter concentration in the effluent [mg/l]
C_o	Organic matter concentration in the influent
C_r	Organic concentration in the effluent at radius r [mg/l]
C_s	Organic concentration at cell surface [mg/l]
C_t	Organic (BOD or COD) concentration at time t [mg/l]
COD	Chemical oxygen demand [mg/l]
d_p	Diameter of packing particle [m]
D_1	Initial dissolved oxygen of diluted samples [mg/l]
D_2	Final dissolved oxygen of diluted samples [mg/l]
D_{eff}	Intraparticle effective diffusivity
D_T	Diameter of column [m]
f	Volume of seed in diluted sample to volume of seed in seed control
f_e	Wetting efficiency
g	gravitation acceleration [m/s^2]
H	Filter height [m]
h	Liquid holdup [m^3/m^3]
h_d	Dynamic liquid holdup [m^3/m^3]
k	Constant at equation 4.13
k	Intrinsic first order biodegradation rate constant[l/h]

k_t	True reaction rate constant [1/h]
k_{app}	Apparent biodegradation rate constant [1/h]
k_m	Mass transfer coefficient [cm/h]
k_v	First order reaction rate per unit volume of catalyst pallet [1/s]
k_s	Volumetric liquid-solid mass transfer coefficient constant without reaction
K_A	Adsorption equilibrium constant
n	Constant at equation 4.13
P	Decimal volumetric fraction of sample used
Q	Liquid flow rate [m^3/s]
Q_i	Liquid flow rate in a cell [m^3/s]
Q_{av}	Average liquid flow rate [m^3/s]
q	Superficial liquid load [m^3/m^2.day]
q_r	Local superficial liquid load at radius r [m^3/m^2.day]
R	Universal gas constant =8.314 [kJ/mol.K]
r	Biodegradation rate [mg/g.h]
r_m	Mass transfer rate [mg/g.h]
T	Temperature [K]
t	Time [s]
q	Superficial liquid load [m^3/m^2.day]
U	Liquid mass flux [kg/m^2.s]
V_r	Volume of the bed [m^3]
x	Number of collecting cells

Greek Symbols

ρ_L	Density of liquid [kg/m^3]
μ_L	Dynamic viscosity of liquid [kg/m.s]

Subscripts

L	Liquid phase
LS	Liquid-Solid phase

Abbreviations

BOD	Biological Oxygen demand
COD	Chemical oxygen demand
LHSV	Liquid hourly space velocity, volume of liquid fed to reactor per hour per volume of reactor
MC	Maldistribution Coefficient
PGME	Propylene glycol methyl ether
ppm	Part per million

Chapter 1

Introduction

1.1 Trickle bed bioreactor

One of the earliest applications of trickle bed bioreactors or so-called trickling filters was in wastewater treatment plants. For about a century, trickle bed bioreactors have been used for the organic removal and nitrification of municipal and industrial wastewater by means of biological reaction. The first trickle bed bioreactor was placed in operation in England in 1893 [1]. Prior to 1970s, a trickle bed bioreactor was used as a secondary treatment. Its effluent quality was not adequate and typically contained 20 to 40 mg/l biological oxygen demand. Therefore, either tertiary treatment was added to improve the effluent quality, or trickle bed bioreactor was replaced with another process such as activated sludge. However, because of low operating cost, reliability, stability and simplicity of operation, the trickle bed bioreactor gained new popularity in 1980s [2]. Although the effluent from trickle bed bioreactor plants of earlier design was of poorer quality than that from activated sludge plants, the performance of trickle bed bioreactors designed more recently is comparable to that of activated sludge plants [3].

A trickle bed bioreactor is basically a fixed bed bioreactor in which the biomass is attached to the surface of supporting medium. The supporting medium can be rock, slag or various plastic packings. The wastewater is introduced at the top of the bed by means of a rotary distributor or fixed nozzle. Fixed nozzle distributors are mostly used in square or rectangular beds or when the reactor is small [1].

Conventional trickle bed bioreactors consisting of rock packing have a maximum hydraulic loading rate to the bed of 0.4 l/s.m^2. They are able to reduce biological oxygen demand up to 80 % [1] and nitrification up to 75% [4]. Moreover, rock beds can be up to

(*weak material similar to glass, which retained after metal has been obtained from rock,*)

1
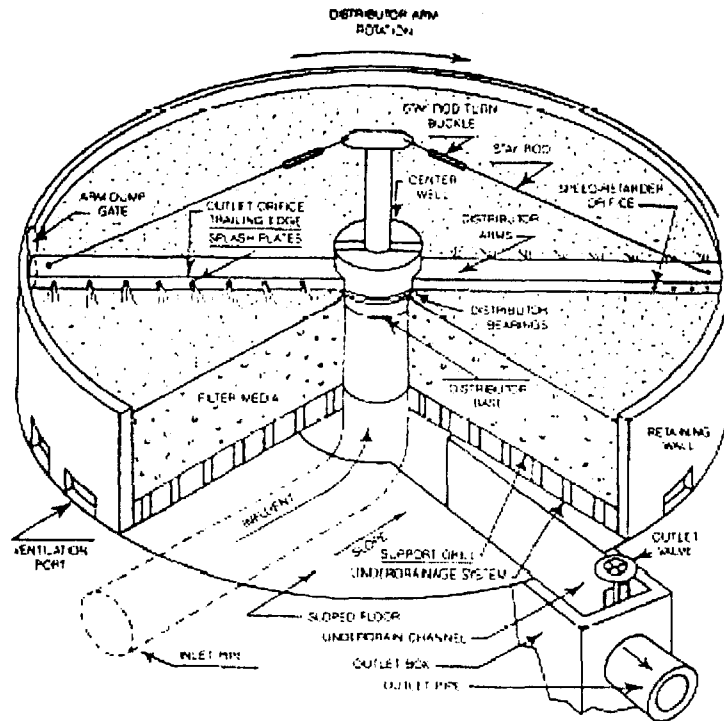
Figure 1.1: A typical trickle bed bioreactor [3]

to 2.5 meters in diameter and from 0.9 to 2.4 meters in depth. The size of rock varies from 2.5 to 10.2 cm [1] with a void fraction ranging from 40 to 55 percent (Figure 1.1). The introduction of plastic media was a great success in trickle bed bioreactor manufacturing .The utilizing of plastic media has permitted much higher loading rates as high as eight times of conventional bed loading rate because of much larger surface area, voidage (about 90%) and permeability of this type of packings. The plastic packing beds can remove biological oxygen demand up to 90 %. Moreover, the low bulk density of plastic media allows deeper bed from 4 to 12 meters with a smaller diameter [1].

In trickle bed bioreactors, the wastewater flows down and trickles over the packing surface where it is in contact with attached microorganisms. The microorganisms consume organic matter from the wastewater and form a slime layer (biofilm) over the

packing surface. The microorganisms convert the biodegradable organics and oxygen to carbon dioxide, water and more microorganisms. When the biofilm is thick enough, both aerobic and anaerobic zone exist in the biofilm. Inner section of biofilm where oxygen doesn't penetrate becomes an anaerobic zone while the outer section which has enough oxygen available for microorganisms becomes an aerobic zone. Thus, a trickle bed bioreactor can perform both aerobic and anaerobic degradation of organics. When the biofilm is very thick, all organic matter is consumed by microorganisms in outer layers and finishes before reaching to inner layer. Therefore, due to the deficiency in carbon source for their energy requirements, the microorganisms near the surface media start endogenous respiration. As a result, the microorganisms lose their ability to adhere to the media surface and are washed out with the flowing liquid. This phenomenon is called sloughing. After sloughing, a new layer of biofilm starts to grow on packing surface. The rate of sloughing and microbial build up is related to hydraulic and organic loading into the bed and the nature of the wastewater [1].

In a trickle bed bioreactor, the organic removal depends on the amount of microorganism available in the bed and the contact time between the wastewater and microorganisms. The amount of microorganisms in the bed is controlled by the rate of sloughing and growth of the microorganisms, which is an indirect function of hydraulic and organic loading rate and the nature of the wastewater. The mean contact time of the liquid with microorganisms is direct function of the hydraulic loading rate and depth of the bed [5].

A proper liquid distribution throughout the bed is essential to utilize all the bed capacity. However, because of maldistribution, the liquid does not distribute uniformly all over the bed and the packings only partially wet in the bed. In other words, some parts of the packing that are not in contact with the liquid remain dry, whereas the other parts are overloaded. The non-wetted areas of packings are not colonized and therefore, these zones cannot contribute to the degradation of organic matter. This consequently limits the performance of the trickle bed bioreactor and reduces the bed efficiency. Besides, proper liquid distribution minimizes plugging and ponding problems and prevents channeling.

Therefore, an optimum contact of waste liquid and oxygen with biofilm is achieved and the organic pollutant is oxidized efficiently [6].

However, the hydrodynamic flow pattern in the trickle bed bioreactor is very complicated and is affected by the liquid flow rate, packing configuration, liquid distributor design, and packing height. A number of studies have been done on liquid distribution in packed towers during the last century. Also, several authors have measured the efficiency of trickle bed bioreactors for BOD removal under different operating conditions [1, 2]. However, little attempts were done to quantify the effect of liquid distribution on the BOD removal in a trickle bed bioreactor. Recently, only Crine et al. [7] have studied the effect of the liquid flow distribution on the removal rate of the organic matter in a trickle bed bioreactor.

1.2. Objective

In the present study, the influence of the liquid distribution on the BOD removal was examined and quantified. To achieve this goal, the liquid distribution in a pilot scale trickle bed bioreactor was studied. The effect of the operating variables on the liquid distribution profile and the dynamic liquid holdup were determined. Then, under various liquid distribution conditions, the performance of the trickle bed bioreactor for soluble organic removal was studied.

Chapter 2

Literature review

This chapter consists of two parts; at the first part, a comprehensive review on the liquid distribution in trickle bed reactor is presented. Moreover, the effect of operating variables on the liquid distribution is described. At the second part, the application of trickle bed bioreactor for wastewater treatment is presented. The second part also deals with the influence of operating variables on the trickle bed bioreactor's performance.

2.1 Liquid Distribution in Trickle Bed Reactors

The performance of a trickle bed reactor highly relies on the uniformity of the liquid distribution throughout the bed. It is well known that the liquid distribution critically affects transport mechanisms, such as mass /heat transfer efficiency and thus the overall reactor performance [8]. Therefore, the prevention of liquid flow maldistribution is one of the major challenges in the design and operation of a trickle bed reactor. Indeed, liquid maldistribution decreases the efficiency of the trickle bed reactor significantly. This phenomenon causes the nonuniform wetting of the packing within the reactor, which in turn reduces the liquid and catalyst interaction leading to inefficient catalyst usage. In other words, no reaction takes place where the catalyst particles are not wetted by the liquid reactant [9].

Several techniques have been proposed in the literature to measure liquid maldistribution, among which the liquid collector technique is the most popular [10]. In liquid collector method, liquid maldistribution is detected using collecting cells installed directly below the packing to measure liquid flux in various segments of the column cross-section. The obtained results can be further proceeded in two ways:

- Some information on liquid maldistribution can be obtained from the measurements of flow rate at the column outlet

- Liquid maldistribution is usually quantified as a maldistribution coefficient that is a measure of deviation from an ideal liquid distribution as described by the following equation [11]

$$MC = \frac{1}{x}\sqrt{\sum_{i=1}^{x}\left(\frac{Q_i - Q_{av}}{Q_{av}}\right)^2}$$

(2.1)

where MC is a dimensionless distribution coefficient, Q_{av} is the average liquid flow rate to a collecting cell, Q_i is the measured liquid flow rate to a cell, and x is the number of collecting cells. Equation 2.1 equals zero at the ideal liquid distribution condition and increases as the liquid distribution becomes less uniform [11].

Another method for detecting liquid distribution is the tomographic measuring method, which includes the X-ray tomography and the capacitive tomography. These methods are very popular in the investigation of the hydrodynamics of multiphase reactors [12-15]

2.1.1 Scale of Liquid Maldistribution

Two types of the liquid flow maldistribution have been recognized in packed columns: small-scale maldistribution or natural flow, and large-scale maldistribution or wall flow [16]. They are both well known to have negative influence on the mass transfer efficiency of packed columns [17].

2.1.1.1 Small Scale Liquid Maldistribution

In randomly packed columns, the liquid flow over packing particles is severely maldistributed. It has been shown that for a uniform initial distribution of liquid, liquid

channeling instantly occurs within a few layer of packing through which most of liquids flows down the column [18]. This type of liquid maldistribution is known as small scale maldistribution or natural flow and is characterized by the number of liquid channels and the standard deviation of the local flow rates [19].

Small-scale maldistribution was suggested by Wang et al. [20] to be the result of the gas, liquid and solid phases interactions over the particle dimension. The liquid streams tend to flow certain courses in preference to others due to channeling in packing and thus give uneven liquid distribution. Channeling of the liquid is considered an inherent property of packings. It is believed that low radial dispersion often causes channeling [21]. The radial spreading coefficient characterizes the liquid distribution requirements for random and structured packings [22]. It is a measure of how quickly a vertical liquid stream is radially spread as it flows down the bed through the packings. The radial dispersion of the liquid takes place at the conjunction point of two packing particles [21]. The occurrence of the channeling phenomena is inversely proportional to the radial spreading coefficient of the packing particles [23]. It was also shown that channeling also occurs as the result of uneven packing loading [24] regardless of the initial liquid distribution, column diameter and bed height [17].

Albright [25] showed that each packing had a natural frequency of distribution that was developed along the bed. Packing with larger spreading coefficient results in the natural frequency of distribution in a start time. In addition, they found that the radial spreading coefficient depends on the shape and the size of the packing. Larger packings tend to have higher spreading coefficient values and result in better radial spread of the liquid.

2.1.1.2 Large Scale Maldistribution

Generally, uniform initial liquid distribution degrades as the liquid flows down the bed. The liquid flow in the wall vicinity increases while the gas flow dominates in

the center of the packed bed. The tendency of the liquid flow towards the wall region is called wall flow or large-scale maldistribution [26].

It is known that the wall induces a loosening of the packing, which results in increasing the voidage at the wall vicinity. The tendency of the liquid to flow in the vicinity of to the wall is attributed to the lower resistance to the liquid flow because of high voidage near the wall. In fact, in the wall region the bed void fraction approaches unity. This peak in the porosity at the wall causes greater flow rate of liquid near the wall vicinity [27].

Wall flow, which is the quantity of liquid flowing down near the reactor wall is measured as the ratio of the total flow in the outermost annulus to the total area of liquid collector in that annulus. Wall flow is known as a major cause of the loss of efficiency in packed beds. Indeed, this phenomenon decreases the mass transfer efficiency due to the reduction of interaction between the liquid and gas phases. Wall flow in trickle bed reactors has been widely investigated and reported in the literature. It is proved that the wall flow depends on the ratio of reactor to packing diameter, liquid and gas flow rates, porosity, shape and orientation of packing as well as physicochemical properties of the liquid such as surface tension, density and viscosity.

2.1.2 Liquid Distribution Pattern

The 1950s literature reported the non-uniformity of the liquid flow distribution in a packed bed. It was found that the velocity distribution in down stream of the bed had uneven velocity profile with the largest value at the wall. More recent research work using more accurate measurements of the velocity distribution, showed oscillating velocity profile with decreasing amplitude and period towards the wall of the bed. Its minimum occurs at about one or two particle radius from the wall followed by an amplitude increase resulting in a maximum of one at the wall. It was noted that the

velocity oscillation profile was in accordance with the oscillation pattern of the voidage over any cross section of the bed [28].

These discoveries formed the basic background for later studies on the liquid flow distribution in a packed bed. Various models have been proposed in the literature to simulate the flow distribution of the liquid phase in randomly packed beds. The diffusion model, proposed by Chila and Schmidt [29] used a partial differential equation to balance axial convection with radial dispersion. However, the uncertainty of the boundary condition limited its application [27]. Later on, Farid [30] improved on Chila's model and proposed a differential equation to describe liquid distribution in the packing. The author demonstrated the existence of a potential force for the radial velocity in a packed bed due to the difference in the permeability between the bulk and the wall region of the packing, and set a new boundary condition.

Albright [23], Hoek et al. [19] and Song et al. [31] proposed a model based on the continuous splitting and recombination of the liquid on the scale of the packing elements. The model, named Natural Flow Model, described the tendency of the liquid to redistribute in a natural flow while flowing down the bed. Bey and Eigenberger [32] developed a mathematical model for liquid distribution profile derived from the Brinkman [33] equation for velocity distribution in a packed bed of spheres, rings, and cylinders in terms of the radial void fraction profile and the effective viscosity. The model was also able to determine radial void fraction profile independently.

Subagyo et al. [34] proposed a model for liquid velocity for single phase fluid flow in packed beds. The model was based on the analysis of a bed as a combination of continuous and discontinuous systems for fluid flow between voids in the bed. The bed cross section was divided into two regions based on the voidage; the continuous approach was applied for the region where the voidage was higher than 0.5 and the discontinuous approach was applied for the rest. In the continuous approach, it was assumed that the fluid interaction occurs between voids. In the discontinuous approach, which was applied for the region in which the voidage was less than 0.5, it was assumed that there was no

fluid interaction between voids, and the fluid flow in the packed bed was similar to fluid flow inside a bundle of tangled tubes. In comparison with other researcher's velocity distribution models, Subagyo's model was in better agreement with the experimental data.

While most of the investigations on the radial liquid distribution were restricted to the single phase flow, Jiang et al. [35] developed a discrete cell model to characterize the liquid and gas flow distributions in trickle bed reactors. The model assumed that the liquid and gas distribution were governed by the minimum rate of the total energy dissipation in the bed and incorporated the effect of structural non-uniformities and different initial liquid distribution as well as particle wetting characteristics.

Later on, Kunjummen et al. [28] developed a model to predict the water velocity profile in the presence of air based on single-phase velocities of water and air, and dynamic liquid saturation. They proposed a dynamic liquid saturation factor to take into account the effect of gas flow rate on the radial liquid velocity profile for two-phase flow systems.

Zimmerman and Ng [36] modeled liquid distribution in single phase trickle bed reactors by using a computer- generated, two dimensional packed columns of uniform spheres. The model was able to predict the effect of liquid flow rate, liquid density and surface tension on the liquid distribution. However, they did not take into account the effect of the gas flow on the liquid distribution.

2.1.3 Effect of Operating Variables on the Liquid Distribution

The liquid distribution in a packed column under various operation condition has been comprehensively investigated in the literature [20]. Weimann [37] studied the distribution of water in a packed bed of rings and found that the portion of the liquid, which flows close to the column wall, depends on the size of the packings and the column

diameter. Gunn [38] found that the wall flow in a larger column is less pronounced compared to a small column. Other studies showed that the structure of voidage between the particles, which formed the passage around the packing particles, is a function of the ratio of the column diameter to the particle diameter (D_T/d_p). Consequently, the liquid distribution strongly depends on the ratio of the tower diameter to the diameter of the packing [39]. A large portion of liquid flow down the bed in the vicinity of the wall for smaller column diameters and larger packing sizes. Backer et al. [39] studied the liquid distribution for various packing sizes, in 3 to 24 inches towers. They found that the liquid distribution was less uniform for the larger packing size. For a ratio of D_T/d_p less than 8/1, a high fraction of the liquid flows down the tower wall. Different values of D_T/d_p above which wall flow no longer exists or diminishes considerably have been reported in the literature [32, 37, 40-45]. The discrepancies in the suitable value of D_T/d_p found in the literature for minimum liquid maldistribution is due to the difference in the type of the packing used and the way packings were set in the column [46]. Herskowitz and Smith [42] observed that for granular particles, uniform liquid distribution was achieved at lower ratios of D_T/d_p and at lower bed depth as compared to beds packed with spherical or cylindrical particles. The data obtained from radial distribution studies by Tsochatzidis et al. [47] also showed that the spherical packing provides a better liquid distribution compared to the cylindrical ones.

Several researchers [20, 26, 39, 40, 48] have been studied the liquid distribution under different gas and liquid flow rates. Porter and Templeman [40] showed that for a given ratio of the column to packing diameter, the increase in the liquid flow rate reduced the wall flow. Kundu et al. [26] also investigated the influence of the liquid and the gas flow rates on the wall flow and found that the introduction of gas flow into the liquid solid system improved the uniformity of the liquid distribution. This was attributed to the competition between the liquid and the gas phase to fill the interstitial pore space. They also found that the liquid flow rate has more effect on the wall flow than the gas flow rate regardless of the type of the packing used. Although at a constant liquid flow rate, for the gas flow rate below a certain value, the wall flow was practically not affected by gas flow rate, an increase in both the liquid and gas flow rates improve the liquid distribution and

reduce the wall flow. On the other hand, Wang et al. [20] showed that the wall flow was almost constant at different gas flow rates. Similar observation was reported by Herskowitz and Smith [42]. They also found that the influence of the liquid flow rate on the large-scale maldistribution was less significant than that on the small-scale maldistribution. These findings suggested that the small-scale maldistibution was controlled by gas liquid interaction while the large-scale maldistribution was believed to result from heterogeneous bed structure, such as high porosity in the vicinity of the wall and /or uneven voidage at the central area of the bed.

Backer et al. [39] studies on the liquid distribution also revealed the insignificant influence of gas flow on the liquid distribution. They also found that except for the case of severe initial maldistributions, the liquid distribution was not very sensitive to the liquid flow rate. Their studies showed that except for the case with a single delivery point, the maldistribution coefficient was considerably low even at low liquid flow rates. A slight improvement was observed when the liquid flow rate was increased.

The liquid distribution at different packed bed heights has been well studied. Al-Samadi et al. [11] measured the liquid distribution at different depths of a packed bed using a 4-feet diameter packed tower under various initial distribution conditions. They found that the small-scale maldistribution decreased within the first 6 ft of the packing . A study by Doan and Fayed [49] showed that even in the case of severe initial maldistributin (for a one point source liquid delivery), as the liquid flowed down, the radial liquid distribution profile became smoother, which was attributed to the internal distribution characteristics of the packing.

Williams and Xie [12] observed that the improvement of liquid distribution at the top section of the packed bed is temporary; as the liquid flows down the bed, the wall flow will start to appear finally due to the contribution of the packing in spreading of liquid outwards. Similar results were also reported by Albrite [23]. The author showed that non-uniform liquid distribution occurs in a packed bed if it is sufficiently deep, regardless of the uniformity of the initial liquid distribution. Seader and Henley [50]

found that the large-scale liquid maldistribution could occur at bed depths of more than 20 ft.

Backer et al. [39] observed that liquid distribution varied down the bed to a depth of packing equal to ten times the tower diameter and then remained unchanged. Other researchers also observed continuous variation of liquid distribution over a packing depth up to 40 times the tower diameter [36, 51]. Kouri et al. [52] illustrated that the bed depth at which the wall flow became stable was dependent on the ability of the packing to spread the liquid radially. Previously, Hoek et al. [19] studied the effect of initial liquid distribution and packing size and shape on the depth at which wall flow occurs. They used 15 mm and 50 mm Pall rings and compared the results obtained for the both uniform initial distribution and non-uniform initial distribution. They observed that under the uniform initial distribution, the wall flow started to develop at equal bed depths for both sizes of packings. However, in the case of non-uniform initial distribution, the wall flow occurred at smaller depths for the packings with larger sizes. Song et al. [53] also showed that the depth at which the wall flow occurs is strongly dependent on the initial distribution. They found that in the case of uniform initial liquid distribution, the wall flow was formed more rapidly than the non-uniform initial liquid distribution. A similar trend of the liquid velocity profile and the bed depth was reported for structured packings. Very rapid wall flow formation using the structured packing was observed, which could be explained by the relatively large radial spreading coefficient of this type of packings.

2.1.4 Liquid Distributor Design

Initial liquid distribution strongly affects the efficiency of a packed column. Indeed, the performance of a packed bed depends on the distributor to spread a uniform quantity of liquid over the entire surface of the packing to create a sufficient area for mass transfer [22]. A proper design of liquid distributor is one of the critical factors to achieve a uniform liquid distribution throughout the bed. It was also believed the that

large-scale maldistribution resulted from non-uniform initial distribution over the packed column [38].

According to Perry et al. [22], the quality of liquid distribution for each distributor depends on three factors: number of distribution points (distribution density), geometric uniformity of distribution point across the cross section of the tower, and uniformity of liquid flow from the distribution point.

A broad range of the numbers of liquid distribution point per unit area is used in packed beds. An adequate number of delivery points is critical for liquid distribution in a packed bed. The regarded number of liquid delivery points varies with the packing geometry due to the variation of the radial spreading coefficient. For a packing with a high radial spreading coefficient, a distributor with a relatively small number of delivery points would be adequate [11]. Therefore, the packing with a superior ability to spread the liquid is more desirable. These types of packing not only provide a high efficiency for mass transfer through the bed, but also eliminate the need for expensive liquid distributors.

Leva [54] achieved better liquid distribution in a bed filled with S-LVK packing with a single point liquid distributor, rather than a 3-delivery point distributor, which was attributed to a relatively large value of the spreading coefficient of this type of packing. It must be noted that this experiment was done in relatively small tower (16 inches diameter) and for the case of larger diameter towers, it may differ.

Al –Samadi et al [11] performed about 300 liquid distribution experiments in the packed bed of No.2 S-LVK^{TM} using 1, 5, 9, 13 and 24 delivery points distributors. A significant improvement in liquid distribution was observed when the number of liquid delivery points was increased from 1 to 5. A similar observation was reported by Doan and Fayed [49] for a 4-ft diameter packed bed of 2 in. ceramic Intalox saddles under 1, 5, 9, 13, 24 liquid delivery point. They measured the liquid flow rate over the bed cross section at the 8 ft depth of the bed. With one liquid delivery point distributor, a very

large liquid flow rate in the central region of the bed was observed signifying a poor liquid distribution of one point liquid distributor. By increasing the number of delivery points, the liquid distribution over the bed cross-section became more uniform. On the other hand, comparable profiles of 13 liquid delivery points ($1.0/ft^2$) and 24 liquid delivery points ($1.9/ft^2$) indicated that there tend to be an optimum liquid delivery point density above that point, no considerable improvement in liquid distribution or even deterioration of liquid distribution may occur. The optimum liquid delivery points changes with the type of the packing. Most distributors are designed for 4 to 10 delivery point per square foot. It was found that the distribution of 9 point/ft^2 is adequate for most sizes of random and structured packings [22].

Another important factor is the distribution of the liquid delivery points across the tower cross-section (geometric uniformity). Improper arrangement of the liquid delivery points results in irrigation of the wall zone because of presence of liquid delivery point very close to the tower wall. Although a uniform spreading of delivery points seems to provide a uniform liquid distribution over the entire tower cross section, in practice a good distribution is not achieved by this way of delivery points organization. Norton Co. suggested a useful method to check the geometric uniformity. In this method, the tower cross section was divided into three equal radial zones and the number of delivery point in each area should be equal. Using this method, designers can improve the design by adding adequate number of liquid delivery point wherever they are needed [22].

2.1.5 Liquid Holdup and Wetting Efficiency

Liquid holdup and wetting efficiency of the solid particles are main parameters that affect trickle bed reactor operation. Indeed, they are closely interrelated with reactor performance, power consumption and mass transfer.

2.1.5.1 Liquid Holdup

Liquid holdup is one of the important hydrodynamic parameters, which is used in the description of the liquid retention in a packed bed [55]. It is also regarded as a measure of wetting effectiveness [56-57]. It has been long recognized that the liquid holdup distribution affects the mass transfer and consequently, the overall yield of the reactor.

Liquid holdup is defined as the volume fraction of the bed occupied by the liquid at a given condition and categorized into three parts: internal, residual and dynamic (or free-draining) holdup. Internal holdup is the liquid held inside a porous particle by capillary action. It is important parameter only for the bed packed with porous particles. It was found that the internal holdup is not affected by the variation of the liquid or gas flow rates and is usually complete even at very low liquid flow rate due to capillary force [58, 59]. The residual holdup defines as the part of the liquid remains after the reactor has been completely filled with liquid and then drained. The static hold up is the summation of the residual holdup and the internal holdup. The fraction of liquid collected at the bottom of the column after a sudden shutoff of the liquid feed is called dynamic holdup [55, 45].

It was found that the liquid holdup distribution is not uniform in the bed and is affected by liquid and gas flow rates, liquid initial distribution, packing size and shape, and wetting characteristics of the packing [60]. Packing with a large specific surface can hold more liquid [61-63]. Moreover, the liquid hold up increases as liquid density decreases, but decreasing of the liquid flow rate and surface tension decreases the liquid holdup. Liquid viscosity has no impact on liquid holdup [61-63]. It was found that when the reactor operates at atmospheric pressure, the liquid hold up is independent of the gas flow rate [64], but when it operates at high pressure, the effect of the gas flow on the liquid holdup is significant. This is because of the existence of the drag force in the liquid- gas interface. As pressure increases, the drag force at the liquid –gas interfaces increases, which results in the reduction of the liquid holdup [65].

16

Fukushima and Kusaka [66] proposed a correlation for liquid holdup in terms of the gas and liquid Reynolds number and the void fraction. They showed that the ratio of liquid holdup to void fraction is a function of the gas and liquid Reynolds number, but independent of d_p/D_T. Specchia and Baldi [56] also proposed a liquid holdup model that was a function of the liquid flow rate and packing specifications.

Yin et al. [67] measured the liquid holdup distribution in a 0.6 m diameter packed column filled with 25.4 mm metal Pall rings using a gamma ray tomography system. They found that the liquid holdup was not uniformly distributed over any cross-section of the bed, regardless of the uniformity of the initial distribution. This was because of the local heterogeneity in the bed structure. They also showed that the liquid holdup distribution was strongly dependent on the liquid flow rate and the initial liquid distribution. The liquid holdup distribution tends to be more uniform at a higher liquid flow rate due to increase of the liquid radial spreading which in turn smoothes out the local flow irregularities. They observed that when the liquid was introduced into the column via a single point source distributor, it took more than 0.6 m of the bed depth for liquid to move away from the centerline and reach to the column wall.

Tsochatzidis et al. [68] found that the effect of the initial distribution on liquid hold up is not significant in trickling flow regime (low liquid flow rate) while in the pulsing flow regime (high liquid flow rate), the uneven liquid distribution was associated with higher dynamic holdup values. They also observed that the liquid holdup varied with the type of packing. For spherical packings, it was found that the liquid holdup values tend to increase as the packing size was reduced. Moreover, spherical packing exhibited lower holdup values than cylindrical packing.

2.1.5.2 Wetting Efficiency

Wetting efficiency, which is defined as the fraction of the external catalyst area wetted by the flowing liquid down the bed, determines the extent of catalyst utilization. Partial wetting can cause incomplete catalyst utilization. This occurs when the gas and liquid flow into the reactor is low; hence, full coverage of all catalyst particles in the column with a continuous liquid film is not realized. In contrast, the wetting efficiency increases with liquid and gas flow rates, and complete wetting can be achieved at very high liquid flow rate [69].

The wetting efficiency has been determined using two methods; reaction method and tracer method. In the reaction method, the rates of the reaction in a three gas-liquid-solid phase flow trickle bed reactor and in a reactor completely filled with the liquid (complete wetting of the packings) are measured and compared. Table 2.1 presents the models published in the literature.

Table 2.1: Wetting efficiency models

Satterfield [70]	k_{app}/k_t
Colombo et al. [71]	$f = \dfrac{\left(D_{eff}\right)_{2-phase}}{\left(D_{eff}\right)_{liquid-filled}}$
Schwartz et al. [72]	$f = \dfrac{\left(K_A\right)_{apparent}}{\left(K_A\right)_{liquid-filled}}$
Dudukovic [73]	$f = \sqrt{\dfrac{\left(D_{eff}\right)_{2-phase}}{\left(D_{eff}\right)_{liquid-filled}}}$
Lakota and Levec [74]	$f = \dfrac{\left(k_S a_{LS}\right)_{2-phase}}{\left(k_S a\right)_{liquid-filled}}$

An alternative method for determination of the wetting efficiency is use of tracer techniques. The method is based on producing an impulse concentration of a tracer at the entrance to a trickle bed reactor and obtaining the time distribution of concentration at the outlet [75]. Mills and Dudukovic [73], Ring and Missen [76] and Al-Dahhan and Dudukovic [43] determined wetting efficiency using tracer technique.

Effects of gas and liquid flow rates on wetting efficiency have been studied and reported in the literature. Schwartz et al. [72] conducted dynamic studies of trickle-bed reactors. They observed that the liquid flow rate had minor effect on the wetting efficiency. On the other hand, Herskowitz and Mosseri [77] found that wetting efficiency (f_e) increased with the liquid flow rate but decreased with the gas flow rate. The effect of gas flow rate was even smaller at very high liquid flow rates. The wetting efficiency value ranged from 0.5 to 1 for relatively low gas flow rates under trickle flow regime. Pironti et al. [65] determined the extent of wetting of the catalyst as a function of gas and liquid velocities and the size of the packing. Leung et al. [78] showed that the uniformity of liquid and gas distribution within the catalyst bed had positive effect on the wetting efficiency.

Recently, Larachi et al. [79] developed a correlation for wetting efficiency in trickling flow reactors. The approach is relying on the combination of neutral network computation and dimensional analysis. The model is not restricted for specific operating condition and produces a relatively low error.

While most of the correlations for prediction of wetting efficiency in trickle bed reactors rest on the data obtained at atmospheric pressure, Al-Dehhan and Dudukovic [43] developed a model to predict the wetting efficiency at elevated pressure and high gas flow rate. Wetting efficiency increased with increase in the liquid flow rate because of increase in both pressure drop and liquid holdup. For a given liquid flow rate, wetting efficiency improved significantly at high pressure and gas flow rate. The effect of gas flow rate, pressure drop and liquid holdup on wetting efficiency was more at elevated

pressure. Indeed, the presence of high gas flow rate or pressure intensified the spread of liquid holdup over the external packing area.

2.2 Application of Trickle Bed Reactors for Wastewater Treatment

One of the oldest fixed film bioreactors, used for treating wastewater for many years, is the trickle bed bioreactor. Among various existing fixed film bioreactors, there is a great attraction toward trickle bed bioreactors for municipal and industrial wastewater treatment because of their simplicity of operation and their low energy requirement and operating cost. They have been considered as secondary treatment for most wastewater amenable to aerobic biological processes.

2.2.1 Trickle Bed Bioreactor Theory

Trickle bed bioreactors are fixed film bioreactors consisting of a bed filled with inert pellets on which biomass are immobilized. As the wastewater trickles over the bed and flows down, the organic pollutants are consumed by the biomasses and removed from the wastewater. The biofilm is attached to a surface of the inert pellets and continuously exposed to the falling liquid. Microorganisms form within the biofilm and grow by consuming the organics. The required oxygen for the biological oxidation is partially supplied from the air circulation through the bed and partially from the dissolved oxygen in the wastewater. Usually, natural ventilation, which is generated due to the temperature gradient between the wastewater inside the bed and the ambient, is sufficient to ensure air renewal and aeration of the water; otherwise, forced ventilation should be used. Oxygen either transfers to the biofilm directly or diffuses through the liquid film [80]. Diffusion is known as a main process for transportation of soluble substrate from

the bulk liquid into the biofilm and the microbial byproduct from the biofilm to the bulk liquid. In the case of particulate substrate, the substrate must be adsorbed on the surface of the biofilm and hydrolyzed to be able to diffuse through the biofilm. This phenomenon is known to erode the biofilm surface [81].

2.2.2 Effect of Operating Variables on the Performance of a Trickle Bed Bioreactor

Alexandra [80] suggested that adequate hydraulic and organic loading and proper ventilation helps to achieve maximum efficiency. Under such conditions, trickle bed bioreactors can produce an effluent equal to that of the suspended growth systems. The liquid retention time in the trickle bed bioreacror is only a few minutes provided that there is an adequate amount of biomass to remove the organic pollutants during that time interval. Proper liquid distribution and efficient contact of wastewater and biofilm is also necessary for optimum performance.

2.2.2.1 Organic Loading Rate

The organic loading rate and influent organic concentration are among the main factors affecting the trickle bed bioreactor efficiency for wastewater treatment and have been long used as a design and operating parameter. The volumetric organic loading rate is defined as the amount of BOD or COD applied to the trickle bed bioreactor volume per day and is expressed in kg BOD/m^3.day or kg COD/m^3.day [1]. It has been found that the performance of a trickle bed bioreactor was controlled by the organic loading rate [82, 83]. In addition, the volumetric BOD loading has been correlated well with the BOD removal [1].

21

Previous studies on the removal of organic compounds by trickle bed bioreactors showed that the percentage of the BOD removal is inversely proportional to the organic loading rate, whereas, the rate of BOD removal is a direct function of the organic loading rate [84-87]. However, Schulze [88] found that while the BOD removal rate increased with increasing the organic loading, the BOD removal efficiency was independent of the organic loading for values below 6.5 kg/m^3.day at a constant hydraulic loading.

Other study [89] examined the effect of the initial organic concentration on the efficiency of the COD removal in a cross flow nitrifying trickle bed bioreactor. It was found that the percentage COD removal was an inverse function of the influent COD concentration. However, the rate of COD removal increased with the increase of the influent COD concentration. Moreover, the plot of the organic loading rate versus the organic removal rate exhibited two regions of linear behavior. At lower organic loading rates, the rate of the organic removal sharply increased with the organic loading rate up to a certain point, beyond which the slope of the curve of the organic loading rate versus organic removal rate became moderate. This indicated that the removal rate reduces at the relatively high organic loading rates. Raj and Murthy [90] found that an increase in the influent substrate concentration and hydraulic loading rate resulted in a higher concentration gradient between bulk liquid and biofilm, and thinner liquid layer on the biofilm surface, respectively. This resulted in an improvement in the mass transfer of the substrate to the biofilm, which in turn increased the removal efficiency of the bed.

Randall et al. [91] also reported similar results while investigating the removal efficiency of a vertical flow medium trickle bed bioreactor for synthetic fiber wastewater treatment. They showed that although the amount of organics removed in the bioreactor increased with increasing the organic loading, there was a maximum beyond which no more enhancement in removal efficiency with increasing the loading rate was observed. This phenomenon was related to the fact that the organic matters are removed from wastewater by adsorption on the biofilm surface. Once the biofilm becomes saturated, no more additional organic removal occurs [92]. Previously, the National Research Council's [4] data had shown that for rock media beds, the organic loading should not

exceed 0.19 kg BOD$_5$/ m^3. day in order to obtain 75% ammonia removal. Also, Vaynas et al. [93] observed that when the initial ammonia concentration was higher than 4 mg/l, a significant amount of ammonia remain in the effluent.

2.2.2.2 Hydraulic Loading Rate

Another important design parameter of trickle bed bioreactors is the hydraulic loading rate. Indeed, trickle bed bioreactors are categorized according to the applied hydraulic loadings. The hydraulic loading rate is the total volume of liquid entering the reactor per unit time, per unit area of the bed.

Several studies [94, 95, 96] showed that in trickle bed bioreactors, the organic removal is inversely proportional to an exponential function of hydraulic flow rate and an increase in the hydraulic loading rate reduces the removal efficiency. In fact, the hydraulic loading rate determines the liquid retention time in the bed. At low hydraulic loading rates, the liquid retention time in the bed is long and the organics can be consumed by the biomasses completely. At high hydraulic loading rates, the liquid retention time is relatively short and the biodegradation of the organics may not be completed; therefore, a considerable portion of the organic matter leaves the reactor without any change [87-90]. Also, the improvement of the removal rate with an increase in the hydraulic loading rate can be due to the reduction in thickness of the stagnant liquid film and the increase of the wetted area [86, 97].

Dicks and Ottengraf [96] found that the biofilter efficiency increased with an increase in the liquid flow rate and attributed this to the improved wetting efficiency. They observed that at low liquid flow rates, the bed was not completely wet and only parts of packing material was covered with the biomasses. Therefore, biomass activities limited to the wetted areas. Moreover, Tekerlekopoulou and Vayenas [87] showed that at very low hydraulic loading rates, the biofilm thickness decreases, specially in the region near to the bottom of the bed. As a result, the upper portion of the bed become the main

participant in the organic degradation at low hydraulic loading rates and the liquid, which reaches the lower part of the bed, does not contain a significant amount of organic matter. At high loading rates, the substrate retention time in the bed reduces. Therefore, no considerable reaction occurs in the bed and high BOD concentration remains in the reactor effluent.

Parker and Richards [98] also reported the inverse effect of the hydraulic and organic loading rates on the percentage ammonia removal for nitrification in a trickle bed bioreactor. They observed that when the organic loading increased from 6 to 15 kgBOD$_5$/m^2.day, the percentage ammonia removal reduced by 85%. Moreover, Parker et al. [98] showed that increasing the hydraulic loading rate improves the bioreactor efficiency by increasing the wetted area of the packings.

Bosco et al. [99] investigated the influence of the superficial liquid velocity on the production of exoenzymes in a biological trickle bed reactor. It was discovered that the superficial liquid velocity not only affected the wetting of the bed, but also controlled the mass transfer from both the liquid film to the biofilm and the gas to the liquid film. At low superficial liquid velocities substrate mass transfer limitation happened. At these low velocities the wetting of the support was limited and thus, the substrate supply might not be available for the biomass in the entire bed. On the other hand, at high liquid velocities, the oxygen transfer limitation problem arises. In fact, the entire surface of support particles becomes wet under high liquid velocities; therefore, direct access of the biomass to the gas phase is hindered. In this case, oxygen must be provided from the liquid phase and consequently the rate is reduced rapidly. However, further increase in the liquid superficial velocity leads to an increase in the oxygen mass transfer in the liquid phase and the overall transfer rate of oxygen improves partially. Besides, higher liquid velocities induce higher shear stresses, which may detach the biomass from the packing surface.

In contrast, Lunan et al. [100] observed that the total BOD removal efficiency slightly decreases with the increasing hydraulic loading rate. This was explained by the

very fast consumption of simple compounds .The reduction in the percentage of BOD removal with increasing the hydraulic loading rate was also observed by Logan et al. [101] and Raj and Murthy [102].

2.2.2.4 Depth of Bed

There is a disagreement among various authors on the effect of media depth on the trickle bed bioreactor performance. Some investigators believe that volume of the bed, irrespective of the depth, controls the bioreactor performance [82]. Others suggested that for a fixed volume, the bioreactor performance was enhanced as the depth of the bed was increased [103]. The improved performance with increasing the tower depth at a fixed volume of media was attributed to better liquid distribution that in turn increases the wetting efficiency in the bed[104] and the higher retention time of the wastewater in the bed [4, 105-107]. However, some recent trickle bed models [104] predict only a minor improvement in the bioreactor performance with increasing the bed height at a fixed bed volume.

Although most researchers found that the removal efficiency increased with increasing the bed depth, there were several evidences indicating that there was an optimum depth beyond which no further improvement in the removal efficiency was observed. This was most likely due to the reduction of the concentration of the dissolved BOD in the lower section of the bed. It was shown that the soluble BOD concentration was a controlling factor for diffusion of the substrate into the biofilm. When the BOD concentration was relatively low, it could not diffuse into the biofilm and thus the BOD concentration did not change significantly [92,102].

Chapter 3

Experimental Methodology

3.1 Experimental Setup

This study was carried out in a pilot scale trickle bed bioreactor. A schematic diagram of the experimental set up is shown in Figure 3.1. The trickle bed consists of a vertical column of clear PVC with a liquid distributor at the top and a liquid collector at the bottom. The height and diameter of the column are 1.8 m and 0.3 m respectively. The column was filled with 2-cm plastic spheres. The packing height was varied between 0.7and 1.4 m. There was an opening on top of the tower for natural ventilation.

A synthetic wastewater was prepared in a 350 L feed tank. Liquid from the tank was pumped to the liquid distributor at the top of the packed bed. Two types of liquid distributors were used in the present study: single-delivery-point and 25-delivery-point liquid distributors (Figure 3.2). The single-point liquid distributor was a vertical tube with an opening diameter of 1.5 cm, whereas the 25-delivery-point distributor was a cross type distributor with six liquid delivery points in each arm and one liquid delivery point on the intersection of arms. The size of the liquid delivery nozzles was 0.3 cm. The distributors were installed at the top of the reactor in very close proximity of the packing to prevent water spreading to the column walls. It is known that a distributor with point density of 65 to 100 is adequate for initial distribution [22, 108]. However, it was observed that the liquid flow rate from each liquid delivery point of the cross type distributor was not equal. Therefore, the cross-type distributor did not distribute liquid uniformly over the top of the packing. The other distributor was a central single point distributor. This distributor could only supply liquid to the central part of column. The drip point density of this distributor is 14 points per square meter.

A liquid collector was installed at the bottom of the column at 7.5 cm below the packing support. This was used for measuring flow distribution leaving the packed bed. It was designed to collect data not only over a cross sectional area of the bed, but also in various diagonal and concentric paths. The liquid collector was made of 37 collecting cells (Figure 3.3). Each collecting cell was a 15 cm cylinder with a diameter of 3 cm. The bottom of each collecting cell was connected with a drain tube.

The effluent from the reactor was collected into a 120 liter holding tank located underneath the liquid collector. In the batch mode, the reactor effluent was recycled from the holding tank directly to the top of the bed. The influent flow rate to the reactor was adjusted using a valve. A flow meter (model Blue-White F-450) was used to monitor the flow rate. During the experiment, the influent flow rate varied from 0.184 to 0.918 kg/m^2.s. Five different flow rates of 0.184, 0.376, 0.551, 0.734, and 0.918 kg/m^2.s were used in the present study.

At the present study, two packed bed heights of 0.7m and 1.4 m were employed. The height of the bed was reduced by removing some packings from the top of the bed. The position of liquid distributor was adjusted according to the variation of packed bed height, and carefully leveled after installation.

OPENING
FOR AIR

DISTRIBUTOR

PACKED
COLUMN

FLOW
METER

FEED TANK

LIQUID
COLLECTOR

HOLDING
TANK

PUMP
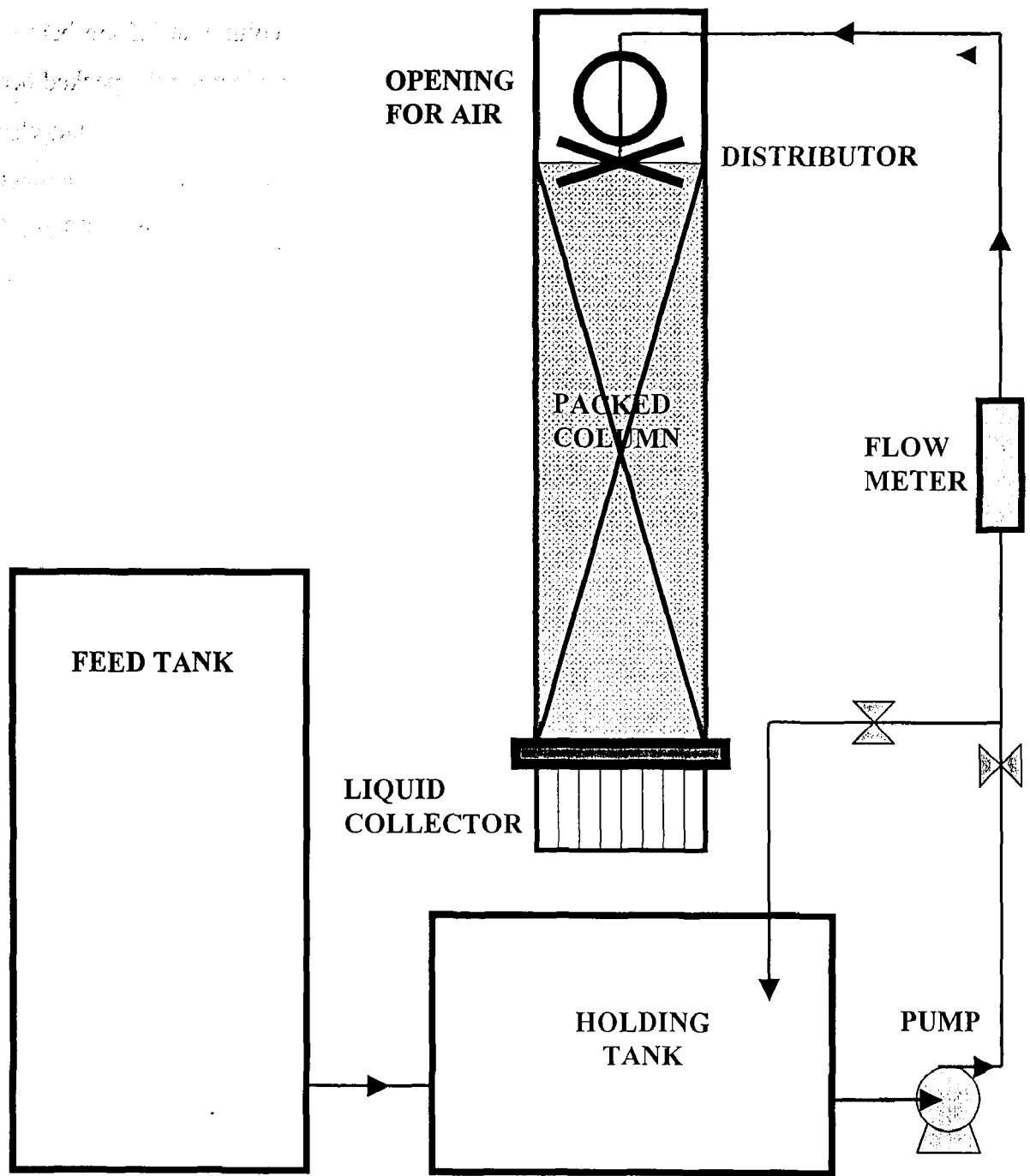
Figure 3.1: Schematic diagram of the experimental set-up

3.2 Experimental Procedure

3.2.1 Liquid Distribution Study

The initial phase of this study was on liquid flow distribution and dynamic liquid holdup. The operating conditions for liquid distribution study are summarized in Table 3.1.

Table 3.1: Operating conditions for liquid distribution study

Variable	Range
Liquid Flow Rate	0.184 - 0.918 kg/m^{-2}.s^{-1}
Packed Bed Height	0.7 – 1.4 m
Initial Liquid Distribution	1- 25 point Distributor

The liquid flow distribution studies were performed by measuring the liquid flow rate at the bottom of the column using a specially designed liquid collector. The liquid flowing out of each cell of the liquid collector was collected and measured in a graduated cylinder over a specific period of time and recorded. The radial liquid flow pattern and maldistribution coefficient were then determined based on these measured liquid flow rates. The effects of the liquid flow rate, the height of the bed and the initial liquid distribution on the liquid distribution profile and maldistribution coefficient were determined.

Dynamic liquid holdup was measured by the draining method [109] in the present study. The liquid inflow was stopped after a stable hydrodynamic condition in the bed was achieved. The liquid was let to drain for a period of 30 minutes and its volume was measured. The dynamic liquid holdup (h_d) was then calculated based on following:

$$h_d = \frac{V_d}{V_r}$$

(3.1)

where the V_d is the volume of the drained liquid, and V_r is the volume of the bed .

3.2.2 Biological Organic Removal Study

In the second phase, the performance of the trickle bed bioreactor for the organic removal under the same operation condition was investigated. The operating conditions for biological organic removal study are summarized in Table 3.2.

Table 3.2: Operating conditions for biological organic removal study

Variable	Range
Initial Propylene Glycol Methyl Ether Concentration	100 – 500 ppm
Liquid Flow Rate	0.184 - 0.918 kg.m^{-2}.s^{-1}
Packed Bed Height	0.7 – 1.4 m
Initial Liquid Distribution	1 - 25 point distributor

A start-up period was required for the microorganism to build up on the surface of the packing material and acclimate to the propylene glycol methyl ether (PGME).
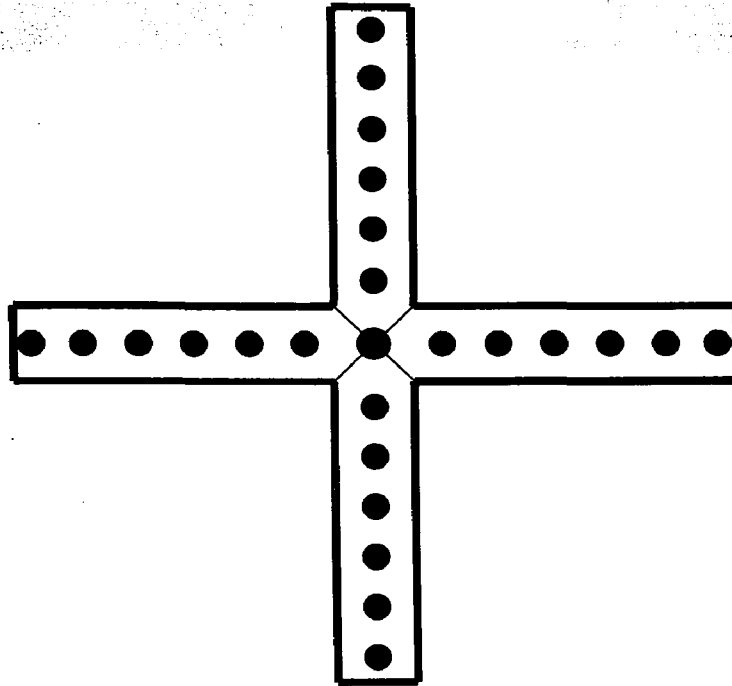
Multi delivery point distributor
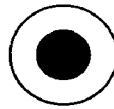
Single delivery point distributor

Figure 3.2: Liquid distributor design
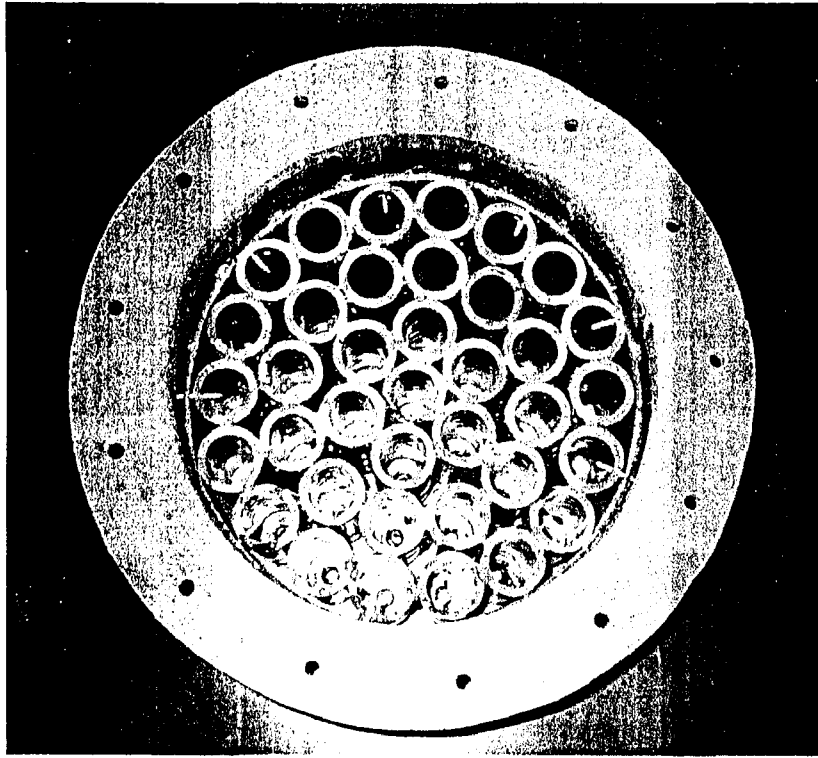
Top view of liquid collector
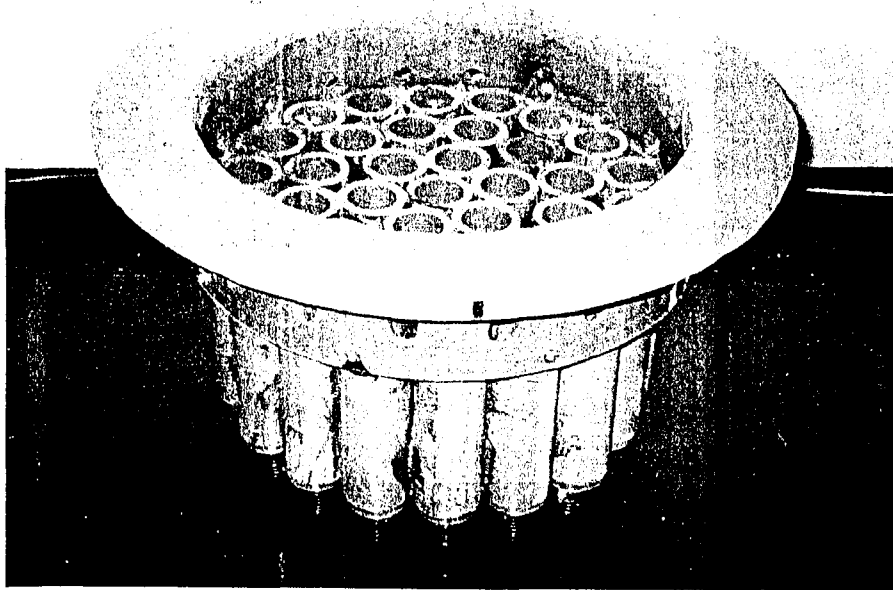
Side view of liquid collector

Figure 3.3: Liquid collector

In the beginning, the reactor was seeded with polyseed® (InterBio Inc. Texas) and run in the batch mode for 6 weeks. During this period, the reactor was fed with highly biodegradable substrate such as glucose solution. Ammonium chloride and sodium phosphate were added to the feed solution as nitrogen and phosphorous source with a C: N: P ratio of 100:5:1. The COD concentration of the feed was increased in four steps of three-day intervals, from very low concentration of 70 mg COD/l.day up to 550 mg COD/l.day and then kept constant. Table 3.3 shows the composition of synthetic wastewater during start-up period. During this period, water samples were taken daily from the holding tank. The pH and the BOD_5 of the samples were measured as indicators of the biological activity. The pH was decreasing due to the formation of some organic acid as an intermediate compound. In order to maintain pH at 7, an appropriate amount of 0.1 M sodium hydroxide solution was added to the wastewater. The BOD_5 of wastewater was decreased with time, which was the evidence of biological activity and growth.

Table 3.3: Composition of wastewater during start-up period

Constituent	Concentration
Glucose	0.5 gr/l
Ammonium chloride (NH_4Cl)	0.105 gr/l
sodium phosphate (Na_2HPO_4, $7H_2O$)	0.0475 gr/

After the start-up period, when good population of microorganisms was developed on the packing surface, the composition of the feed was changed. The microorganisms were progressively adapted to PGME by increasing its concentration in the feed from 0 to 100 mg/l while the glucose concentration was gradually decreased. This was done to maintain the total COD at 550 mg COD/l. Samples were taken each time before and after adding the mixture of PGME and glucose for measurement of BOD_5. The constant reduction in the BOD_5 showed that the acclimation was proceeding successfully. This process was continued until the concentration of PGME and glucose

in feed reached 550 and 0 mg COD/l. It took about two weeks for the biomass to acclimate to PGME.

The effects of the liquid flow rate, the packed bed height, the liquid distributor design, and initial organic concentration on the percentage removal and the biodegradation rate of the PGME were examined. The synthetic wastewater used for this study was a solution of PGME at five different concentrations of 100 ppm, 200 ppm, 300 ppm, 400 ppm and 500ppm. All the feed solutions were prepared using distilled water.

Water samples were taken daily from the storage tank over the period of 5 days during each run. The BOD and the COD of the samples were measured using standard methods [110]. To investigate the effect of liquid distribution on the organic removal, water samples were taken from selected cells of the liquid collector while the reactor was running in continuous mode. The cells were selected in such a way that the samples located on a diagonal path were looked at. After that, the BOD and COD of these samples were measured. The pH and the dissolved oxygen content and temperature of the liquid entering and exiting the reactor were also measured. To do this, two wastewater samples, one from the bypass flow and another from the central cell of the liquid collector were collected in BOD bottles in a daily basis during each run. All the measurements were done immediately after sampling to insure the accuracy of results.

3.3 Analytical Procedures

3.3.1 Biological Oxygen Demand

The Standard BOD test was performed on all the samples during the biological phase of the research project. The biological oxygen demand is an empirical test; it is used to determine the relative oxygen requirement of waste and treated water. It measures

the amount of oxygen utilized by microorganism for degradation of organic material during a specific period of time (usually 5 days).

The BOD of each sample was measured immediately after taking the sample. Dilution water was prepared according to the standard methods [110] by adding 1.0 mg of phosphate buffer solution, magnesium sulphate solution, calcium chloride solution and ferric chloride solution per liter of distilled water. The dilution water was aerated by inserting a tube connected to the organic free compressed air supply. It was then cooled to 20 ^{0}C prior to use. Since the effluent from the reactor did not contain a sufficient microbial population, it was necessary to add some microorganism to the BOD bottles. Polyseed capsules were used as a source for seed. Dissolving one capsule of polyseed in 500 cm^3 dilution water created the seed solution.

The water samples, collected from the system, were added to a 300 ml BOD bottle depending on the estimated BOD value. 10 ml of the seed solution was added to each BOD bottle of the wastewater. All bottles were then filled with the dilution water. The initial dissolved oxygen was measured immediately by inserting a DO probe of the dissolved oxygen meter (model 52 CE YSI, Yellow springs, Ohio, USA) into the bottles. The bottles were closed tightly, sealed with water and covered with a foil cap to minimize evaporation of the water seal during incubation. Finally, they were incubated (Incubator VWR) at 20 ±1°C for a period of 5 days.

As recommended in standard methods [110], a seed control was performed to ensure the quality of the seed. The seed control was prepared in a similar manner. 10 ml of the seed solution was added to the BOD bottle and filled with the dilution water. It was also incubated at 20 ±1°C for a period of 5 days.

After 5 days, the dissolved oxygen value was measured again and the BOD$_5$ value of the water samples was calculated from the following equation:

$$BOD_5, mg/L = \frac{(D_1 - D_2) - (B_1 - B_2)f}{P}$$

(3.2)

where:

D_1 = Dissolved oxygen of diluted sample immediately after preparation, mg/L

D_2 = Dissolved oxygen of diluted sample after 5 days of incubation at 20 $^{\circ}$C , mg/L

P = decimal volumetric fraction of sample used

B_1 = Dissolved oxygen of seed control before incubation, mg/L

B_2 = Dissolved oxygen of seed control after incubation, mg/L

f = ratio of seed in diluted sample to seed in seed control

3.3.2 Chemical Oxygen Demand (COD)

Chemical oxygen demand (COD) of the collected samples was also measured. The closed reflux colorimetric method was used for the COD test in present study. The procedure was performed according to the Standard methods [110]. The method was for mid-range COD concentration in the range of 20 to 900 mg/l. A Standard 10 ml ampule was used for the COD assay. First, the tubes and caps were washed with 20% sulfuric acid solution to prevent any contamination. Then, the tubes were filled with 1.5 ml digestion solution and 3.5 ml sulfuric acid reagent. A sample was taken from the holding tank every 24 hour during each run. They were filtered to remove any biomass or other organic matter that would affect the COD results prior to each test. Vacuum filtration with a Buchner funnel and low ash 32 Whatman filter paper was used. 2.5 ml of the filtered water was added to the prepared ampules and capped tightly. A blank ampule containing distilled water instead of the sample was also prepared. A block digester (Bioscience, Inc.) was preheated to 150 and then the ampules were placed in it for two hours. Then, they were cooled to room temperature prior to reading their absorbance. The absorbance of the samples was read at 600 nm directly with a Spectrophotometer (Orbeco-Hellige, model 975-MP, Farmingdale, New York). For each sample, multiple COD reading were obtained and average COD concentration was calculated.

3.3.3 pH control

The pH measurements were performed using a pH meter (Model 220, Corning). Prior to each set of measurement, A two point calibration was performed using two buffer solutions of pH = 4 and pH = 7 to insure that the readings were accurate. The pH of the system was maintained between 6 and 7.5 by adding an appropriate amount of a buffer solution (pH=7.2) to the wastewater.

3.4 Data Analysis

The absolute uncertainty associated with liquid flow rate, maldistribution coefficient, and liquid holdup was calculated according to method for the calculation of uncertainty in a function of several variables [111]. Sample calculations for estimating the uncertainty in the liquid flow rate, maldistribution coefficient, and liquid holdup is presented in Appendix B.

The uncertainty in the dissolved oxygen reading was calculated based on the manufacture's (YSI Inc.) instructions. The uncertainty in the BOD_5 was then estimated according to the method for the calculation of uncertainty in a function of several variables [111].A sample calculation for this is also presented in Appendix B. Moreover, uncertainty in chemical oxygen demand was calculated from multipoint readings.

Chapter 4

Result and Discussion

4.1 Liquid Distribution Profile

In the beginning, reproducibility test was conducted for the system at the bed height of 1.4 m with the multipoint liquid distributor. The selected liquid flow rate was 0.734 kg/m^2.s. The result is shown in Figure 4.1, which displays three different runs. The data is plotted in terms of liquid flow rate (averaged over three diagonal paths) against the radial position. As shown in Figure 4.1, the liquid distribution profiles of the three runs are comparable to each other. The overall error was about 15% from the average value.

The liquid distribution experiments were carried out using a 0.3 m diameter column filled with 2 cm plastic spheres covered with biomass. The liquid velocity was measured using a liquid collector, which was installed underneath the column. Samples were taken at three diagonal pathways for each experimental run to investigate the angular variation of radial liquid flow profile relative to the liquid distributor position. The three diagonal pathways and their position relative to the liquid distributor are shown in Figure 4.2. The average radial liquid distribution profile at the reactor outlet was determined by averaging the liquid flow rate obtained at the diagonal pathways.

The results of liquid flow distribution measurements at the reactor outlet showed that the liquid distribution profile was not uniform. A plot of variation of liquid velocity with radial position is shown in Figures 4.3 to 4.5 for three different liquid flow rates. The figures reveal that the liquid distribution profiles are characterized by wavering behavior with minimum amplitude in the region near the wall area. Several investigators have obtained the same behavior of radial liquid distribution profile [31,112, 113].
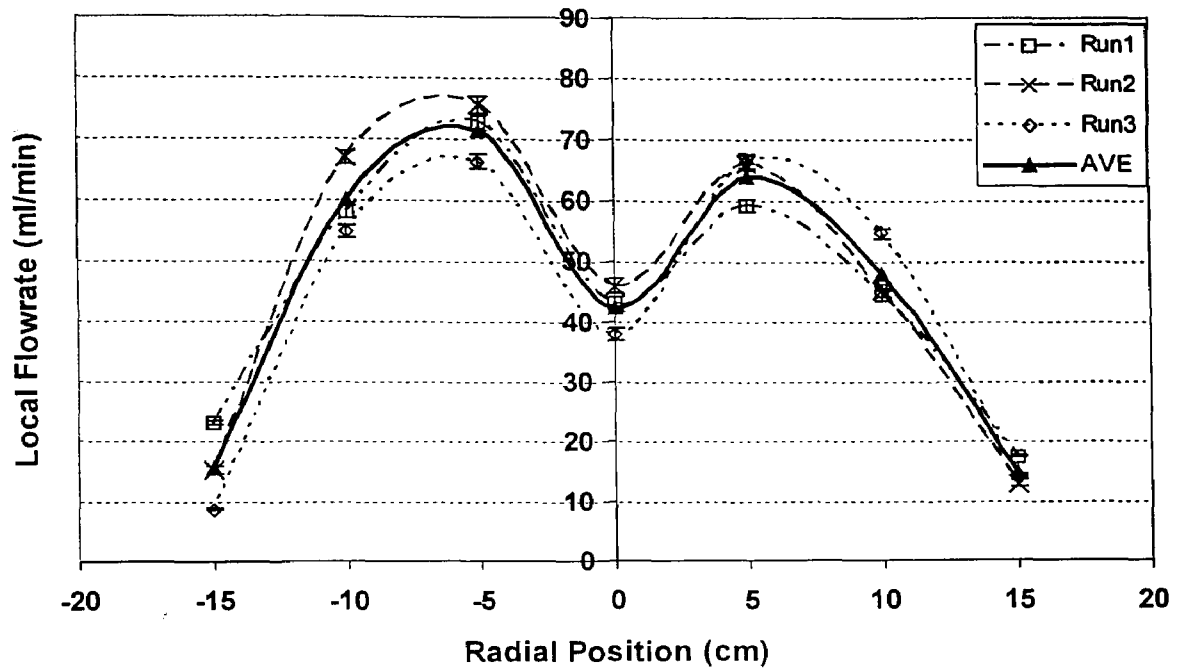
Figure 4.1: Reproducibility test at flow rate of 0.734 kg/m^2.s using multipoint distributor
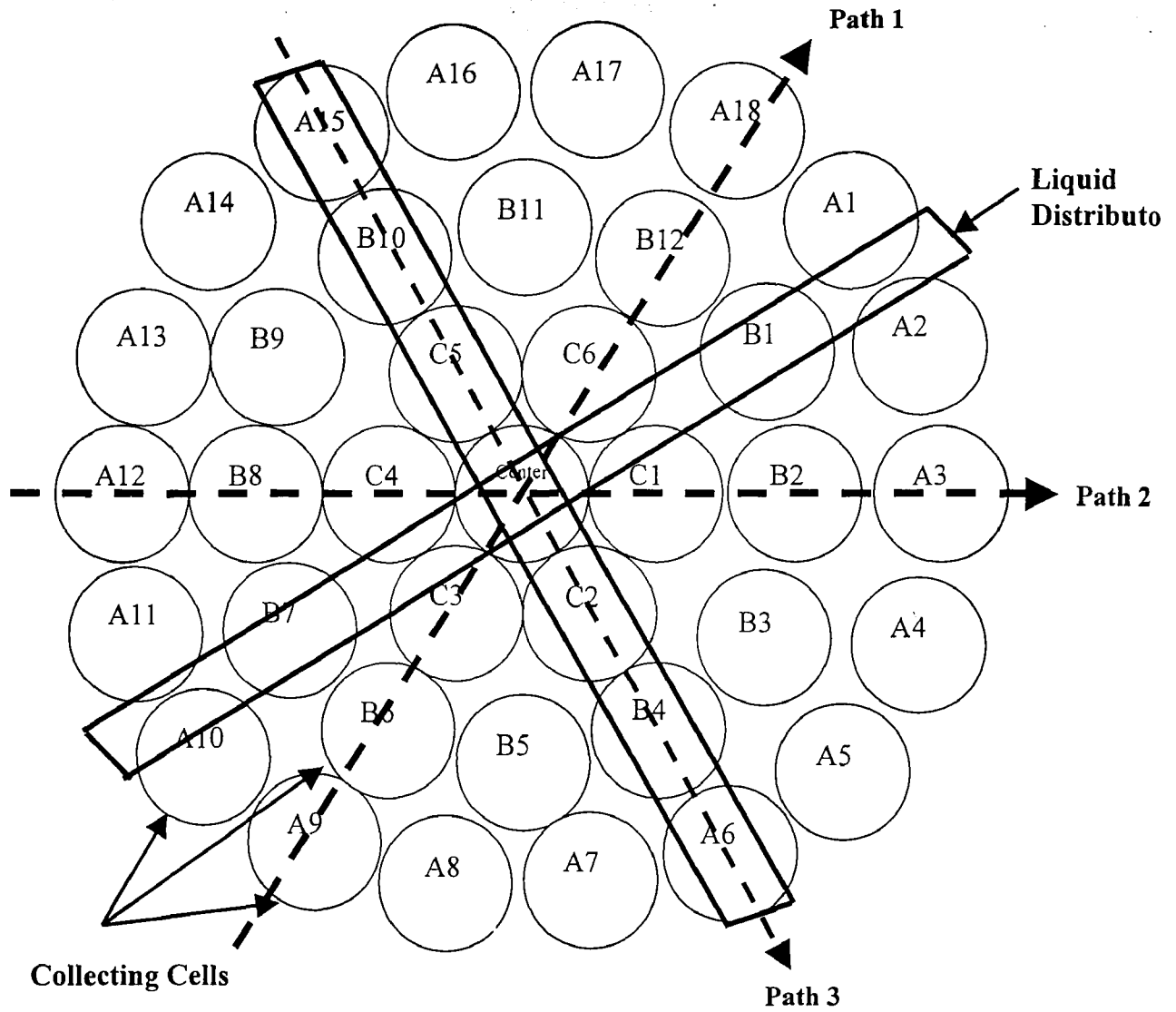
Figure 4.2: Relative position of the liquid distributor and the liquid collector
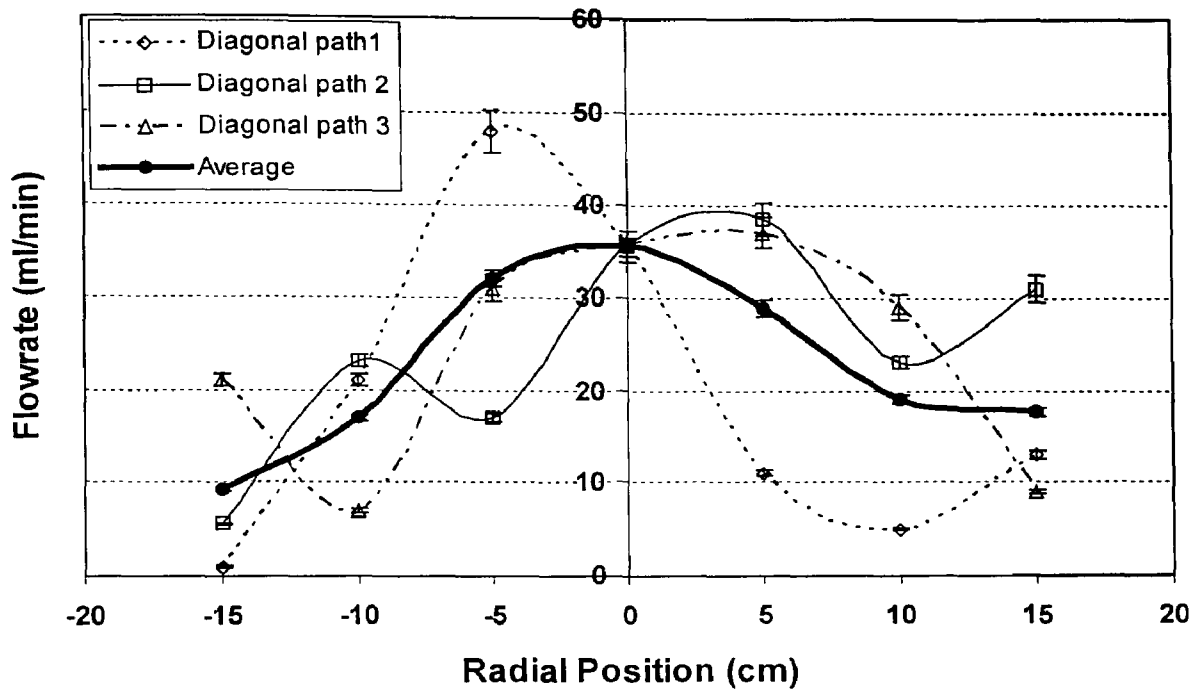
Figure 4.3: Liquid distribution profile for liquid flow rate of 0.367 kg/m^2.s at 1.4 m bed depth using a multipoint cross type distributor
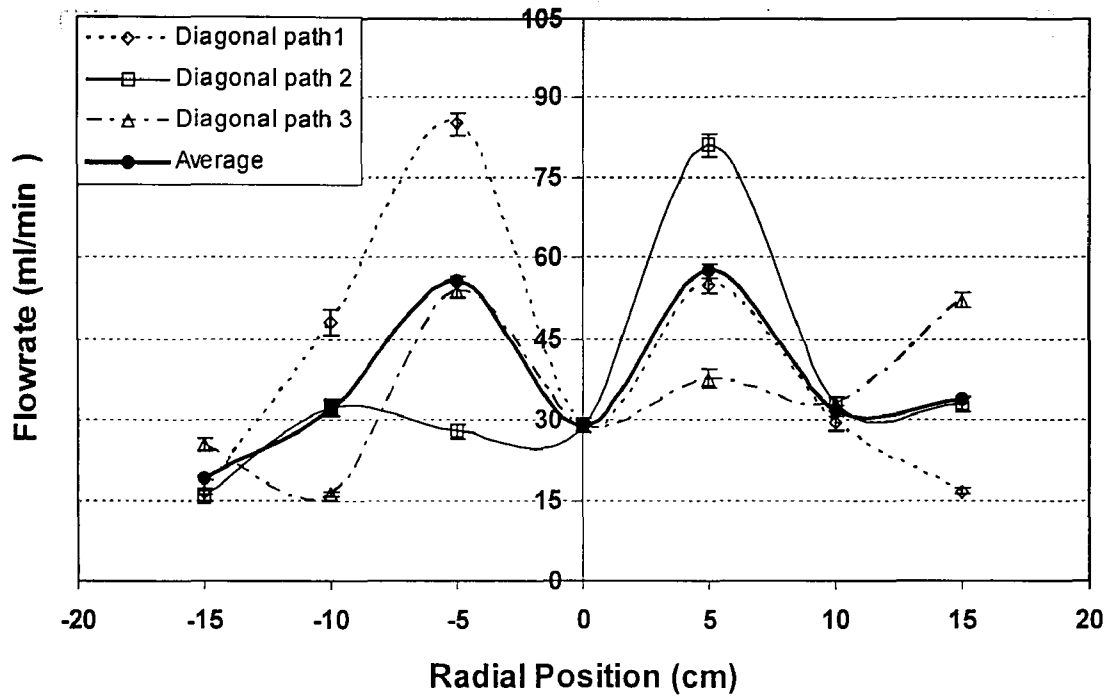
Figure 4.4: Liquid distribution profile for liquid flow rate of 0.551 kg/m^2.s at1.4 m bed depth using a multipoint cross type distributor
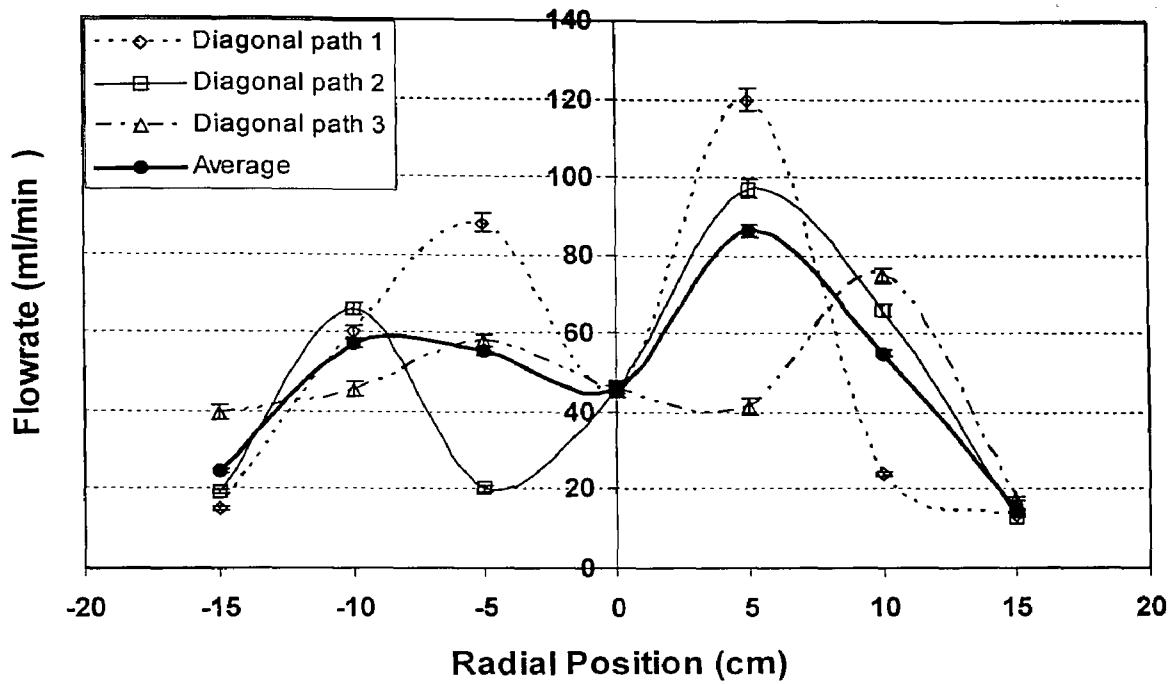
Figure 4.5: Liquid distribution profile for liquid flow rate of 0.734 kg/m^2.s at 1.4 m bed depth using a multipoint cross type distributor

Kunjummen et al. [28] found that radial liquid velocity profile over any bed cross section was corresponded to the oscillation pattern of voidage at that radial direction. This finding was also supported by the mathematical model of velocity distribution of single-phase flow in packed beds, developed by Subgyo et al. [34].

In order to study the effect of liquid distributor position (relative to the liquid collecting cell) on the liquid distribution profile, the radial liquid distribution was measured in three pathways for a given liquid flow rate. The results showed that the radial liquid distribution profile in Path 3 has less variation compared to the other paths. As shown in Figure 4.2, one of the liquid collector's branches lies on the collecting cell in Path 3 and the collecting cells receive the liquid mostly from that branch. However, the collecting cells in Path 2 and 1 collect the liquid coming from both branches of liquid collectors.

4.1.1 Effect of Liquid Flow Rate

The averaged liquid flow profile was determined for five different liquid flow rates ranging from 0.184 kg/m^2.s to 0.918 kg/m^2.s at the bed heights of 0.7 m and 1.4 m. Figure 4.6 presents the profile of liquid distribution at the bed height of 1.4 m for five different liquid flow rates of 0.184, 0.367, 0.551, 0.734 and 0.918 kg/m^2.s. The liquid distribution profile was found to be more uniform at lower liquid flow rates. The oscillation amplitude of the profile increased notably when the liquid flow rate increased to 0.551 kg/m^2.s and beyond.

The liquid distributor used for this experiment was cross type distributor with one nozzle at the intersection of branches and six nozzles on each of its four branches. At low flow rates, due to relatively low liquid pressure inside the pipes, the liquid could not reach the end of the distributor's branches and was distributed on the packing mostly from central nozzles. Figure 4.6 demonstrates that for the case of multipoint distributor at low liquid flow rates of 0.184 kg/m^2.s and 0.367 kg/m^2.s, the local liquid flow rate at

the center of the column is higher than the mean value of the bed cross section. In other words, liquid mainly flows in the center of column. However, more even profile was obtained at the bed outlet in spite of initial non-uniform liquid distribution at these flow rates in comparison with higher liquid flow rates.

When the liquid flow rate was increased from 0.367 $kg/m^2.s$ to 0.551 $kg/m^2.s$, its pressure was high enough to overcome the friction between liquid and pipe, and the liquid flowed all the way through the branches. As a result, all the nozzles of the distributor participated in distribution of liquid on the packing. The nozzle density on the branches was higher than that in the intersectional area of distributor. Consequently, the local liquid flow rate at the center of column was substantially lower than the area next to the center of the column (Figure 4.6). Another possible reason for low local liquid flow rate at the center of the column at high liquid flow rates might be the higher concentration of biomass in central area of the bed which blocked the liquid pathway. In this area, the packing is more likely to be wet and the microorganism could grow on the solid spheres. As a result, a fraction of void space between the packing was occupied by the microorganisms. Thus, the liquid was directed around and flowed through the area next to the center of the column. Further increase in the liquid flow rate (up to 0.918 $kg/m^2.s$) resulted in an increase in the local liquid flow rates all over the column cross-section with similar trend.

Yin et al. [67] found that increasing the liquid flow rate had negligible effect on the liquid distribution in the bulk region, which was due to uniform increase of liquid film thickness within the packing in the bulk region. They performed their experiments in the packed column without biomass. Also the range of liquid flow rate employed in their experiment was between 2.96 and 6.66 $kg/m^2.s$, which was much higher than that of this study.

The wall flow was not measured in these experiments. However, it was observed at high liquid flow rates. This phenomenon was first observed at a low bed height of 0.5 m under liquid flow rate of 0.376 $kg/m^2.s$ when the multipoint distributor was used.
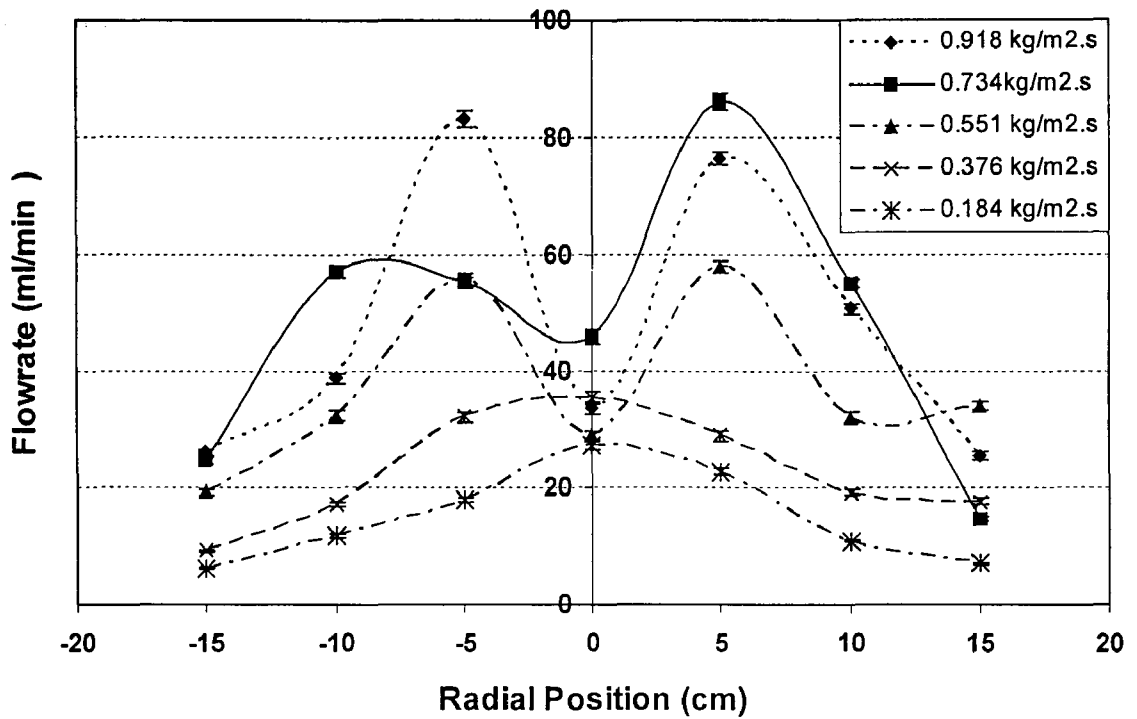
Figure 4.6: Effect of liquid flow rate on liquid distribution profile at the 1.4 m bed height using a multipoint distributor

Generally, the observation revealed that the higher the flow rates, the more the wall flow. This result is in contrast with that of other researchers who have shown that increasing the liquid flow rate reduces the wall flow rate [67]. The similar results could be achieved if these experiments were run under higher liquid flow rates or bed heights. The range of the liquid flow rate employed in present study was generally low and even with multipoint distributor uniform distribution at the top could not be achieved. Moreover, the packings were small and thus their spreading coefficient was low. Accordingly, at the lowest flow rate where the initial liquid distribution was very non-uniform for the both types of liquid distributor, no wall flow was observed and the liquid left the column before reaching the wall.

4.1.2 Effect of Liquid Distributor Design

Liquid distribution was also measured for single point liquid distributor at the range of liquid flow rates varied from 0.184 kg/m^2.s to 0.918 kg/m^2.s.The liquid distribution profile of single point liquid distributor at different liquid flow rate can be found in Appendix A (Figure A.1). The results show that the variation of liquid distribution profile of single point distributor is similar to Figure 4.6.

Liquid flow rate profiles of two liquid distributors, under different liquid flow rates, are compared in Figure 4.7. The liquid distribution profile of multipoint liquid distributor was smoother compare to that of single point distributor. However, as it is evident from Figure 4.7, the liquid distribution profile generated with both distributors follows similar pattern of oscillation. As for the multipoint distributor, the radial liquid flow profiles of the single point distributor had lower local liquid flow rates at the area next to the column wall and the local liquid flow rate at the central region of column was higher than the overall average flow rate based on the column cross section. This indicates that the non-uniform initial liquid distribution at the top generated by single point distributor can be smoothened out gradually as liquid flows along the bed. This is due to the ability of the packing to spread the liquid flow radially.

Because liquid was introduced into the column through central region when using single point distributor, the local liquid flow rate at the center of column was much higher in comparison with that of multipoint distributor, as shown in Figure 4.7. This is because a single point distributor did not spread out the liquid over the packing and the liquid entered the packing from the central region at the top of the bed. Therefore, the local liquid flow rate in central area of column was higher than that of other parts of the bed. In spite of the relatively high liquid flow rate in the column center at the top, the local flow rate at the center of the column is still lower relative to the region next to it at the bed outlet. This is probably due to the high concentration of microorganism in the central area of the bed as it was explained in previous section.

For single point distributor it was observed that the liquid didn't reached the column wall at flow rates lower than 0.551 kg/m^2.s. This means that the packing was only partially wetted and the rest of the packing remained dry. Since the dry part of packings is not able to contribute in mass transfer process, the overall performance of the reactor reduces. This would reveal the importance of initial distribution on a randomly packed bed reactor's operation [22].

4.1.3 Effect of Bed Height

Liquid distribution profile was also determined at the bed height of 0.7 m. Height of the bed was reduced to half of the initial height by removing packing from the top of the bed. Figure 4.8 compares the liquid distribution profile of two different bed heights at the same liquid flow rates using the multipoint distributor. The figure depicts that at the bed height of 0.7 m the liquid distribution is still far from uniformity. At this height of the bed the liquid distribution profile was characterized by very high flow at the center. The liquid distribution profile obtained at the1.4 m bed height was comparatively evener than that of the 0.7 m bed height. Scott [114] suggested that the effect of
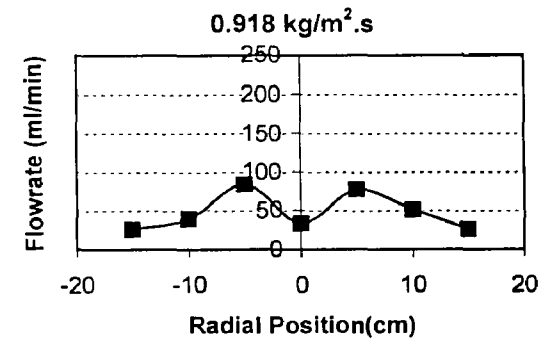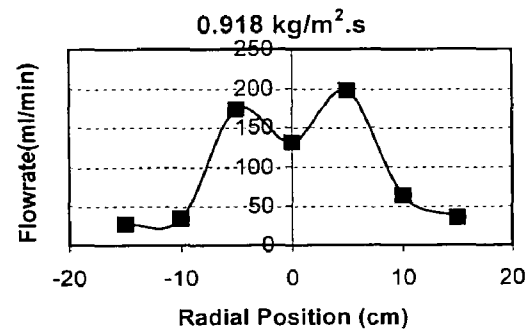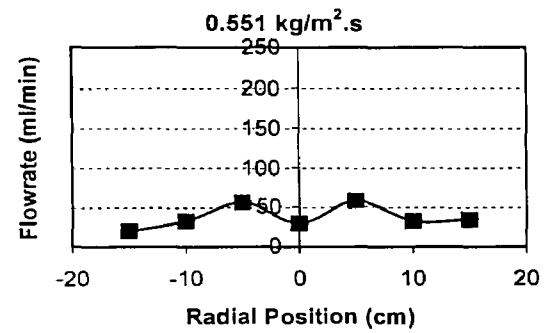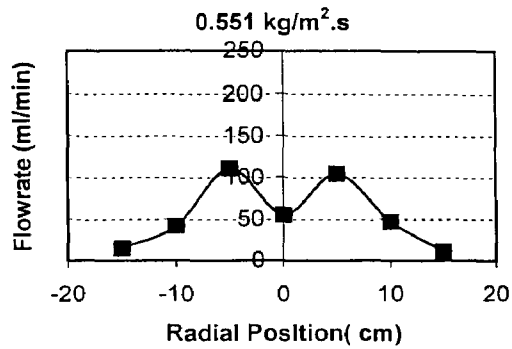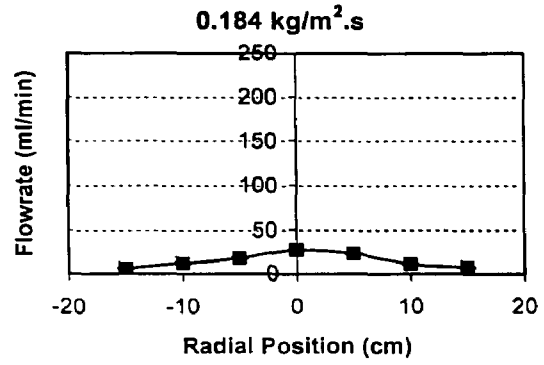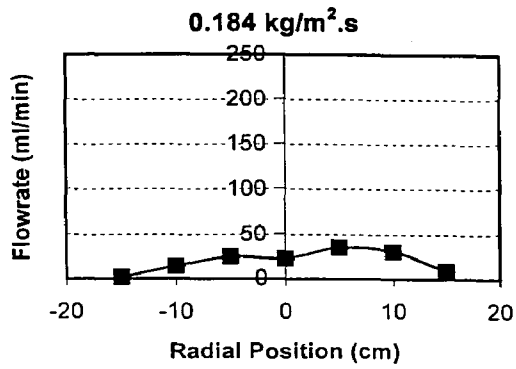
a: Single point distributor   b: Multipoint distributor

Figure 4.7: Effect of liquid distributor design on liquid distribution profile under different liquid flow rate at the bed height of 1.4 m.
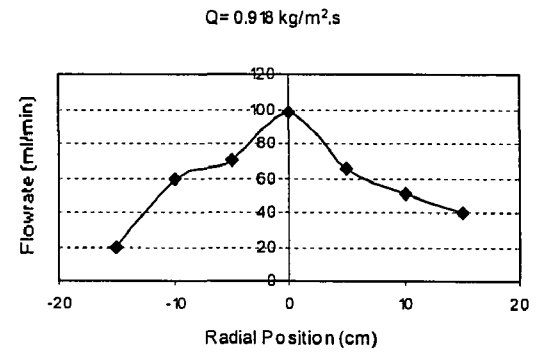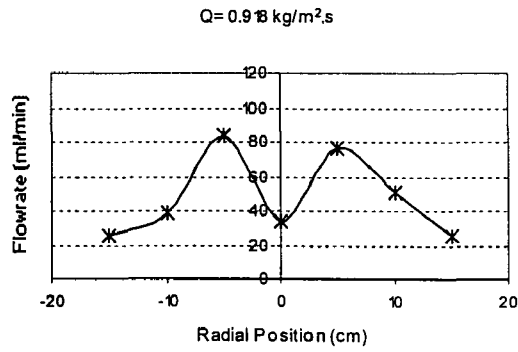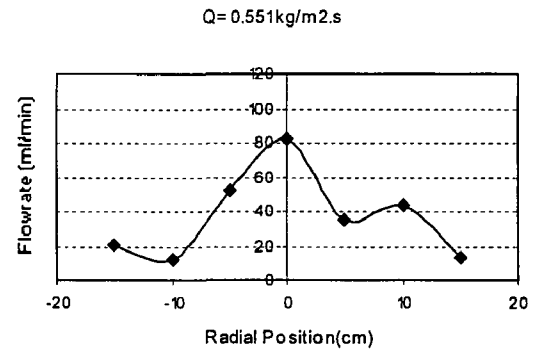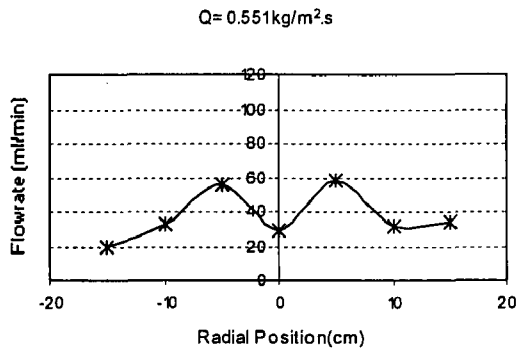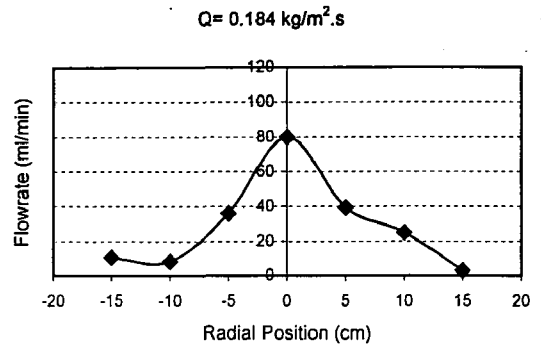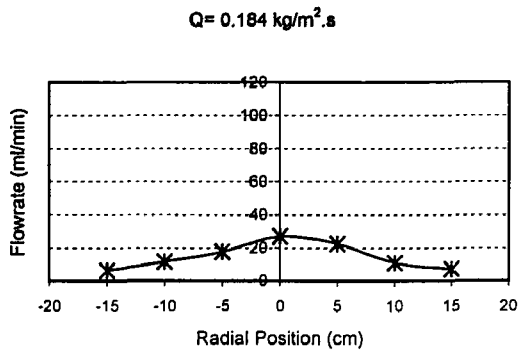
Figure 4.8: Effect of the bed depth on the liquid distribution profile at different liquid flow rate using multipoint distributor

increasing the height of the bed on the liquid distribution was to increase the spread of the liquid towards the walls. Undoubtedly, our results confirm Scott's hypothesis. Backer et al. [39] also found that in order to reach to fully developed state in a 0.3 m diameter column packed with sphere, at least 3.0 m of bed height is needed when central single point distributor is used.

4.2 Quantification of Liquid Distribution

The liquid flow distribution is quantified by a maldistribution coefficient defined as

$$MC = \frac{1}{x}\sqrt{\sum_{i=1}^{x}\left(\frac{Q_i - Q_{av}}{Q_{av}}\right)^2} \qquad (4.1)$$

The maldistribution coefficients were calculated for the range of liquid flow rates (0.184 to 0.918 kg/m².s) at two bed heights of 0.7 m and 1.4m using single point and multipoint distributors. The calculation was done based on the data collected at the column outlet. In general, the results showed that considerable maldistribution of liquid takes place in the bed. It was found that the maldistribution coefficient was mainly depended on the packed bed height and the type of liquid distributor. The liquid flow rate didn't affect the *MC* value significantly at the bed height of 1.4 m. However, when the height of the bed reduced to 0.7 m, the *MC* value decreased sharply with increasing the liquid flow rate.

4.2.1 Effect of the Liquid Flow Rate

The maldistribution coefficient decreased with an increase of the liquid flow rate from of 0.184 kg/m².s to 0.918 kg/m².s at the bed height of 1.4 m when multipoint liquid

distributor was used (Figure 4.9). This is in agreement with the results of other authors [11]. However, very small reduction of maldistribution coefficient was observed with the increase of liquid flow rate from 0.184 kg/m^2.s to 0.918 kg/m^2.s. At the high liquid flow rates, the wall flow started to build up at the shorter depth of the bed, and thus, the liquid wall flow existed at the bed outlet where maldistribution coefficient was measured. Existence of the wall flow increased the maldistribution coefficient at higher flow rates. This in turn negated the improvement of liquid distribution due to high flow rate. However, when the bed height of the bed reduced to 0.7m, no wall flow was observed at any liquid flow rate. Hence, the maldistribution coefficient decreased when liquid flow rate was increased (Figure 4.10).

For the case of the single point distributor, the maldistribution coefficient was appeared to increase with increasing the liquid flow rate. In fact, at the low liquid flow rates of 0.184kg/m^2.s and 0.376 kg/m^2.s, quite smooth profiles of the liquid distribution were attained as depicted in Figure A.1, which might result in the low value of maldistribution coefficient. Also, as liquid flow rate increased, the liquid appeared to flow primarily in the central area of the column possibly due to a low spreading coefficient of the packing. Thus, extremely uneven liquid distribution profile was attained at high liquid flow rates. The highly non-uniform distribution of liquid at the bed outlet led to the high maldistribution coefficient at high liquid flow rates. Finally, the maldistribution coefficient increased when the liquid flow rate increased.

A comparison of the liquid maldistribution coefficient for the two types of liquid distributors is shown in Figure 4.9. Obviously, the initial liquid distribution affected the liquid distribution in the bed as shown in Figure 4.9. The maldistribution coefficient was significantly less for the multipoint delivery distributor compared to that of the single delivery point distributor, which was resulted from the more uniform initial liquid distribution achieved by the multipoint delivery distributor.
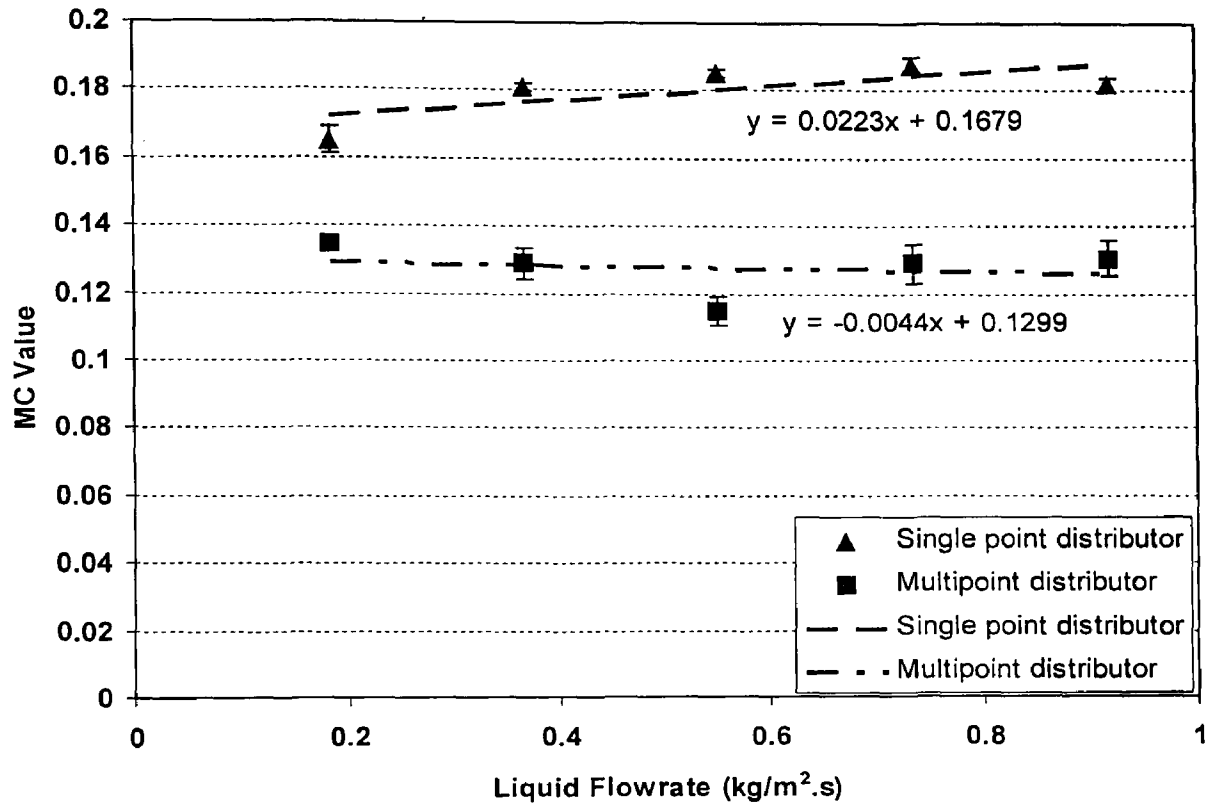
Figure 4.9: Effect of liquid flow rate on liquid maldistribution coefficient at the bed height of 1.4m.
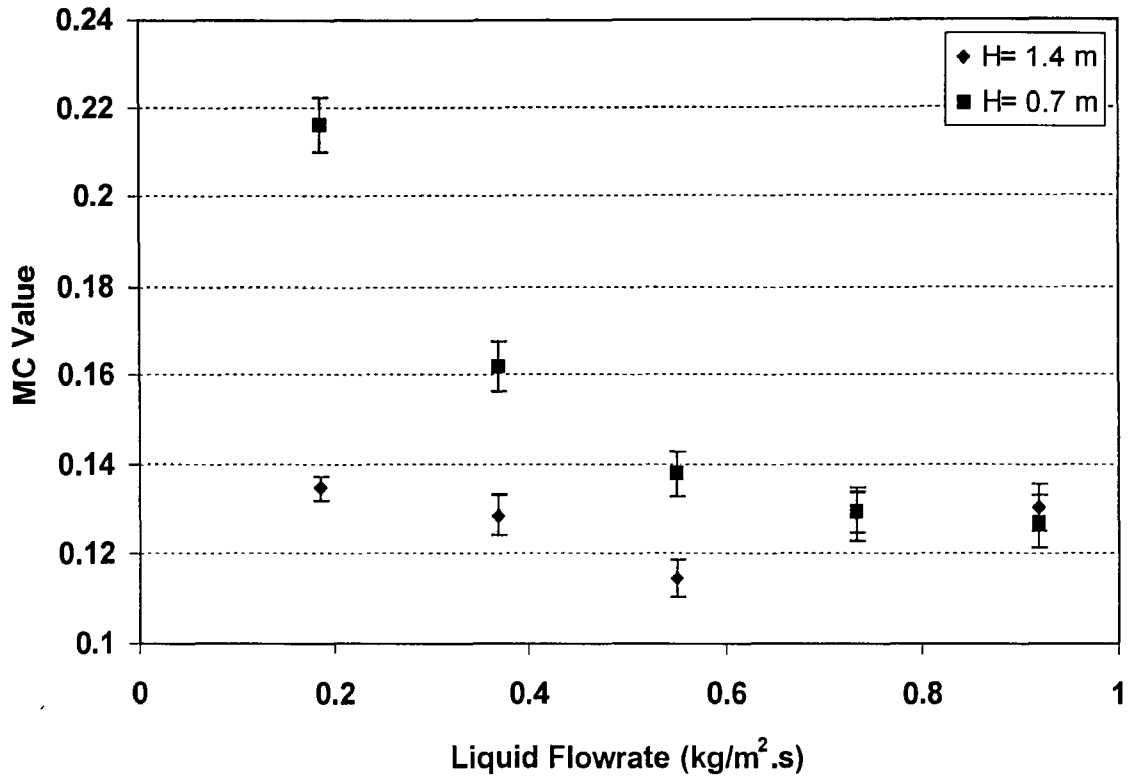
Figure 4.10: Effect of bed height on maldistribution coefficient using multipoint distributor

4.2.2 Effect of the Bed Height

Maldistribution coefficient values at the diffident liquid flow rates was obtained for bed heights of 1.4 m and 0.7 m and presented in Figure 4.10. The figure depicts that at the bed height of 0.7 m, the maldistribution coefficient value decreases considerably with increasing the liquid flow rate. At low liquid flow rates of 0.184 and 0.376 $kg/m^2.s$, where the initial liquid distribution was very non-uniform, the maldistribution coefficient value was high. As the liquid flow rate increased, the maldistribution coefficient decreased as a result of the more uniform initial distribution attained at higher liquid flow rates. Moreover, the comparison of the maldistribution coefficient values at two bed heights shows that the value of the maldistribution coefficient at the 0.7 m bed height approached that of the 1.4 m bed height as the liquid flow rate increased. Indeed, at high liquid flow rates of 0.734 and 0.918 $kg/m^2.s$, the maldistribution coefficient values were the same regardless of the packed bed height. This result indicates that when the initial liquid distribution is non-uniform, an extra height of the bed is required for the liquid distribution to reach uniformity. The above result is in agreement with the results of Yin et al. [67] who showed that the bed height required for the liquid to reach its fully developed state was reduced with increases in liquid flow rate.

4.3 Liquid Holdup

In order to estimate the effective contact between the liquid and the packing in the bioreactor, the dynamic liquid holdup was measured. The dynamic liquid holdup was determined at different liquid flow rates by measuring the volume of the liquid that drained from the bed after the inlet liquid flow was stopped. Then, the dynamic liquid holdup was calculated by dividing the volume of liquid drained from the column to the volume of the bed. The liquid flow rate was varied from 0.184 to 0.918 $kg/m^2.s$ and two bed heights of 0.7 and 1.4 m were used.

The dynamic holdup increased with the liquid flow rate as shown in Figure 4.11. It is generally believed that the dynamic holdup includes liquid films and rivulets [46]. The relative amount of these elements fluctuates primarily with the liquid flow rate [36]. At low liquid flow rates, liquid holdup is formed mainly of liquid films and only a small number of rivulets. As the liquid flow rate increases, the number of the rivulets and their size increase and consequently the liquid holdup increases [115]. The observed increase in the liquid holdup with the liquid flow rate is in agreement with the correlation proposed by Billet [116]. The correlation is written as follows

$$h = \left(12 \frac{1}{g} \frac{\mu_L}{\rho_L} q a^2 \right)^{1/3} \left(\frac{a_h}{a} \right)^{2/3} \qquad (4.2)$$

where h is the liquid holdup, g is the gravity acceleration, μ_L is the dynamic viscosity of the liquid, ρ_L is the density of the liquid, a is the total surface area per unit volume of the packed column and a_h is the hydraulic area of packing per unit volume of the packed column.

The influence of the liquid flow rate on the liquid hold up at the different bed heights was found to be qualitatively similar. However, Figure 4.11 shows the dynamic holdup is affected by the bed height. The holdup values for the bed height of 1.4 m were lower than that of for 0.7 m. These results are in agreement with the results of Lakota and Levec [74]. They related this to the non-uniform liquid distribution in longer bed heights. However, our results showed that the liquid distribution was more uniform at the 1.4 m tall bed than that of the 0.7 m tall bed. On the other hand, for a given liquid flow rate the quantity of the drained liquid for the 1.4m bed height was higher than that of the 0.7 m for (Figure 4.12). In the present study, the measured volume of drained liquid was indeed the sum of the volume of moving liquid inside the bed and the volume of the liquid inside the distributor. The volume of the liquid inside the distributor was the same for both bed heights. This volume of liquid contributed more to the liquid holdup for shorter bed since it was divided to a smaller column volume of the shorter bed. This resulted in an increase in the higher values of the liquid holdup obtained for the shorter bed of 0.7 m height.
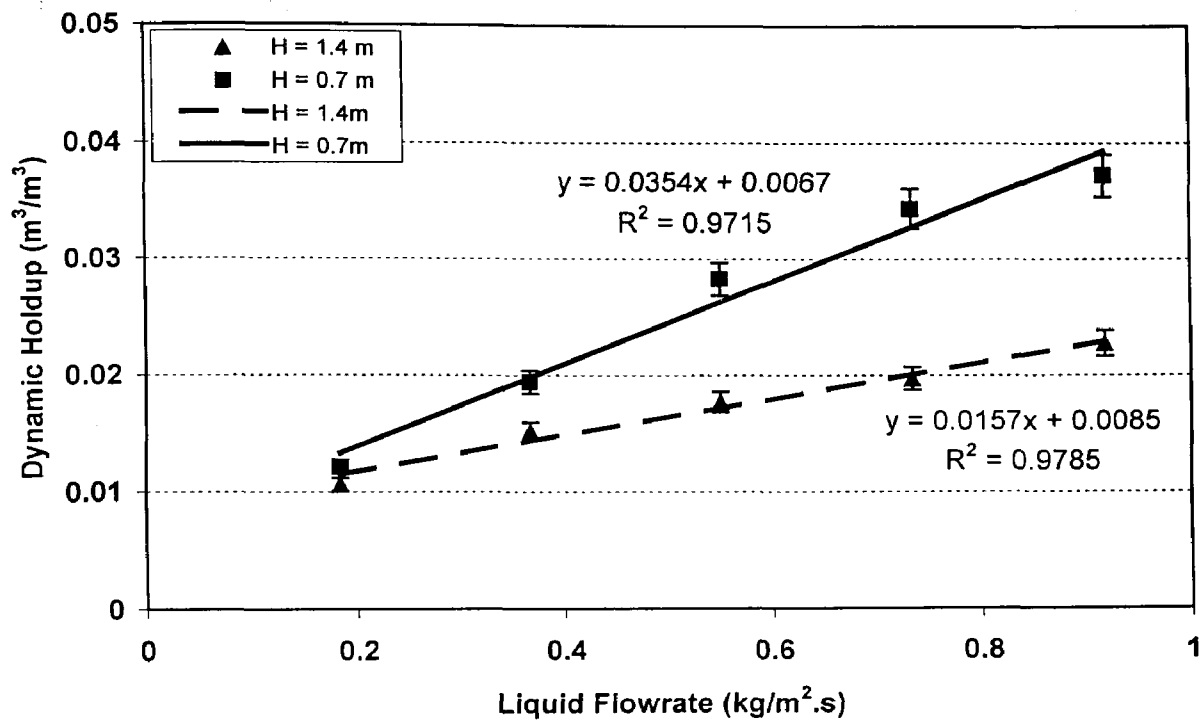
Figure 4.11: Effect of bed height on the dynamic liquid holdup. The data was obtained using the multipoint liquid distributor.
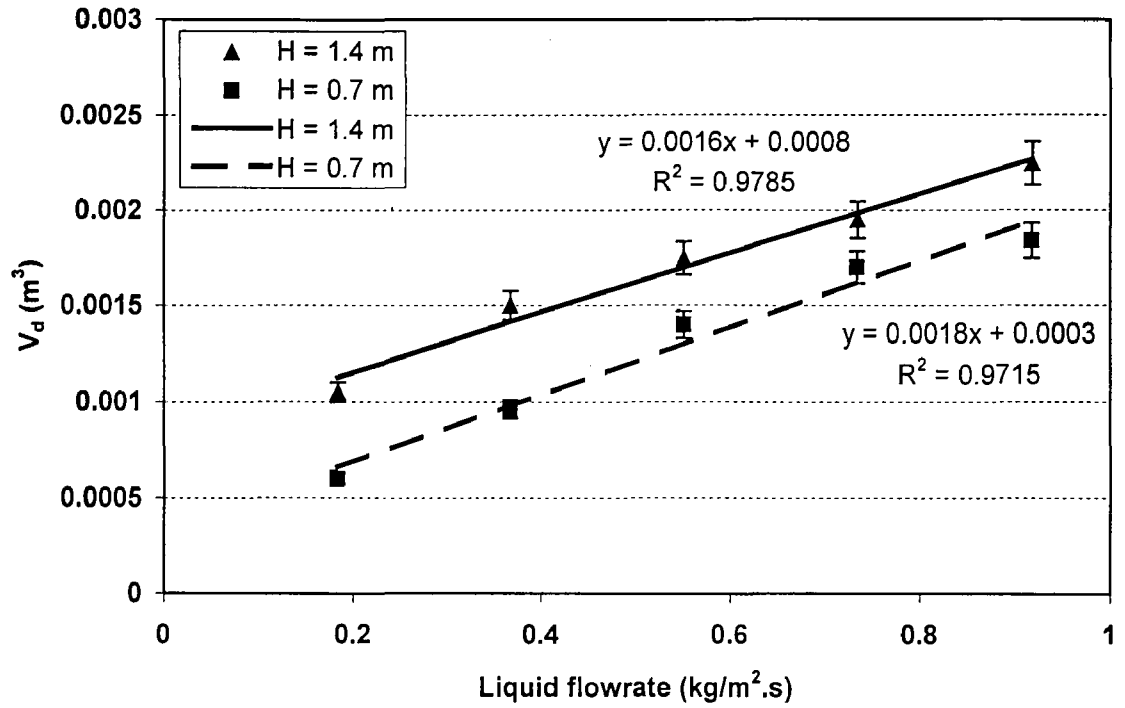
Figure 4.12: Effect of the bed height on the volume of the drained liquid using the multipoint liquid distributor
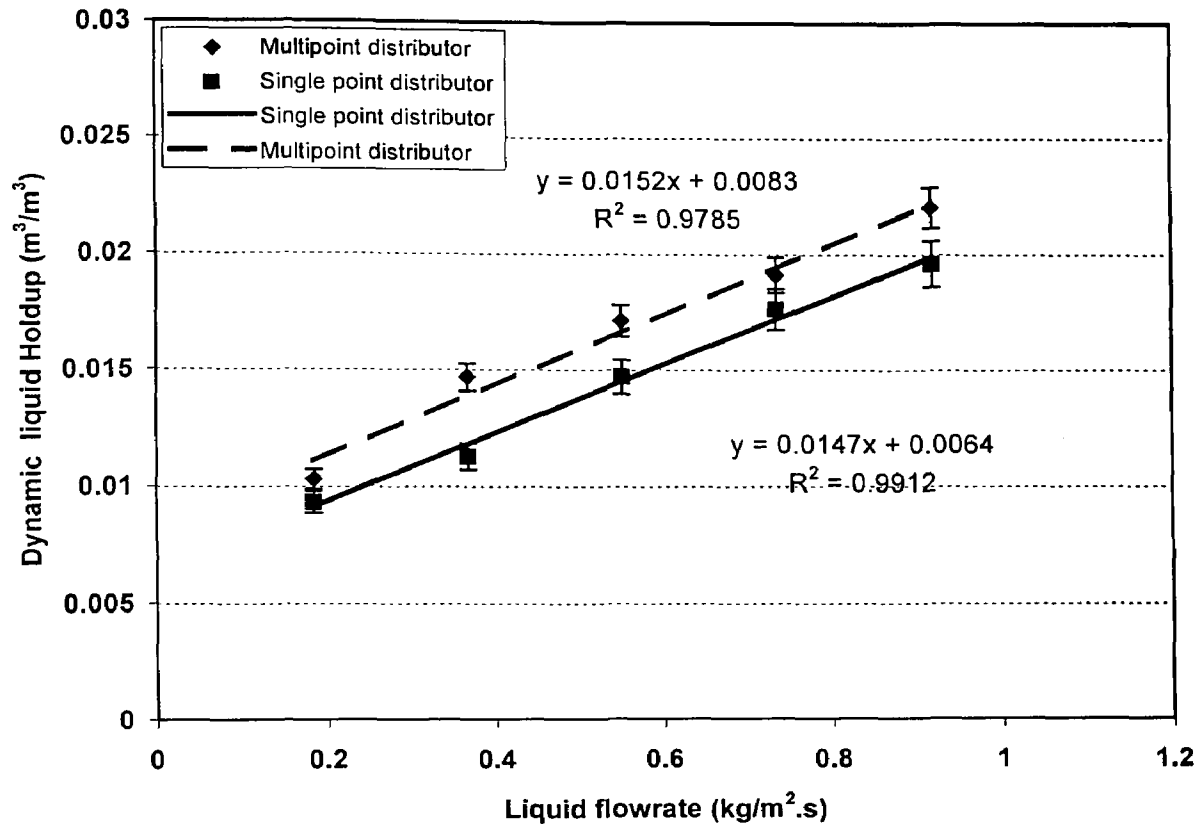
Figure 4.13: Effect of the liquid distributor design on the dynamic liquid holdup at the bed height of 1.4 m.

Liquid holdup values for the single delivery point distributor were compared to those for the multipoint distributor at the same bed height. The dynamic liquid holdup values obtained using the multipoint distributor was higher than that of the single delivery point distributor (Figure 4.13). The values of liquid holdup for both distributors were calculated at the same bed height of 1.4 m, thus, the volume of the liquid inside the distributors contributed to the dynamic liquid holdup calculation equally. Lower liquid holdup values for the case of the single point distributor compare to those of the multipoint distributor possibly resulted from less uniform liquid distribution attained using the single point distributor. This also reflected by the higher *MC* values for the single point distributor as previously shown in Figure 4.9.

Furthermore, the effect of the presence of biofilm on liquid holdup was investigated. The dynamic liquid holdup was measured at various liquid flow rates for the 0.7 m height bed filled with the packing covered with biomass and the clean packing. It appeared that the presence of biomass causes a considerable influence in the dynamic holdup. As shown in Figure 4.14, the dynamic liquid holdup was higher for the packing with the biomass. This phenomenon was more pronounced at higher liquid flow rates. This result is in agreement with the results of other authors who showed that the presence of the biofilm had a positive effect on the wetted area of the packing surface [117,118] and the wetted area increased with the biofilm growth [119].
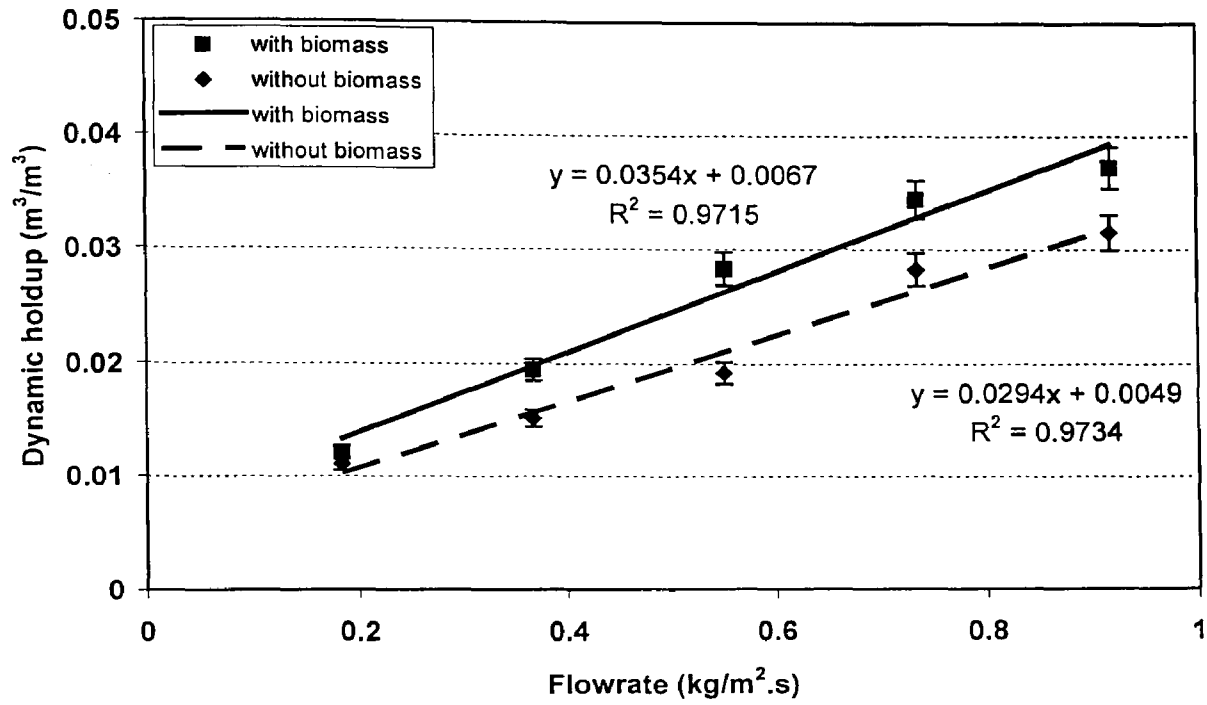
Figure 4.14: Effect of the presence of the biomass on the dynamic liquid holdup. The data was obtained using the multipoint distributor at the bed height of 0.7 m.

4.4 Biological Treatment of Propylene Glycol Methyl Ether

4.4.1 Biodegradation Rate of Propylene Glycol Methyl Ether

To find the kinetic rate constants, the mechanism of biological oxidation should be studied. In the absence of such information of the biooxidation of PGME, the experiments in the present study were used to obtain the overall biodegradation rate reaction. As shown in Figures 4.15, a good linear relationship of $-\ln (COD/CODo)$ versus time was obtained with the regression coefficients of over 0.9 for all initial concentration of PGME used. The degradation rate of PGME in the trickle bed bioreactor appeared to follow first-order reaction kinetics since the plots of $-\ln (COD/CODo)$ versus time were straight lines with different slopes depending on the initial concentration of PGME. The values of the reaction rate constant in the present study were for 72-hours of treatment.

Several authors have shown that the kinetic of biodegradation in a trickle bed bioreactor follows first-order reaction kinetics [1, 120], especially at low substrate concentrations [121]

$$r = k_p C \qquad (4.3)$$

where k_p is an apparent rate constant experimentally determined and C is the removable COD (or BOD) concentration at time t. On the other hand, the reaction rate for attached growth systems is related not only to the removable BOD concentration but also to diffusion-affected factors on and within the biofilm [122].

Generally, three major steps occur in overall process when a substrate is utilized by the biological films [123]:

a) Diffusion of the substrate from the bulk liquid to the interface between the liquid and the biological film

b) Diffusion of substrate within the porous biofilm

c) Biological reaction (substrate consumption) within the biofilm

The overall phenomenon resulting from steps (b) and (c) occurs after step (a) and must be equal to step (a) at steady state [123].

The local mass transfer rate of the substrate from the liquid bulk to the surface of immobilized cells can be expressed as [121]:

$$r_m = k_m A_m (C - C_s) \tag{4.4}$$

where r_m is the mass transfer rate, k_m is the mass transfer coefficient , A_m is the surface area per unit weight of microorganism cells, C is the substrate concentration in the bulk liquid, and C_s is the substrate concentration at the surface of the cell.

On the other hand, first order biodegradation rate on the cell surface can also be written as [121]:

$$r = kC_s \tag{4.5}$$

where k is the intrinsic first order biodegradation rate constant .

Under steady state condition, the rate of external mass transfer and the rate of biodegradation are the same. Therefore,

$$r = r_m \tag{4.6}$$
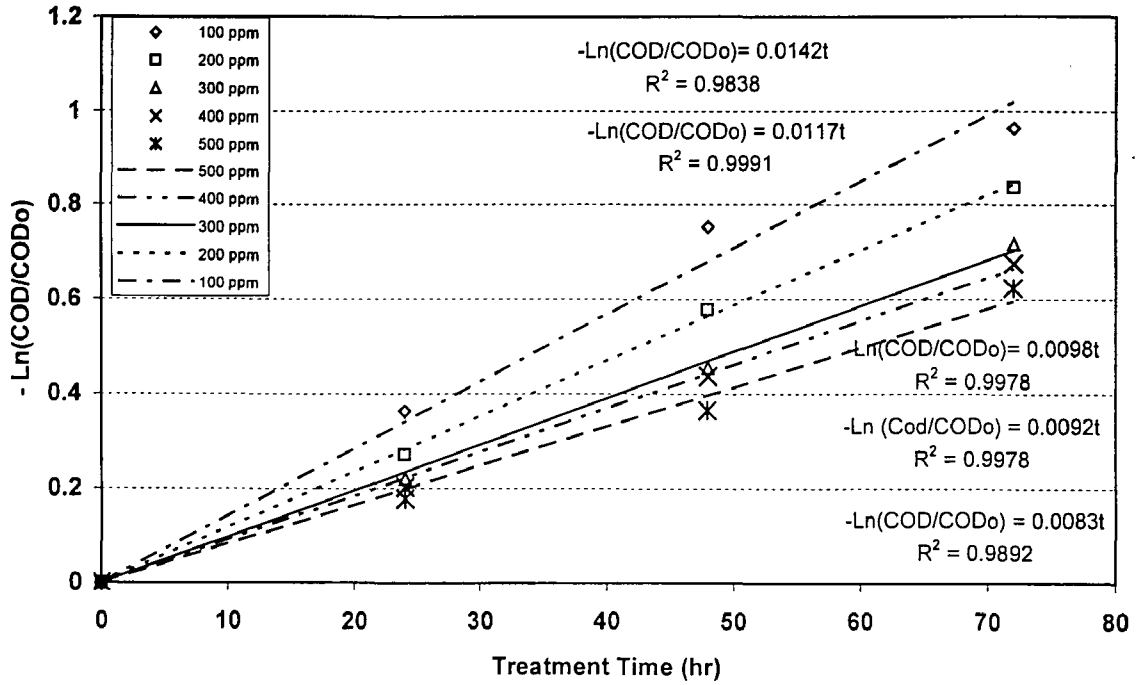
Figure 4.15: Biodegradation of PGME in the trickle bed bioreactor with varied initial concentration of PGME at 0.551 kg/m^2.s liquid flow rate and 1.4 m bed height, using multipoint distributor.

Solving the above equation for the unknown surface concentration gives:

$$C_s = \frac{k_m A_m C}{k + k_m A_m} \qquad (4.7)$$

Then, the effect of biodegradation and mass transfer rates on the actual biodegradation rate will be [121]:

$$k_p = \frac{k k_m A_m}{k + k_m A_m} \qquad (4.8)$$

This explanation is consistent with the obtained experimental data and suggested model.

4.4.2 Effect of Initial Concentration

Initial concentrations of 100, 200, 300, 400, and 500 mg/L of PGME were used to examine the effect of initial concentration on the degradation rate of PGME in a rickle bed bioreactor. The selected liquid flow rate was $0.551 kg/m^2.s$. Figure 4.16 illustrates the effect of initial PGME concentration on the amount of $mgBOD_5$ /l removed. As it can be seen, the amount of BOD_5 (mg/l) removed was higher for the higher initial concentrations of PGME. Atkinson et al. [122] found a similar trend when using glucose as the substrate under the liquid flow rates varied over the range of 0.16 to 1.08 $kg/m^2.s$. Moreover, the correlation between the amount of BOD_5 removed and initial organic concentration exhibits two region of linear behavior with the point of inflection at an initial PGME concentration of 300 ppm. At high organic concentrations of 400 and 500 ppm, the concentration gradient between the bulk liquid and the liquid film, which is a driving force for the mass transfer, was vary high. Therefore, the mass transfer of substrate

65

through the liquid film was high. This indicates that the overall degradation rate was not mass transfer limited in this region and was controlled by the rate of the biodegradation. At the organic concentration of 300 ppm and lower, the rate of the substrate uptake by the microorganisms was faster than the rate of mass transport due to the relatively low concentration gradient between the bulk liquid and the liquid film. Consequently, the mass transfer of the substrate from the bulk liquid controlled the overall rate of organic degradation.

Although the relatively high amount of the PGME was removed with the higher initial PGME concentrations but, the percentage removal was lower than that of the lower initial concentrations. Figure 4.17 shows the profile of the percentage BOD removal during 72 hours of treatment period with different initial organic concentrations of PGME. For the lowest initial PGME concentration of 100 ppm, the percentage BOD removal after 72 hours of treatment was 62%. As the organic initial concentration was increased from 100 to 500 mg/l, the percentage BOD removal decreased from 62 to 37%. This was also illustrated in the plot of the percentage BOD_5 removed after 72 hours of treatment versus initial PGME concentration in Figure 4.18. The figure depicts that an increase in the initial PGME concentration has negative effect on the percentage BOD_5 removal. A similar relationship was obtained for the %COD removal (Figure A.2) when plotted against the initial concentration of PGME. A similar result was reported by Lunan et al. [124]. This phenomenon can be explained by the reduction of the rate of the degradation at the high initial PGME concentration of 400 and 500 ppm as depicted in their profiles in Figure 4.17. The reduction in the rate of degradation is attributable to the saturation of the biofilm surface with PGME [92]. Once the surface of the biofilm becomes saturated, no mass transfer limitation happens and the overall degradation rate is controlled by the rate biodegradation. The biodegradation is a slow process and results in a reduction of the overall degradation rate.

The reduction of the apparent reaction rate constant with the increase of the initial PGME concentration was also shown in Figure 4.19. These data were obtained from the

linear regression of the $-\ln$ (BOD$_5$/ BOD$_{5o}$) versus time at different initial organic concentrations ranging from 100 to 500 ppm.

It is well known that the intrinsic first-order reaction rate constant is independent of concentration and flow rate. However, it is only a function of temperature [125]:

$$k = B \, e^{\left(-E/_{RT}\right)}$$

(4.9)

where k is the reaction rate constant, B is constant, E is the activation energy, R is the universal gas constant and T is the temperature .However, the apparent biodegradation rate constant was found to be a function of both the intrinsic biodegradation rate and the external mass transfer. The external mass transfer process is well known to be affected by the hydrodynamic regimes, biofilm surface geometry, substrate loading rates and diffusivities [126]. Therefore, the variation in apparent reaction rate constant (k_p) with initial PGME concentration can then be explained by the effect of the initial PGME concentration on the mass transfer rate.
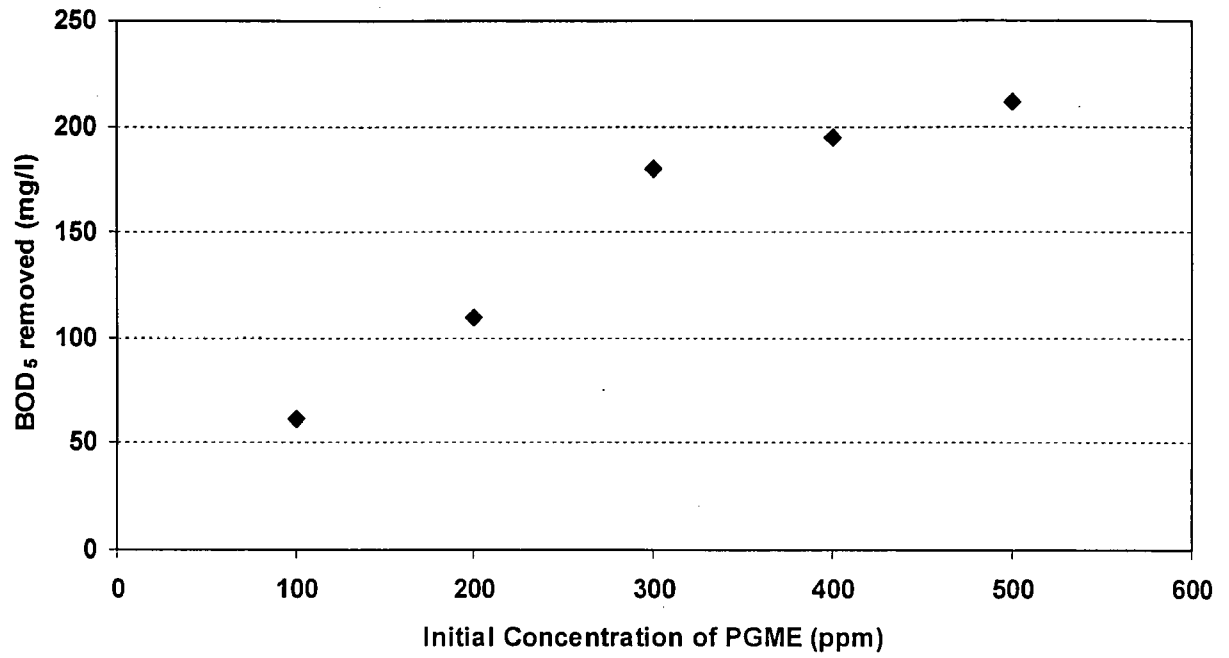
Figure 4.16: Effect of the initial concentration of the PGME on the amount of BOD$_5$ removed at liquid flow rate of 0.551 kg/m^2.s.
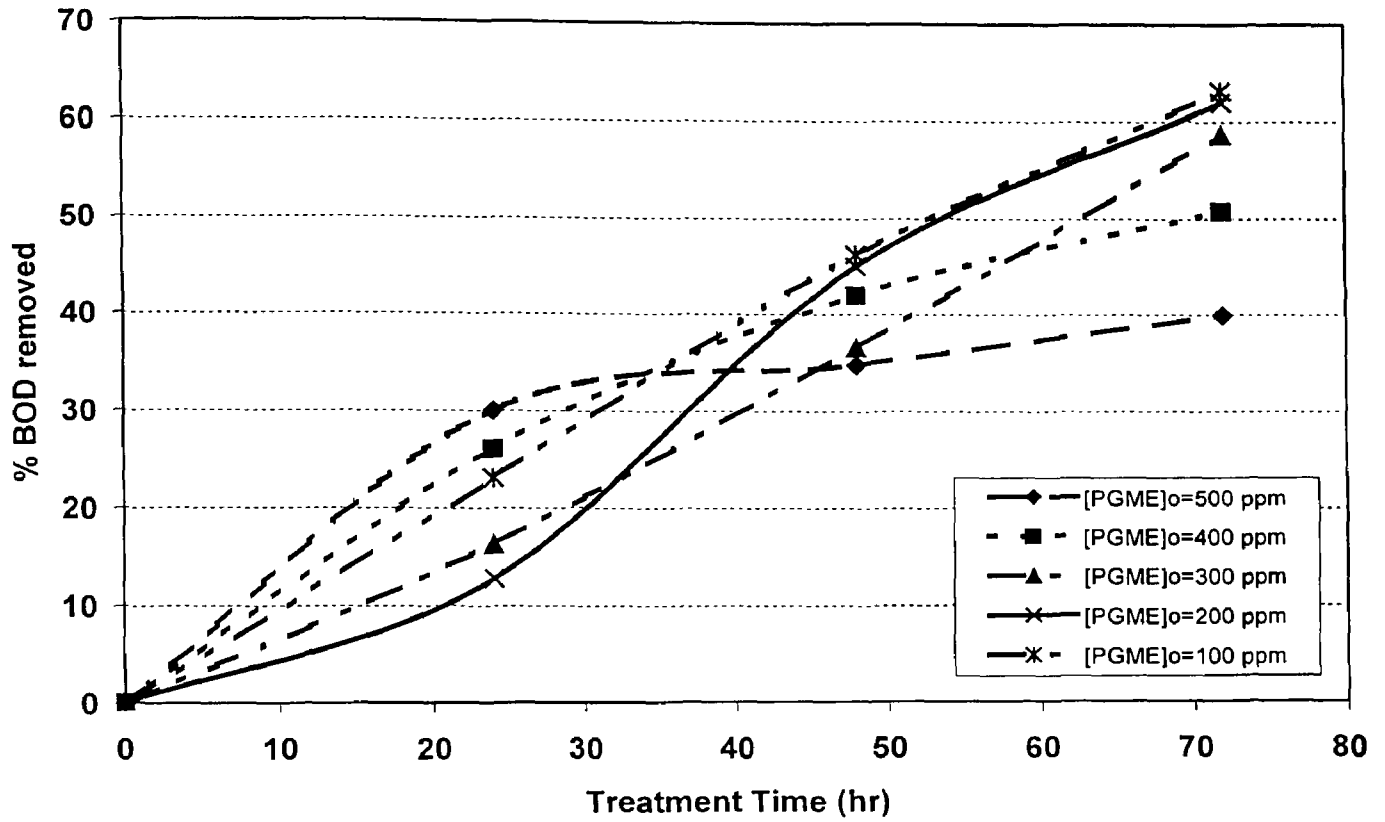
Figure 4.17: Effect of initial concentration of the PGME on the percentage BOD_5 removal at liquid flow rate of 0.551 kg/m^2.s and with the multipoint delivery distributor.
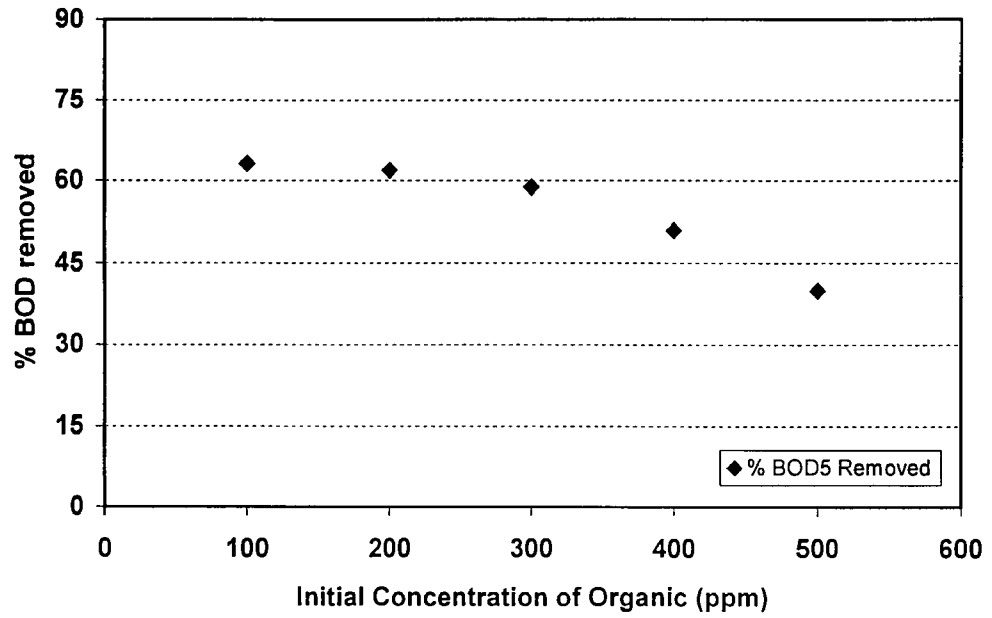
Figure 4.18: Effect of initial concentration of the PGME on the percentage BOD_5 removal after 72 hours of treatment at liquid flow rate of 0.551 kg/m^2.s with multipoint delivery distributor.
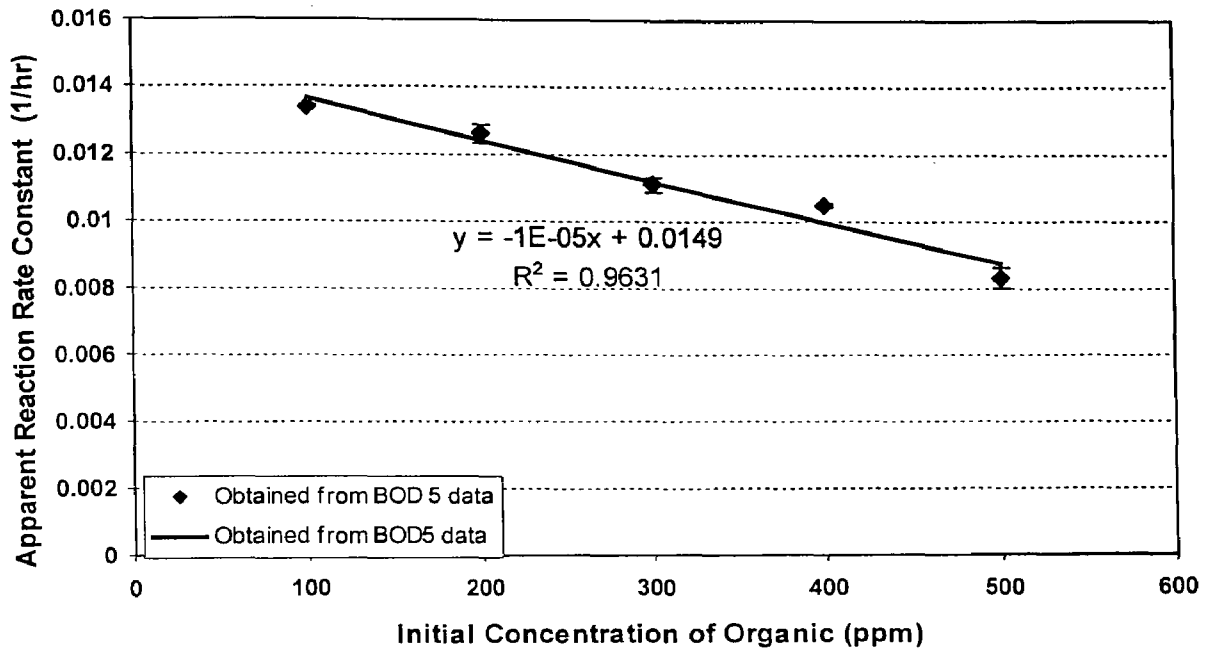
Figure 4.19: Effect of initial concentration of the PGME on the observed reaction rate constant. The treatment time was 72 hours, the flow rate was 0.551 kg/m^2.s and the multipoint delivery distributor was use.

4.4.3 Effect of Liquid Flow Rate

Experiments were carried out to study the effect of flow rate on the biodegradation of PGME in a trickle bed reactor with a constant initial PGME concentration. Five different liquid flow rates were examined, ranging from 0.184 $kg/m^2.s$ to 0.918 $kg/m^2.s$. The initial concentration of PGME was kept at 300 ppm for all runs.

Figure 4.20 depicts the reduction in BOD_5 during the 96 hours of treatment for five different liquid flow rates using the multipoint distributor. During the first 48 hours of treatment, the PGME removal was quite fast with about 75% of the BOD removal. The removal rate then decreased during the next 48-hour of treatment. At first hours of treatment, the concentration of PGME was high. Therefore, the rate of transfer of the organic from the bulk liquid to the surface of biofilm was high. Consequently, the BOD removal rate was high. After that, due to fast degradation of PGME, its concentration was reduced considerably which led to reduction in the mass transfer rate and ultimately the removal rate of PGME decreased. A similar trend was also observed with the percent of organic removal expressed in terms of COD (Figure A.3). A decrease in the removal rate of the COD with decreasing influent COD concentration has been also shown by Raj and Murthy [89-90].

It was observed that the removal of the BOD_5 did not follow any clear trend especially at the region of low removal rate, but, at the end of 96 hours of treatment, higher liquid flow rates appeared to result in a greater percentage removal. In a study on biological oxidation of PGME in an aerated packed column, Doan and Wu [127] observed similar results. The slow kinetics of the biological oxidation is possibly responsible for this observation [128]. The rate of oxygen consumption by the biological oxidation in the wastewater was much lower than the rate of oxygen transfer from the air to water in the packed column. Therefore, the oxygen content was maintained at an

adequate level for BOD reduction. Consequently, the BOD removal was not affected by the liquid flow rate [129].

Figure 4.21 depicts the effect of liquid flow rate on the percentage BOD_5 removed after 96 hours of treatment. At the liquid flow rate of 0.184 $kg/m^2.s$, the percentage BOD_5 removal was about 80%. An increase in the liquid flow rate from 0.184 $kg/m^2.s$ to 0.918 $kg.m^2.s$ resulted in marginal increase in the percentage BOD_5 removal from 80% to 85% after 96 hours of treatment. This indicates that the BOD_5 removal was affected insignificantly by the liquid flow rate over the range used in the present study. This result is in contrast with other published results. Generally, it was found that the removal percentage decreased with increasing the liquid flow rate due to the decrease in the liquid residence time inside the reactor [89-90]. In present study, the trickle bed bioreactor was run in batch mode with continuous recycle of the liquid. In this case, although for each single pass, the liquid residence time decreases with increasing the liquid flow rate, but the number of the passes increased. Thus, for all runs regardless of the applied liquid flow rate, the liquid residence time inside the reactor was in fact the same over the duration of the time.

A slight increase in percentage BOD_5 removal can be attributed to more wetted area of packings for mass transfer, attained at higher liquid flow rates. It is known that the overall microbial activity is proportional to the wetting efficiency [118]. In fact, the more packing get wet, the more biofilm is developed on it [122,129]. In section 4.2.1, it was shown that by increasing the liquid flow rate in the trickle bed bioreactor, the liquid distributed more uniformly in the bed. This in turn increased the dynamic liquid holdup. The increase of the dynamic liquid holdup, which is the wetting efficiency extent [57], was beneficial since it improved the contact of the wastewater and biofilm. Hence, the organic removal improved. The increase of the % BOD removed with the dynamic liquid holdup is shown in Figure 4.22. Furthermore, in order to clarify the effect of the liquid distribution on the organic removal rate, percentage BOD_5 removal and maldistribution coefficient versus liquid flow rate were plotted in Figure 4.23 for the bed heights of 1.4 m. The result elucidates that while the maldistribution coefficient decreases with

increasing the liquid flow rate, the percentage BOD$_5$ removal increases. At the higher liquid flow rates, where liquid distribution is more uniform and the maldistribution coefficient is comparatively lower, the higher percentage of BOD$_5$ is removed. The same experiment was also done at the bed height of the 0.7 m and the plot can be found in appendix A (Figure A.4). The variation of the maldistribution coefficient and percentage BOD$_5$ removal versus the liquid flow rate had the same trend of Figure 4.23.

In addition, Satterfield [70] has shown that the apparent reaction rate constant is proportional to liquid hold up.

$$k_p \propto k_v h \qquad (4.10)$$

The increase of reaction conversion with the liquid hold up can be clearly seen from the following empirical correlation for a first order reaction [70]

$$\ln \frac{C}{C_o} \propto \frac{-k_v h}{LHSV} \qquad (4.11)$$

where C and C_o are the organic concentration in the influent and effluent, k_p is the apparent rate constant k_v is the first order reaction rate constant, h is the liquid holdup and $LHSV$ is the volume of liquid fed to reactor per hour per volume of reactor. This explanation is consistent with the results obtained in the present study. As shown in Figure 4.24, the increase in liquid flow rate has positive effect on the apparent reaction constant due to the improvement of liquid distribution in the bed and thus, the increase of dynamic liquid holdup.
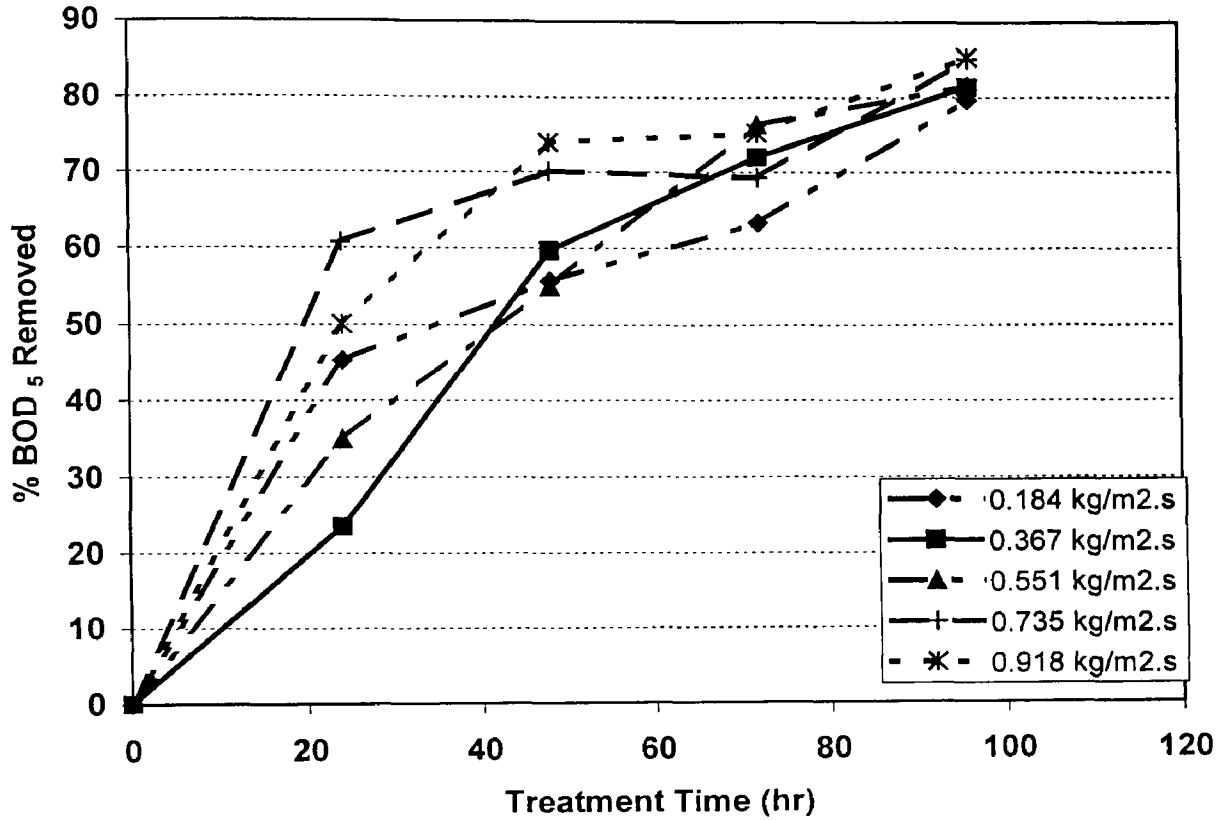
Figure 4.20: Effect of the liquid flow rate on the BOD_5 removal of the wastewater containing 300ppm $[PGME]_0$ using the multipoint delivery distributor.
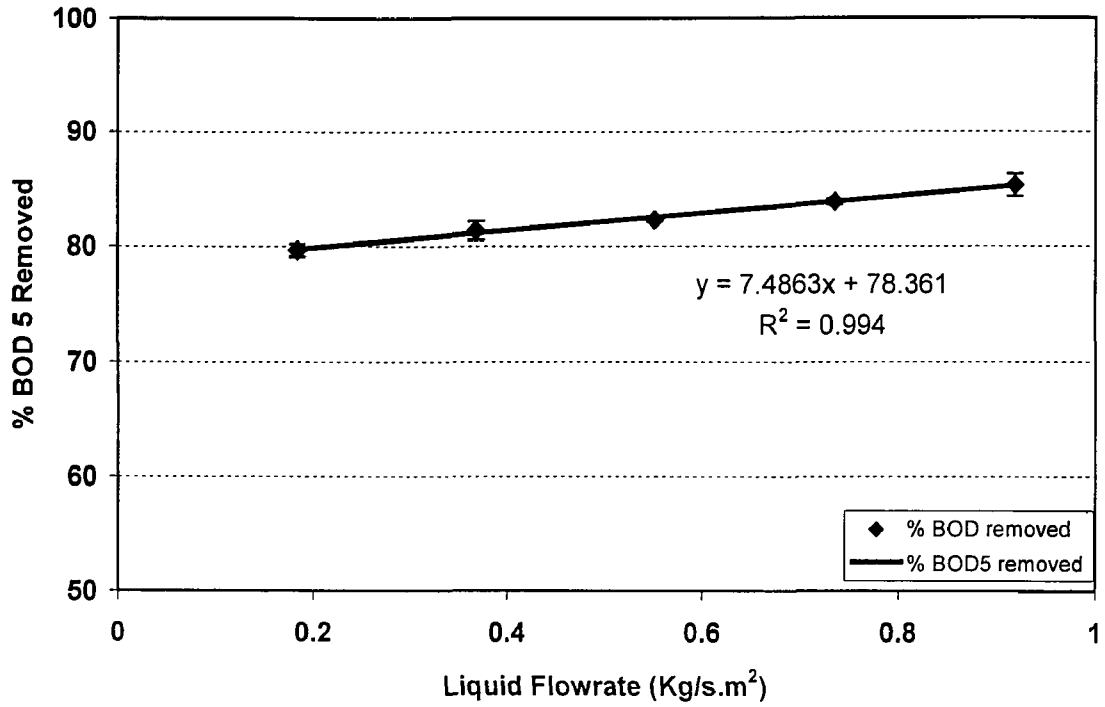
Figure 4.21: Effect of the liquid flow rate on the BOD5 removal. The data was obtained after 96 hours of treatment with 300ppm initial concentration of PGME using the multipoint delivery distributor.
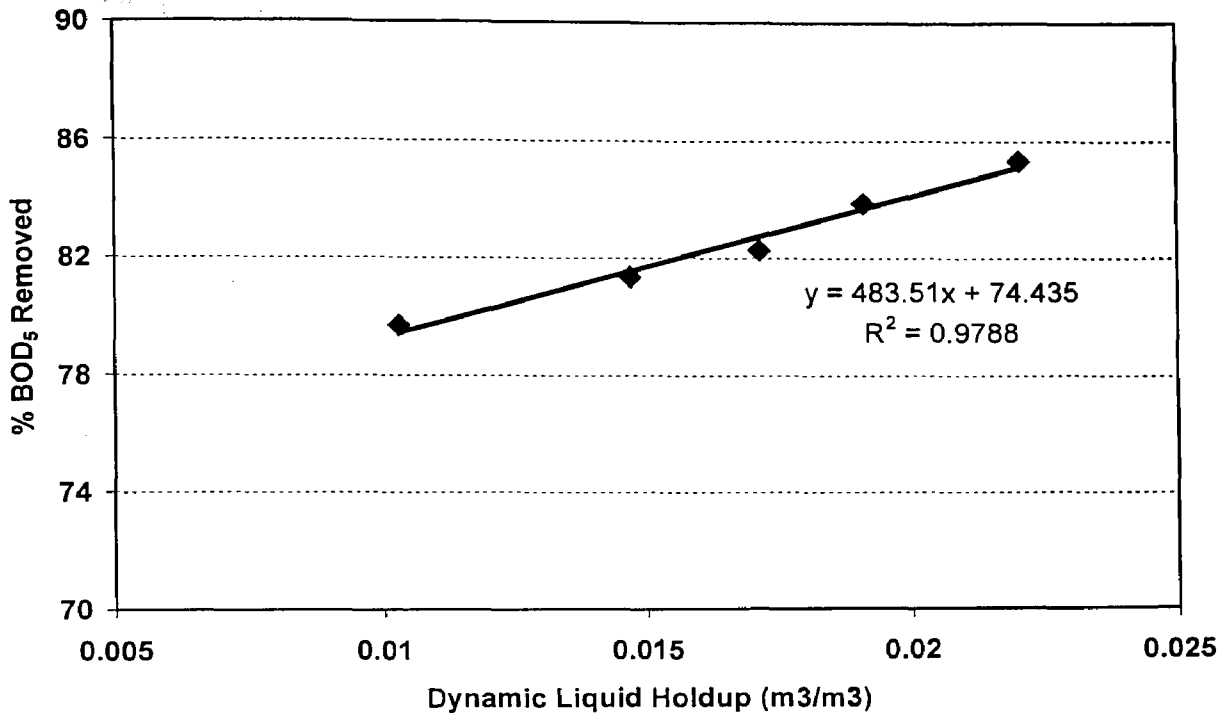
Figure 4.22: Percent BOD5 removed as a function of dynamic liquid holdup. The data were obtained at five different flow rates of 0.184, 0.367, 0.551, 0.734 and 0.918 kg/m^2.s using the multipoint distributor for bed height of 1.4m. Initial concentration of the PGME was 300 ppm and it was treated for 96 hours.
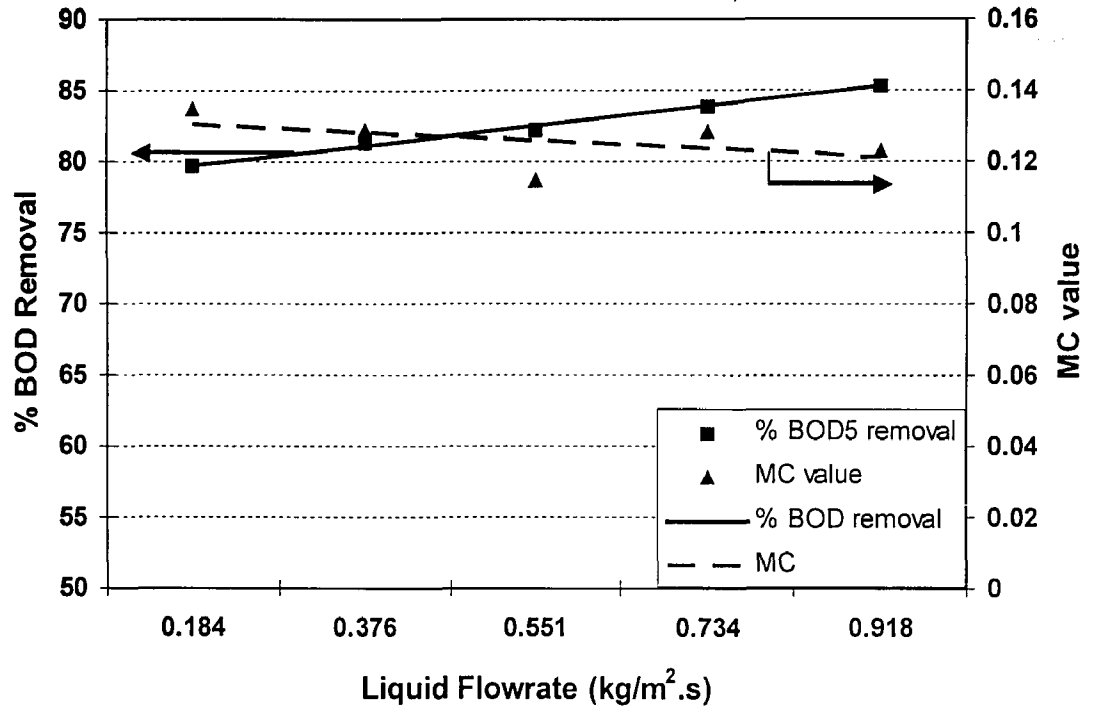
Figure 4.23: Percentage BOD$_5$ removal and maldistribution coefficient versus liquid flow rate at the bed height of 1.4 m with the use of multipoint distributor
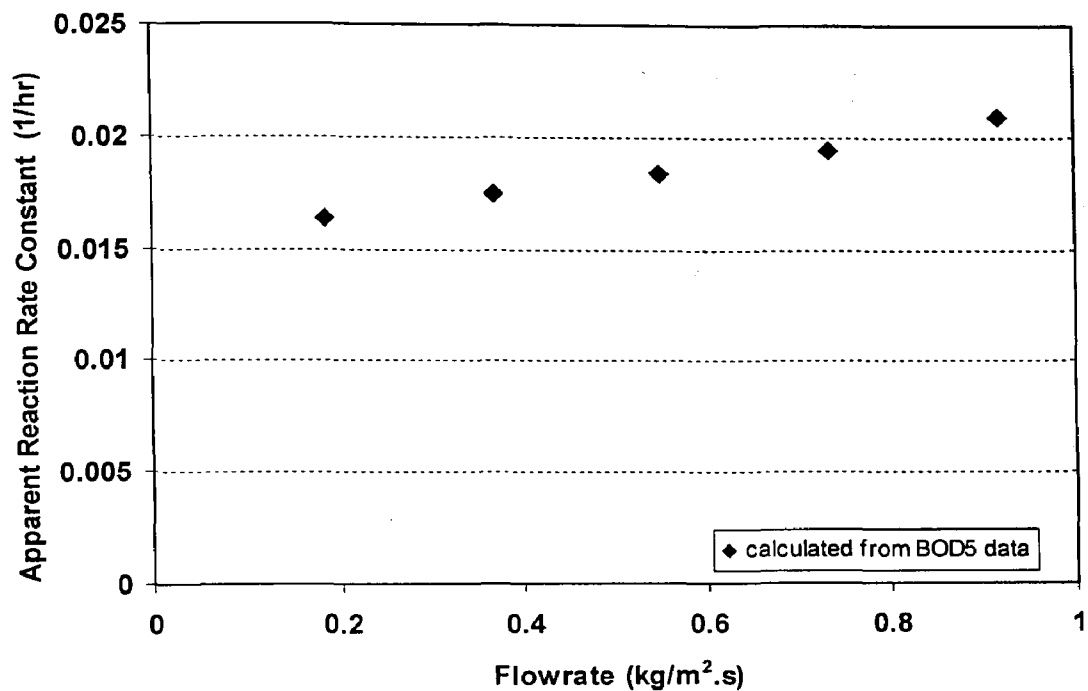
Figure 4.24: Effect of the liquid flow rate on the observed reaction rate constant. The data is obtained after 96 hours of treatment with $[PGME]_o$=300ppm using multipoint delivery distributor.

4.4.4 Effect of Initial Liquid Distribution

The effect of the initial liquid distribution on the BOD removal efficiency was investigated using two types of the liquid distributor: a single delivery point distributor and a multipoint delivery distributor. For each of the liquid distributors, the experiment was performed at three liquid flow rates of 0.184, 0.551 and 0.918 kg/m^2.s. The height of the bed and the initial PGME concentration were 1.4 m and 300 ppm respectively. The COD and BOD$_5$ concentrations were measured over a period of 72 hours for each run.

Figure 4.25 to 4.27 compares the COD profiles of the multipoint distributor and the single point distributor during 72 hours of treatment. As shown in figure 4.25, at the low liquid flow rate of 0.184 kg/m^2.s, the use of multipoint liquid distributor did not show any advantage over the single point distributor. It was previously shown that at the low liquid flow rate of 0.184 kg/m^2.s, both of the liquid distributors operate similarly. Therefore, the wetted area of the bed and consequently the amount of the organic removed at any time was equal for both types of liquid distributor used. As the liquid flow rate increased, the higher percentage of COD was removed when the multipoint distributor was used at a given time and liquid flow rate. Since at higher liquid flow rates, the multipoint distributor spread the liquid out more uniform than the single point distributor, the fraction of the packing, which was wetted, was higher than that of the single point distributor. The increase in the wetted area had a positive effect on the organic biodegradation rate via increasing the surface for mass transfer and thus, increased the percentage COD removal.

In Figure 4.28, the percentage BOD$_5$ removal is plotted as a function of liquid flow rate for both types of liquid distributors. As shown in Figure 4.28, the percentage BOD$_5$ removal improved with increasing the liquid flow rate regardless of the initial liquid distributor design. In the case of multipoint liquid distributor, the increase in the BOD removal is due to improvement of the liquid distribution by increasing liquid flow rate as elucidated in Figure 4.23. But for the single point distributor, the increase of liquid
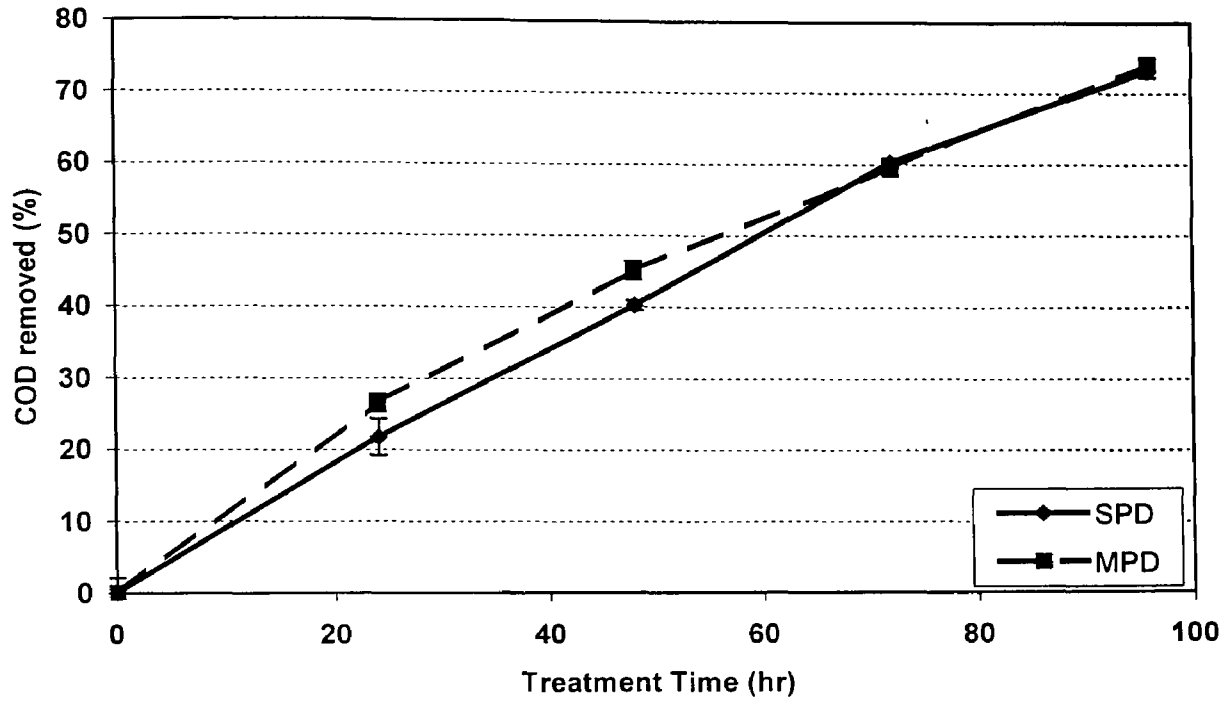
Figure 4.25: Effect of the initial liquid distribution on the COD removal at 0.184 kg/m^2.s. Treatment time was 96 hours and the initial concentration of the PGME was 300ppm.
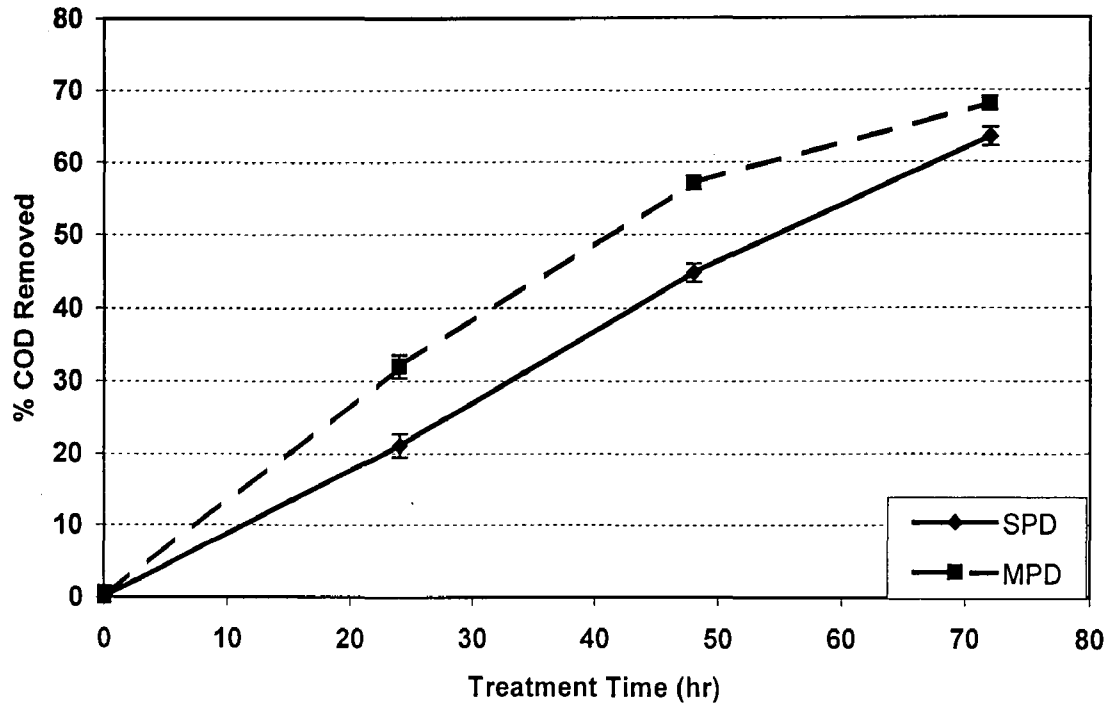
Figure 4.26: Effect of the initial liquid distribution on the COD removal at 0.551 kg/m^2.s. Treatment time was 72 hours and the initial concentration of the PGME was 300ppm.
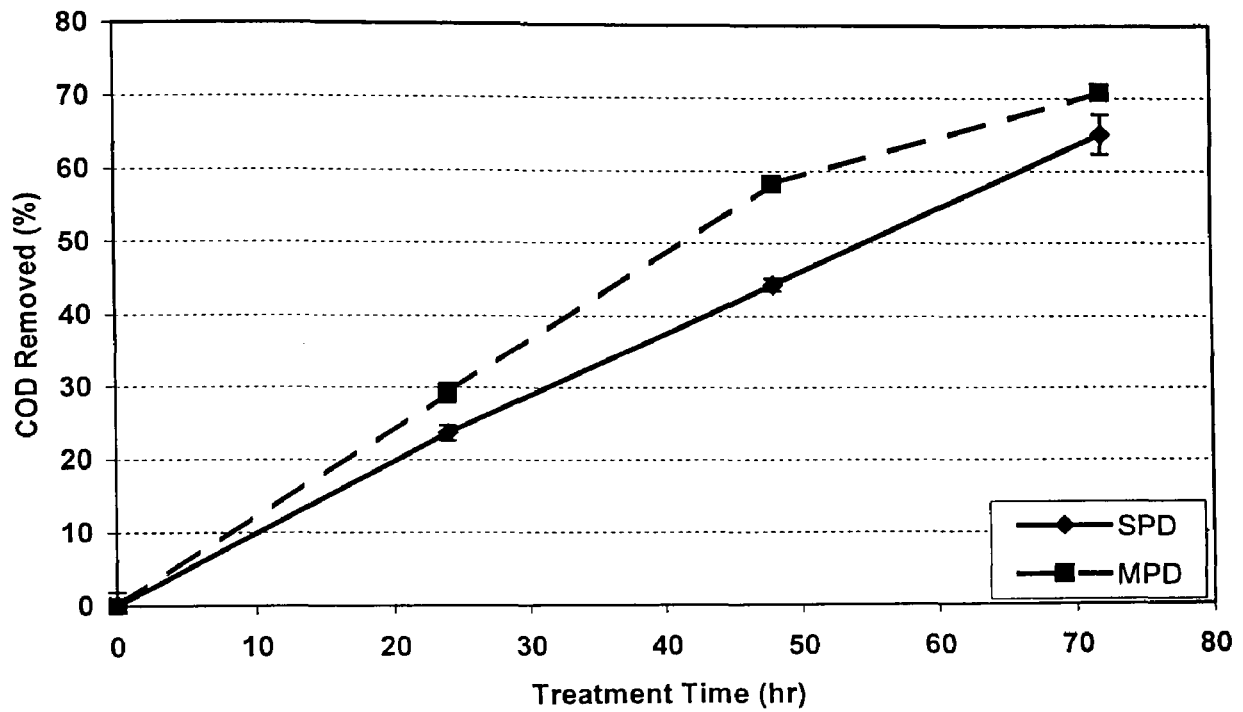
Figure 4.27: Effect of the initial liquid distribution on the COD removal at 0.918-kg/m^2.s. Treatment time was 72 hours and the initial concentration of the PGME was 300ppm.
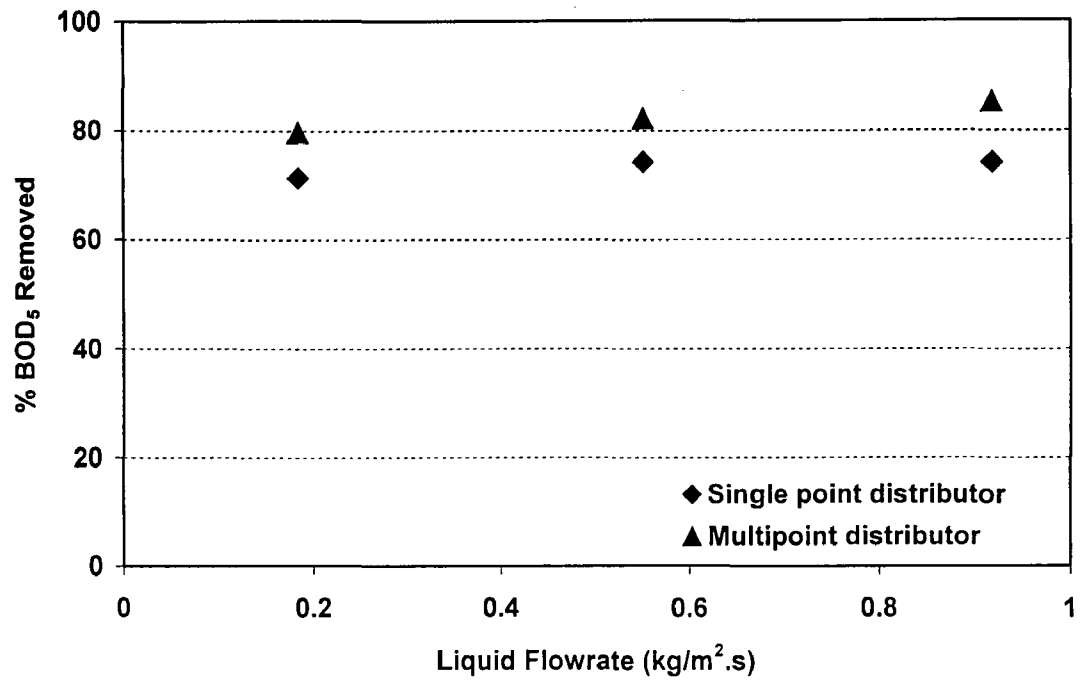
Figure 4.28: Comparison of the performance of the single delivery point distributor and multipoint distributor.
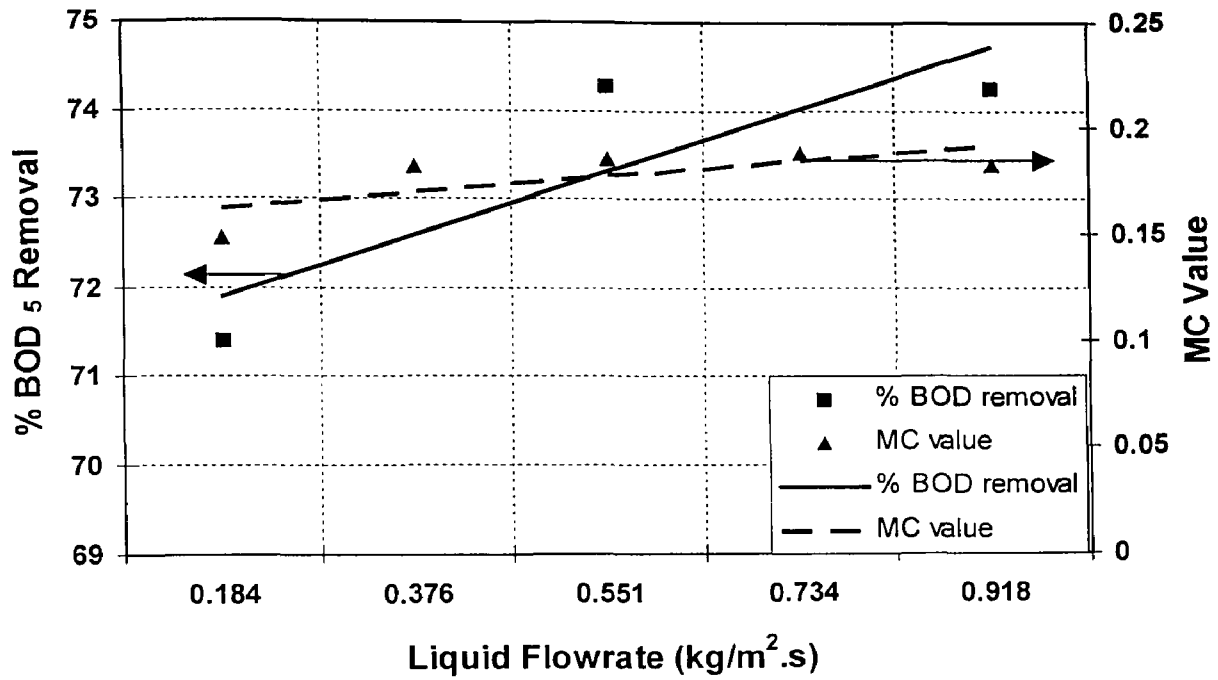
Figure 29: Percentage BOD5 removal and maldistribution coefficient versus liquid flow rate at the bed height of 1.4 m with the use of single point distributor

flow rate not only did not improve the uniformity of the liquid distribution, but also degraded it. In fact, for the single point distributor, both the maldistribution coefficient and the percentage BOD_5 removal increased with the liquid flow rate as shown in Figure 4.29. The increase of the percentage BOD_5 removal with the liquid flow rate was possibly due to the improvement of mass transfer rate by increasing the liquid flow rate [126].

4.4.5 Effect of Filter Height

The amount of BOD_5 removed over 72 hours of treatment was measured at bed heights of 0.7 m and 1.4 m under liquid flow rates of 0.184 to 0.918 $kg/m^2.s$. The obtained data are presented in Figure 4.30. The results showed that the percentage BOD_5 removal for 1.4m bed height was greater than that of the 0.7 m bed at any liquid flow rate (Figure 4.30). The improvement of the percentage BOD_5 removal with the bed height can be due to the increase of the liquid retention time in the bed when the height of bed increased. As a result, the organics has more time to contact with biomass and be removed. Many published researches have also shown that the fraction of the BOD removed is a function of the liquid retention time inside the biofilter [107, 105, 130]. Besides, Howland [131] showed that the liquid retention time is directly proportional to the depth of bed.

Furthermore, the uniformity of the liquid distribution was improved when the bed height was increased. This is also reflected in smaller maldistribution coefficient values of the taller bed compare to those of the shorter bed as shown in Figure 4.9. The better liquid distribution at the higher bed height created more wetted area for mass transfer. Therefore, the biodegradation rate increased with bed height.

Figure 4.30 also depicts that when the liquid flow rate was increased, the percentage organic removal of the shorter bed increased and approached the value of the higher bed. Indeed, at the liquid flow rate of the 0.918 $kg/m^2.s$, only 4% more organic was removed when the height of the bed increased from 0.7 to 1.4m. Whereas, at the

liquid flow rate of 0.184 kg/m^2.s , the increase of the bed height, increased the percentage organic removal by about 20%. A similar trend was observed for maldistribution coefficient values of 1.4 m and 0.7 m bed heights with increasing the liquid flow rate (Figure 4.10).

Satterfield [70] has also reported the increase in the rate of conversion with the bed height at a given liquid velocity and attributed it to the reduction in axial dispersion and the increased liquid holdup with increasing the bed height. Also, Henry and Gilbert [60] reported a similar relationship between the organic removal rate and the bed height and proposed the following correlation.

$$\ln \frac{C}{C_o} \propto \frac{-k_v H^{1/3}}{(LHSV)^{2/3}} \tag{4.12}$$

where k_v is the first order reaction rate constant per unit volume of catalyst pellet, H is the height of reactor , $LHSV$ is the volume of liquid fed to reactor per hour per volume of reactor.
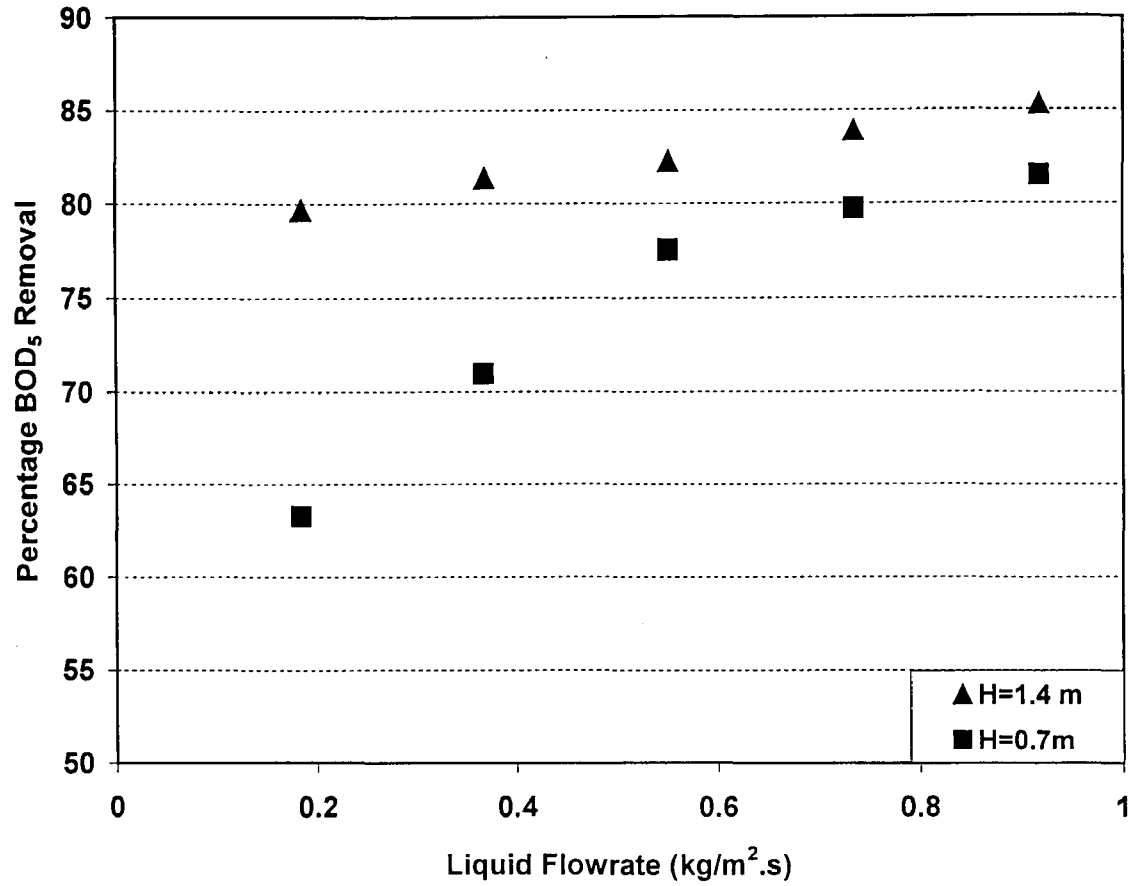
Figure 4.30: Effect of the bed height on the BOD$_5$ removal. The data was extracted after 96 hours of treatment with [PGME]$_o$ using the multipoint delivery distributor.

4.5 Effect of Liquid Distribution on Local BOD Removal

In order to determine the effect of the liquid distribution on the local BOD_5 removal a series of experiments were conducted. For this purpose, the reactor was run in continuous mode. A set of the liquid collecting cells, located at a diagonal pathway, was chosen and the rate of the liquid flowing in these cells was measured. The same samples were further analyzed for their BOD_5 and COD contents. This experiment was performed using the single point distributor at three flow rates of 0.184, 0.551 and 0.918 kg/m^2.s. The initial PGME concentration of 300 ppm was used for all runs.

The results are shown in Figures 4.31 to 4.33. The figures plot the percentage BOD_5 removed and the liquid flow rate versus radial position at a given liquid flow rate. It can be seen that, similar to the liquid distribution, the BOD removal was not uniform over the bed cross section. The regions with higher liquid flow rates corresponded to the lower BOD_5 removal, while, the percentage BOD_5 removal was relatively high at the regions with low local flow rates. In other words, the percent of BOD_5 removed was inversely proportional to the local flow rate of the wastewater in the bed.

It is well known that for a given height of the bed, the liquid retention time is an inverse function of the liquid flow rate and decreases as the liquid flow rate increases. On the other hand, the biodegradation is a slow process requiring a specific retention time of the polluted water in the bed. Accordingly, in the bed, wherever the liquid flow rate was low, due to relatively long liquid retention time, the microorganisms have more time to complete the biodegradation and the more organic was removed. However, anywhere the liquid flow rate was high, the retention time of the wastewater in the bed was short and microorganisms did not have enough time to complete the degradation. Therefore, more organic remained in the effluent.
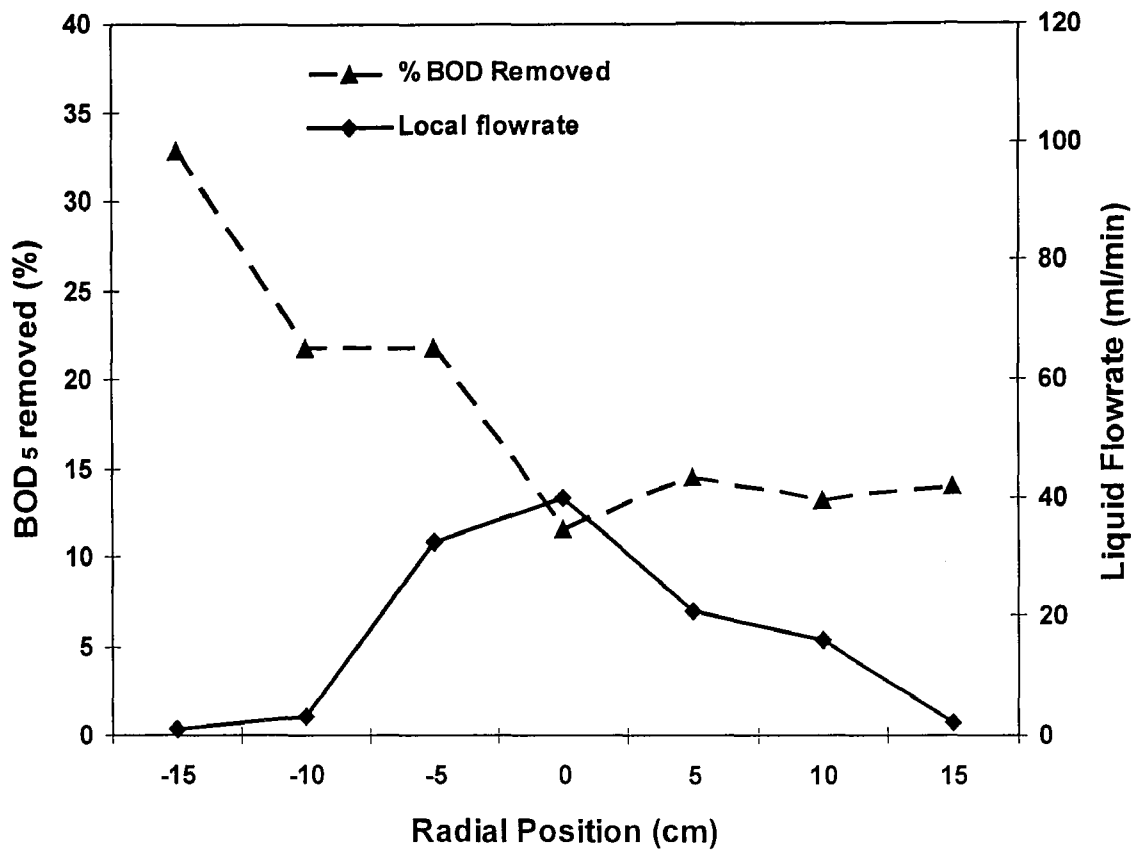
Figure 4.31: Effect of liquid distribution on the local BOD₅ removal for the single delivery point distributor with the liquid flow rate was 0.184 kg/m².s and the initial concentration of the PGME of 300 ppm.
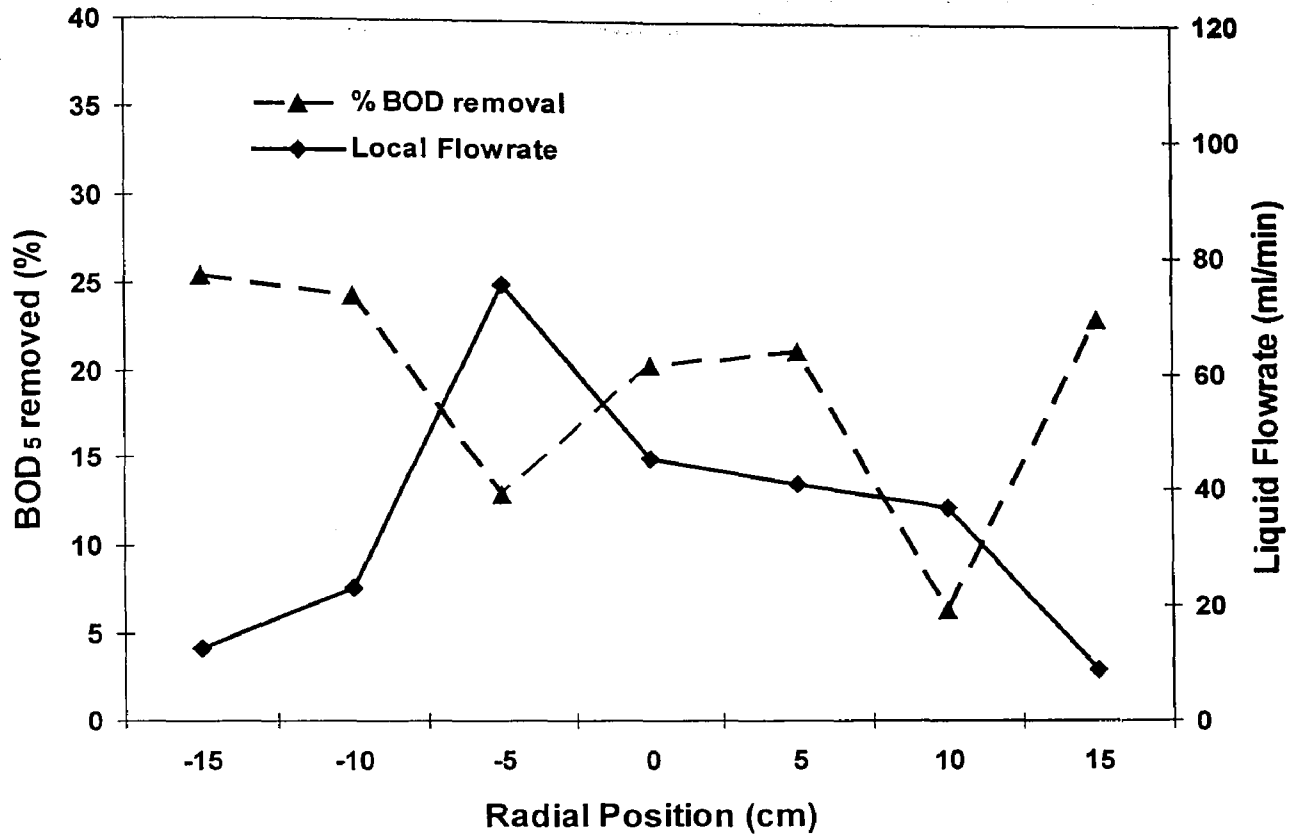
Figure 4.32: Effect of liquid distribution on the BOD₅ removal for the single delivery point distributor with the liquid flow rate was 0.551 kg/m².s and the initial concentration of the PGMEof 300 ppm.
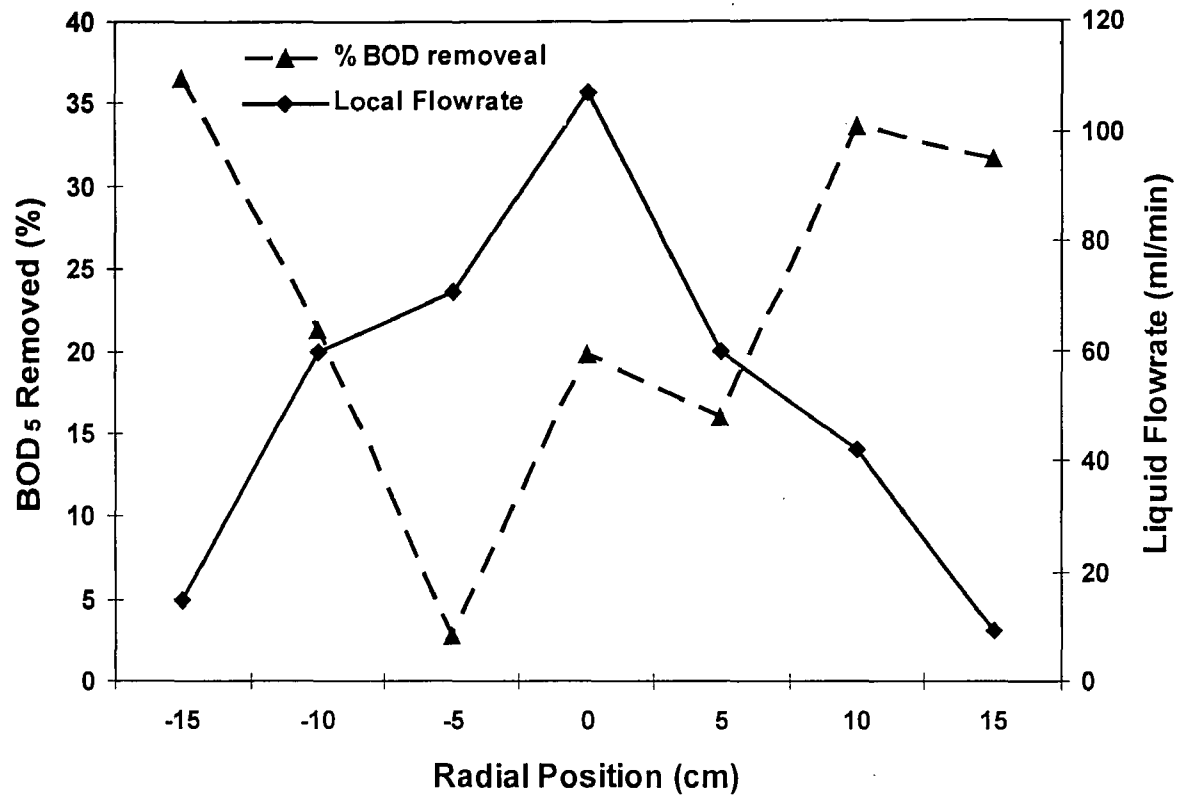
Figure 4.33: Effect of liquid distribution on the local BOD5 removal for the single delivery point distributor with the liquid flow rate was 0.918 kg/m².s and the initial concentration of the PGME of 300 ppm.

Usually, the relationship between the conversion of the substrate and the liquid retention time, which is determined based on the superficial liquid load, is expressed as [97]:

$$\frac{C}{C_o} = e^{-\kappa.H/q^n} \tag{4.13}$$

where C is the organic matter concentration in the effluent (mg/l); C_o is the organic matter concentration in the influent (mg/l); H is the filter height (m); q is the superficial liquid load (m^3/m^2.day); and κ and n are constants.

By assuming that a trickle bed reactor's column is a group of parallel columns, each one having the diameter equal to the collecting cell diameter and the height equal to the trickle bed reactor's column height, the conversion at each radial position as a function of local superficial liquid load can be estimated by the following correlation [130]:

$$\frac{C_r}{C_o} = e^{-\kappa.H/q_r^n} \tag{4.14}$$

where C_r is the organic matter concentration in the effluent (mg/l) at radius r (m), and q_r is the local superficial liquid load at r (m^3/m^2.day).

Chapter 5

Conclusion

The following conclusion could be drawn from the thesis:

- Liquid distribution affects the BOD_5 removal efficiency in trickle bed bioreactors greatly. Under the most uniform liquid distribution condition achieved in this study (with 1.4 m bed height, using multipoint distributor and 0.918 kg/m^2.s liquid flow rate) about 85% of the BOD_5 could be removed by biological oxidation in a trickle bed bioreactor after 4 days of treatment. Whereas, under poor liquid distribution condition with single point distributor and 0.7 m bed height at 0.184 kg/m2.s, only 65% of the BOD_5 was removed.

- The liquid distribution in the trickle bed bioreactor was not uniform. The uniformity of the liquid distribution was found to be affected by the liquid flow rate, the liquid distributor design, and the height of the bed.

- The uniformity of the liquid distribution affects the dynamic liquid holdup. Under more uniform liquid distribution condition, the liquid holdup was higher. Moreover, the growth of biofilm on the packing surface was found to affect the dynamic liquid holdup in the bed and increased the dynamic liquid holdup up to 32 % compare to that of clean bed.

- The biodegradation rate of the PGME in the trickle bed bioreactor followed first order reaction kinetics. The apparent biodegradation rate constant was found to be a function of the liquid flow rate, the liquid distribution design, the packed bed height and the initial organic concentration. The apparent biodegradation rate constant increased from 0.0164 to 0.0212 1/hr with the increase of the liquid flow

rate from 0.184 to 0.918 kg/m^2.s. However, it decreased from 0.0134 to 0.0083 1/hr when the initial organic concentration decreased from 100 to 500 ppm.

- Increasing the liquid flow rate resulted improved the organic removal in the continuous trickle bed bioreactor. The percentage BOD$_5$ removal increased by 6% when liquid flow rate increased from 0.184 to 0.918 kg/m^2.s.

- Increasing the initial concentration of the substrate had negative effect on the percentage BOD$_5$ removal and reduced it by 37% when the initial organic concentration increased from 100 to 500 ppm. However the amount of the 150 mg/l more BOD$_5$ was removed when the initial organic concentration increased up to 500 ppm.

- The use of multipoint distributor showed up to 12% improvement in percentage BOD$_5$ removal and 16% increases in apparent reaction rate constant at the liquid flow rate of 0.918 kg/m^2.s.

- Increases of the bed height led to the increase of in the BOD$_5$ removal efficiency, especially at low liquid flow rates. At the liquid flow rate of 0.184 kg/m^2.s, the percentage BOD$_5$ removal increased by 20 % when the bed height increased from 0.7 to 1.4m. Whereas, when the liquid flow rate was increased to 0.918 kg/m^2.s, the percentage BOD$_5$ removal was only 4% higher at the bed heights of 1.4 m than that fat the 0.7m bed height.

- The radial distribution of BOD$_5$ removal was not uniform across the bed cross-section and it was affected by the liquid flow distribution across the bed cross-section.

Chapter 6

Recommendation

Liquid flow rate and liquid distribution influences the biomass growth and sloughing. In the present study, it was assumed that the rate of growth of biomass and the rate of biomass sloughing was equal, and therefore, the biofilm thickness was constant. However, this is not true for the trickle bed bioreactot operating under high liquid flow rates since high liquid flow rates induce high shear stress that can cause higher sloughing of the biofilm. It is recommended to investigate the effect of biomass growth and sloughing on the trickle bed bioreactor performance and the BOD_5 removal efficiency under continuous operation trickle bed bioreactor.

This experiment was carried out in a pilot plant trickle filter with relatively small diameter. The similar study should be done using a real scale trickle bed bioreactor under continuous operating conditions.

In the present study, effect of liquid distribution on the organic removal was studied through dynamic liquid holdup. The dynamic liquid holdup was used as a measure of wetting efficiency under various liquid distribution conditions. For the further study, the direct measurement of wetting efficiency, instead of measuring the dynamic liquid holdup, is recommended.

References

1. Metcalf and Eddy, Wastewater Engineering: Treatment, Disposal and Reuse, 4th edition, McGraw-Hill Book Company, New York, 2002, 545-940

2. Norris, D.P., D.S. Parker, M.L. Daniels, and E.L. Owens, High rate trickling filter effluent without tertiary treatment, Water Pollution Control Fed.,1982Vol.54, No. 7, 1087 –1098

3. http://www.usace.army.mil/publications/armytm/tm5-814-3/chap12.pdf, May 24, 2004

4. Mohlman, F.W., Sewage treatment at military installation, Sewage Works Journal, Vol. 18, 1946, 789

5. Eckenfelder, W., Wesley Jr., Industrial Water Pollution Control, McGraw-Hill Book Company, New York, 3rd edition, 2000

6. Pozo, R., V. Diez, S.E. Garrido, M. Morales, and R. Osorio, Hydraulic distribution effect on a real-scale trickling filter, Environmental Engineering Science, Vol. 19, No. 3, 2002,151-157

7. Crine, M., M. Schlitz, and L. Vandevenne, Evaluation of the performance of random plastic media in aerobic trickling filters, Water Science and Technology, Vol.22, No.1/2, 227-238,1990

8. Wen, X., Y. Shu, K. Nandakumar, and K. T. Chuang, Predicting liquid flow profile in randomly packed beds from computer simulation, AIChE Journal, Vol. 47, No. 8, 2001, 1770-1778.

9. Vergel Hernandez, C. A., J. P. Euzen, P. Trambouze, and J. P. Wauquier, Two phase flow catalytic reactor, influence of hydrodynamics on selectivity, Chemical Engineering Science, Vol. 50, 1995, 3303-3312.

10. Marcandelli, C., A.S. Lamine, J.R. Bernard, and G. Wild, Liquid distribution in trickle bed reactor. Oil and Gas Science and Technology, Vol. 55, No. 4, 2000, 407-415.

11. Al- Samadi, R. A., C. M. Gordon, M. E. Fayed, and M. A. Leva, A study of liquid distribution in an industrial scale packed tower. Paper presented at A.I.Ch.E. Spring National Meeting, Houston, Texas, U.S.A. April 3, 1989.

12. Williams, R. A. and C. G. Xie, Tomographic techniques for characterizing particulate processes, Particle & Particle Systems Characterization: Measurement and Description of Particle Properties and Behavior in Powders and other Disperse Systems. Vol. 10, 1993, 252-261.

13. Beck, M. S., T. Dyakowski, and R. A. Williams, Process tomography- the state of the art, Proc. Frontiers in Industrial Process Tomography II, Delft, The Netherlands, 1997, 357-362.

14. Chaouki, J. F., F. Larachi, and M. P. Dudukovic, Noninvasive tomographic and velocimetric monitoring of multiphase flows, Industrial & Engineering Chemistry Research, Vol. 36, 1997, 4476-4503.

15. Reinecke, N., G. Petritsch, D. Schmitz, and D. Mewes, Tomographic measurement techniques-visualization of multiphase flows, Chemical Engineering & Technology, Vol. 21, 1998, 7-18.

16. Zuiderweg, F. J., J. G. Kunesh, and D. W. King, A model for the calculation of the effect of maldistribution on the efficiency of a packed column, Chemical Engineering Research & Design, Vol. 71, part A, 1993, 138-44.

17. Zuiderweg, F. J. and P. J. Hoek, The effect of small-scale liquid maldistribution (natural flow) on the separating efficiency of random packings, I. Chem. E. Symposium Series No. 104, B247-B254.

18. Sundaresan, S., Liquid distribution in trickle-bed reactors, Energy and Fuels, Vol. 8, 1994, 531-535.

19. Hoek, P. J., J. A. Wesselingh, and F. J. Zuiderweg, Small-scale and large-scale liquid maldistribution in packed columns, Chemical Engineering Research & Design, Vol. 64, November 1986, 431-449.

20. Wang, Y., Z. Mao, and J. Chen, Scale and variance of radial liquid maldistribution in trickle bed, Chemical Engineer Science, Vol. 53, No. 6, 1998, 1153-1162.

21. Moller, L. B., C. Halken, J. A. Hansen, and J. Bartholdy. Liquid and gas distribution in trickle bed reactors, Industrial & Engineering Chemistry Research. Vol.35, 1996, 926-930.

22. Perry, D., D. E. Nutter, and A. Hale. Liquid distribution for optimum packing performance. Chemical Engineering Progress, January 1990. 30-35.

23. Kan, K. M. and P. F. Greenfield, Multiple hydrodynamic states in cocurrent two-phase down flow through packed beds, Industrial & Engineering Chemistry, Process Design and Development. Vol. 17, No. 4, 1978, 482-485.

24. Koros, R. M., Engineering aspects of trickling bed reactors. In chemical engineering reactor design and technology, Delasa, H., Eds., Martinus Nijhoff: Dordrecht, The Netherlands, 1986, 579-630.

25. Albright, M. A., Packed tower distributors tested, Hydrocarbon Processing, Vol. 63, 1984, 173-177.

26. Kundu, A., A. K. Saroha, and K. D. P. Nigam. Liquid distribution studies in trickle-bed reactors. Chemical Engineering Science, Vol. 56, 2001. 5963-5967

27. Gotz, J., K. Zick, C. Heinen, and T. Konig. Visualization of flow processes in packed beds with NMR imaging: determination of local porosity, velocity vector and local dispersion coefficient. Chemical Engineering and Processing, Vol. 41, 2002. 611-629.

28. Kunjummen, B., T. S. Prasad, and P. S. T. Sai. Radial liquid distribution in gas-liquid concurrent downflow through packed beds. Bioprocess Engineering, Vol. 22, 2000. 471-475.

29. Chila, Z. and O. Schmidt, A Study of the flow of liquid when freely trickling over the packing in cylindrical tower, Coll. Czech. Chem. Commun., Vol. 22, 1957, 896-905.

30. Farid, M. M., and D. J. Gunn. Liquid distribution and redistribution in packed columns- II. Chemical Engineering Science, Vol. 33, 1978, 1221-1231.

31. Song, M., F. H. Yin, K. T. Chung, and K. Nandakumar, A stochastic model for the simulation of the natural flow in random packed columns, Canadian Journal of Chemical Engineering, Vol. 76, 1998, 183-189.

32. Bey, O., and G. Eigenberger. Fluid flow through catalyst filled tubes. Chemical Engineering Science, Vol. 52, No. 8, 1997. 1365-1376.

33. Brinkman, H. C., A calculation of the viscous force extracted by a flowing flowed on a dense swarm of particles, Applied Scientific Research, A1, 1947, 27.

34. Subaygo, N. Standish, and G. A. Brooks. A new model of velocity distribution of single fluid flowing in packed beds. Chemical Engineering Science, Vol. 53, 1998, 1375-1385.

35. Jiang, Y., M.R. Khadilkad, M. H. Al-Dahhan, and M. P. Dudukovic. Tow-phase flow distribution in 2D trickle-bed reactors. Chemical Engineering Science, Vol. 54, 1999. 2409-2419.

36. Zimmerman, S. P. and K. M. Ng, Liquid distribution in trickling flow trickle-bed reactors, Chemical Engineering Science, Vol. 41, No. 4, 1968, 861-866.

37. Weimann, M., Porter, K. E., and M. C. Jones, A theoretical prediction of liquid distribution in a packed column with wall effect, Trans. Instn. Chem. Engrs, Vol.41, 1963, 240-247.

38. Gunn, D. J. Liquid distribution and redistribution in packed columns-I. Chemical Engineering Science, Vol. 33, 1978, 1211-1219.

39. Backer, T., T. H. Chilton, and H. C. Vernon. The course of liquid flow in packed towers, Trans. Am. Inst. Chem. Engrs. Vol. 31, 1935, 269-274.

40. Porter, K. E., and J. J. Templeman. Liquid flow in packed columns-Part III: wall flow. Trans. Instn Chem. Engrs, Vol. 46, 1968, T86-T94.

41. Prchik, J., J. Soukup, V. Zapletal, and V. Ruzicka, Liquid distribution in reactors with randomly packed porouse beds, Coll. Czech. Chem. Cimmun., Vol. 42, 1975, 845

42. Herskowitz, M. and J. M.mith, Liquid distribution in trickle bed reactors, Part I: flow measurement, AIChE Journal, Vol. 24, 1978, 450-454.

43. Al- Dahhan, M., and M. P. Duducovic, Pressure drop and liquid holdup in high pressure trickle bed reactors, Chemical Engineering Science, Vol. 49, 1994, 5681-5698.

44. Hanley, B. The influence of flow maldistribution on the performance of columns containing random packings: a model study for constant relative volatility and total reflux. Separation and Purification Technology, Vol. 16, 1999. 7-23.

45. Mcwhirter, J. D., M. E. Crawford, and D. Klein. Wall region porosity distribution for packed beds of uniform spheres with modified and unmodified walls, Transport in Porous Media, Vol. 27, 1997. 99-118.

46. Ng, K.M., and C.F. Chu, Trickle bed reactors, Chemical Engineering Progress, 1987, 55-63.

47. Tsochatzidis, N. A., A. J. Karabelas, D. Giakoumakis, and G. A. Huff. An investigation of liquid maldistribution in trickle beds, Chemical Engineering Science, Vol. 57, 2002. 3543-3555.

48. Saroha, A. K., and K. D. P. Nigam. Trickle bed reactors, Reviews in Chemical Engineering, Vol. 12, 1996, 207-347.

49. Doan, H. D., and M. E. Fayed. A study of liquid distribution in a packed bed of ceramic Intalox saddles and super-levapak, Proceedings The First Minia International Conference for Advanced Trends in Engineering, Minia, Egypt, March 14-16, 1999.

50. Seader, J. D., and E. J. Henley. Separation process principles, John Wiley & Sons, Inc., New York, U.S.A. 1998. 325-346.

51. M. Weimann, Beihefte zu den Zeits. Ver. Deut. Chem. No.6, Abstract in Chem. Fabr, 1933, 411.

52. Kouri, R. J., and J. Sohlo, Liquid and gas flow patterns in random packing, Chem. Eng. J. Vol. 61, 1996, 95-105.

53. Song, M., F. H. Yin, K. Nandakumar, and K. T. Chuang. A three –dimensional model for simulating the maldistribution of liquid flow in random packed beds, The Canadian Journal of Chemical Engineering, Vol. 76, April, 1998, 161-166.

54. Leva, M., Effect of liquid distribution on absorption performance of randomly dumped tower packings. Paper presented at A.I.Ch.E. Spring National Meeting, Orlando, Florida, U.S.A. March 18-22, 1990.

55.   de Klerk, A., Liquid holdup in packed beds at low mass flux, AICHE Journal, Vol. 49, No. 6, 2003, 1597-1600.

56.   Specchia, V. and G. Baldi, Pressure drop and liquid holdup for two phase concurrent flow in packed beds, Chemical Engineering Science, Vol. 32, 1977, 515.

57.   Alicilar, A., A. Bicer and A. Murathan, The relation between wetting efficiency and liquid holdup in packed columns, Chemical Engineering Communications, Vol.128, 1994, 95-107.

58.   Burghardt A., A. S. Kolodziej and M. Jaroszynski, Experimental studies of liquid –solid wetting efficiency in trickle-bed cocurrent reactors. Chemical Engineering and Processing, Vol. 28, No. 1, 1990, 35-49.

59.   Mills, P. L. and M. P. Duducovic, Evaluation of liquid solid contacting in trickle bed reactors by tracer methods, AICHE Journal, Vol. 27, 1981, 893-904.

60.   Ramachanddran, P. A. and R. V. Chaudhari, Three phase catalytic reactors, Gordon and Breach Science Publishers, NY, 1983.

61.   Piche, S., I. Iliute, B. P. A. Grandjean, and F. Larachi, A unified approach to the hydraulics and mass transfer in randomly packed towers. Chemical Engineering Science, 2001, 56, 6003-6013

62.   Ellenberger, J. and R. Krishna. Counter-current operating of structured catalytically packed distillation columns: pressure drop, holdup and mixing. Chemical Engineering and Science, Vol. 54, 1999, 1339-1345.

63.   Toye, D., P. Marchot, M. Crine, A. M. Pelsser, and G. L'Homme. Local measurement of void fraction and liquid holdup in packed columns using X-ray computed tomography, Chemical Engineering and Processing, Vol. 37, 1998, 511-520.

64.   Elgin, J. C., and F. B. Weiss. Liquid holdup and flooding in packed towers, Industrial Engineering and Chemistry, Vol. 31, 1939, 435-445.

65.   Pironti, F., D. Mizrahi, A. Acosta and D. Gonzalea-Mendizabal, Liquid –solid wetting factor in trickling reactors: its determination by a physical method, Chemical Engineering Science, Vol. 54, 1999, 3793-3800.

66.   Fukushima S., and K. Kusaka. Gas-liquid mass transfer and hydrodynamic flow region in packed columns with cocurrent upward flow, Journal of chemical Engineering of Japan, Vol. 12, No. 4, 1979. 296-301.

67.   Yin, F., A. Afacan, k. Nandakumar, k. T. Chuang. Liquid holdup distribution in packed columns: gamma ray tomography and CFD simulation, Chemical Engineering and Processing, Vol. 42, 2002, 473-483.

68.   Tsochatzidis, N.A., A.J. Karabelas, D. Giakoumakis, G.A. Huff, An investigation of liquid maldistribution in trickle beds, Chemical Engineering Science, Vol.57, No. 17, 2002, 3543-3555.

69.   Luciana, Y., D. Gonzalez-Mendizabal, and F. Pironti, Trickle bed wetting factors from pressure drop and liquid holdup measurements, Chem. Eng. Comm., Vol. 189, 2002, 1653-1670.

70.   Satterfield,C. N., Trickle-bed reactors, AIChE J., 1975, 21,209-228

71.   Colombo, A. J., G. Baldi and S. Sicardi, Solid-liquid contacting effectiveness in trickle bed reactors, Chemical Engineering science, Vol. 31, No. 12, 1976, 1101-1108.

72.   Schwartz, J. G., E. Weger and M. P. Duducovic, A new tracer method for determination of liquid solid contacting efficiency in trickle bed reactors, AIChE Journal, Vol. 22, 1976, 894.

73.   Dudukovic, M.P., Catalyst effectiveness factor and contacting efficiency in trickle bed reactors, AICHE Journal, Vol. 23, 1977, 940.

74.   Lakota, A., and J. Levec, Solid liquid mass transfer in packed beds with cocurrent downward two-phase flow. AICHE Journal, Vol.36, No.9, 1990, 1444-1448.

75.   Burghardt, A., A. S. Kolodziej And M. Jaroszynski, Experimental studies on liquid solid wetting efficiency in trickle bed cocurrent reactors, Chemical Engineering Process, Vol.28, 1990, 35-49.

76.   Ring, Z. E. and R. W. Missen, Trickle bed reactors, tracer study of liquid holdup and wetting efficiency at high temperature and pressure, Canadian Journal of Chemical Engineering, Vol.69, 1991, 1016-1020.

77. Herskowitz, M. and S. Mosseri, Global rates of reaction in trickle bed reactors: effects of gas and liquid flow rates. Ind. Eng. Chem., Fundam., Vol. 22, 1983, 4-6.

78. Leung P. C., F. Recasens and J. M. Smith, Hydration of isobutene in a trickle bed reactor: wetting efficiency and mass transfer, AIChE J., 1987, 33, 996-1007.

79. Larachi, F., L. Belfares and B. P. A. Grandjean, Prediction of liquid solid wetting efficiency in trickling flow reactors, Int. Comm. Heat Mass Transfer, Vol. 28, No. 5,2001, 595-603.

80. Alexandria, Va., Design of municipal wastewater treatment plants, Water Environment Federation, 4th edition. 1998.

81. Wik, T. and C. Lindeborg, Modeling the dynamics of a trickling filter for wastewater treatment, IEEE Conference on Control Applications - Proceedings, Vol. 2, 1994, 1035-1040.

82. Bruce, A. M., and J. C. Merkens, Recent study of high rate biological filtration, Water Pollution Control, 1970, vol. 72, pp 499-523.

83. Bruce, A. M., and J. C. Merkens, Further studies of partial treatment of sewage by high-rate biological filtration, Journal Institute Water Pollution Control (G.B) Vol. 72, no. 5, 449

84. Richards, T. and D. Reinhart, Evaluation of plastic media in trickling filters, Water pollution Control Federation, Vol. 58, No. 7, 1986, 896-902.

85. Logan, B.E., S.W. Hermanowicz and D.S. Parker, A fundamental model for trickling filter process design, Water Pollution Control Federation, Vol.59, No.12, 1987, 1029-1041.

86. Sarner, E., Removal of particulate and dissolved organics in aerobic fixed film biological process, Water Pollution Control Federation, Vol.58, No. 2, 1986, 165-172.

87. Tekerlekopoulou, A.G. and D.V. Vayenas, Operational and design consideration of a trickling filter for ammonia removal from potable water, Environmental Modeling and Assessment, Vol. 8, 2003, 55

88. Schulze, K.L., Load and efficiency of trickling filters, Water Pollution Control Federation, Vol.32, No. 3, 1960, 245.

89. Raj, S.A. and D.V.S. Murthy, Comparison of the trickling filter models for the treatment of synthetic dairy wastewater, Bioprocess Engineering, Vol. 21, 1999, 51-55.

90. Raj, S.A. and D.V.S. Murthy, Synthetic dairy wastewater treatment using cross flow medium trickling filter, Journal of Environmental Science and Health, Vol. A34, no. 2, 1999,357-369.

91. Randall, A.A., J. Sullivan and J. Dietz, Journal of the Environmental Engineering Division, Vol. 123, No.11, 1997, 1072

92. Germain, J.E., Economical treatment of domestic waste by plastic medium trickling filters, Water Pollution Control Federation, Vol.38, No. 2, 1966, 192-203.

93. Vayenas, D.V., S. Pavlou and G. Lyberatos, Development of a dynamic model describing nitrification and nitrification in trickling filters, Water Research, Vol. 31, No. 5, 1997, 1135-1147.

94. Velz, C. J. a basic law for performance of biological filter, sewage work journal, Vol. 20, 1948, 607.

95. Howland, W. F. Flow over porous media as in Trickling filter, Proc. 12th Ind. Waste Conf., Purdue Univ, 1957, 435

96. Dicks, R. and S. Ottengraf, Verification studies of a simplified model for removal of dichloromethane from waste gases using biological trickling filter, Bioprocess Engineering, Vol. 6, 1991, 131.

97. Parker, D., M. Lutz, B. Andersson and H. Aspegren, Effect of operating variables on nitrification rates in trickling filters, Water Environment Research, Vol. 6, No. 7, 1995, 1111-1118.

98. Parker, D.S., and T. Richards, Nitrification in trickling filters, Water Pollution Control Federation, Vol.58, No. 9, 1986, 896-902.

99. Bosco, F., B. Ruggeri, and G. Sassi, Performances of a trickle bed reactor for exoenzymes production by Phanerochaete chrysosporium: influence of

superficial liquid velocity, Chemical Engineering Science, Vol. 54, 1999, 3163-3169.

100.   Lunan, W.E., C. Harden and K. Krupa, Pilot trials of a trickling filter for treatment of effluent from a newsprint mill, International Environmental Conference Proceeding, 1995, 241-247.

101.   Logan, B.E., S.W. Hermanowicz and D.S. Parker, Engineering implication of a new trickling filter model. Water Pollution Control Federation, Vol.59, No. 12, 1987, 1017-1028.

102.   Williamson, K. and P.L. McCarty, A model for substrate utilization by bacterial films, Water Pollution Control Federation, Vol. 48, 1976, 9.

103.   Parker, D. S., Research needs for trickling filter design: a consultant's perspective, Proc. 2nd international conf, Fixed Film Biol. Processes, Arlungton, 1984, 1155-1166

104.   Logan, B.E., S.W. Hermanowicz and D.S. Parker, A fundamental model for trickling filter process design, Water Pollution Control Federation, Vol.59, No.12, 1987, 1029-1042.

105.   Gullick, H.A. and J.L. Cleasby, Cold climate nitrification biofilters: design and operation consideration, Water Pollution Control Federation, Vol.62, 1994, 50-57.

106.   Gullick, H.A. and J.L. Cleasby, Nitrification performance of a pilot-scale trickling filter, Water Pollution Control Federation, Vol.62, 1994, 40-49.

107.   Balakrishnan, S., W.W. Eckenfelder, and c. Brown, Organics removal by a selected trickling filter media, Water and Wastewater Engineering/ Industrial, A-22 - A25.

108.   Olujic, Z. and de Graauw, J., Experimental studies on the interaction between the initial liquid distribution and the performance of structured packings, Separation Science and Technology, Vol. 25, No. 13-15, 1990, 1723-1735

109.   Sant' Anna, G., H. Roques, K. T. Nyadziehe and R. Ben Aim, Hydrodynamics of plastic media trickling filters, Environmental Technology Letters, Vol. 3, 1982, 395-404

110. Standard methods for the examination of water and wastewater, 20th ed., APHA, AWWA, New York, 1998

111. Taylor, J.R., An introduction to error analysis, 2nd edition, University Science Books, Sausalito, California, 1997.

112. McGreavy, C., E. A. Foumeny, and K. H. Javed, Characterization of transport properties for fixed bed in terms of local bed structure and flow distribution. Chemical Engineering Science, Vol. 41, 1986, 787-797.

113. Ziolkowska, I. And D. Ziolkowski, Modeling of gas interstitial velocity radial distribution over a cross section of a tube packed with a granular catalyst bed. Chemical Engineering Science, No.48, 1993, 3283-3292.

114. Scott, A. H., Liquid distribution in packed towers, Transactions Institution of Chemical Engineers, 1935, 211-217

115. Sederman, A. J. and L. F. Gladden, Magnetic resonance imaging as a quantitative probe of gas-liquid distribution and wetting efficiency in trickle-bed reactors Chemical Engineering Science, 56, (2001), 2615-2628.

116. Billet, R., Prediction of mass transfer columns with dumped and arranged packing, Trans. IchemE, 77, Part A,498,1999.

117. Atkinson, B. and M. E. Abdel Rahman Ali, The effectiveness of biomass holdup and packing surface in trickling filters, Water Research, Vol. 12, 1978, 147-156.

118. Lekhlif, B., D. Toy, P. Marchot and M. Crine, Interaction between the biofilm growth and hydrodynamics in a aerobic trickling filter, Water Science and Technology, Vol. 22, No. 10-11, 1994, 423-430

119. Hinton, S. W. and H. D. Stensel, Experimental observation of trickling filter hydrodynamics, Water Research, Vol. 25, No.11, 1991, 1389-1398.

120. Hosono, Y. and H. Kubita, Characteristic evaluation of trickling filter process, Water Research, Vol. 14, 1980, 581-590.

121. Asku, Z. and G. Bulbul, Investigation of the combined effects of external mass transfer and biodegradation rates on phenol removal using immobilized *P. putida* in a packed bed column reactor, Enzyme Microb. Technol., Vol.22, April 1998, 397-403.

122. Atkinson, B. and M. E. Abdel Rahman Ali, Wetted area, slim thikness and liquid phase mass transfer on packed bed biological film reactors (trickling filters) Transactions of the Institution of Chemical Engineers, Vol. 54, No. 4, 1976, 239-250.

123. LaMotta, E.J., Internal diffusion and reaction in biological films, Environmental Science and Technology, Vol. 10, No. 8, August 1976, 765-769.

124. Lunan, W.E., C. Harden, K. Kupa, Pilot trials of a trickling filter treatment of effluent from newsprint mill, International Environmental Conference, Exhibit, and Short Course, Vol. 1, 1995, 241-247.

125. Perry, R. H. Maloney. J. O., Green D. W., Perry's Chemical engineers handbook, McGraw-Hill, New York, 6th edition, 1984.

126. Bishop, P. L., J. T. Gibbs and B. E. Cunningham, Relationship between concentration and hydrodynamic boundary layers over biofilm, Environtal Technology, Vol.18, 1997,375-386.

127. Doan, H. and J. Wu, Biological treatment of wastewater from polymer coating process, Journal of Chemical Technology and Biotechnology, Vol. 77, No. 9, 2002, 1076-1083.

128. Mitzakov, R., Combined electrochemical and biological treatment of industrial wastewater using porous electrodes and packed bed aerator, Masters thesis, Ryerson University, Department of Chemical Engineering, Chapter 4, 2004.

129. Sarner, E., Removal of particulate and dissolved organics in aerobic fixed film biological processes, Journal of Water Pollution Control Federation, Vol. 58, No. 2, 1986, 165-172.

130. del Pozo, R., V. Diez, S.E. Garrido, M. Morales, and R. Osorio, Hydraulic distribution effect on a real-scale trickling filter, Environmental Engineering Science, Vol. 19, No. 3, 2002,151-157.

131. Howland, W. E., Flow over porous media as in a trickling filter, Proceedings of the 12th Induustrial Waste Conference, 1958, 435.

Appendices

Appendix A
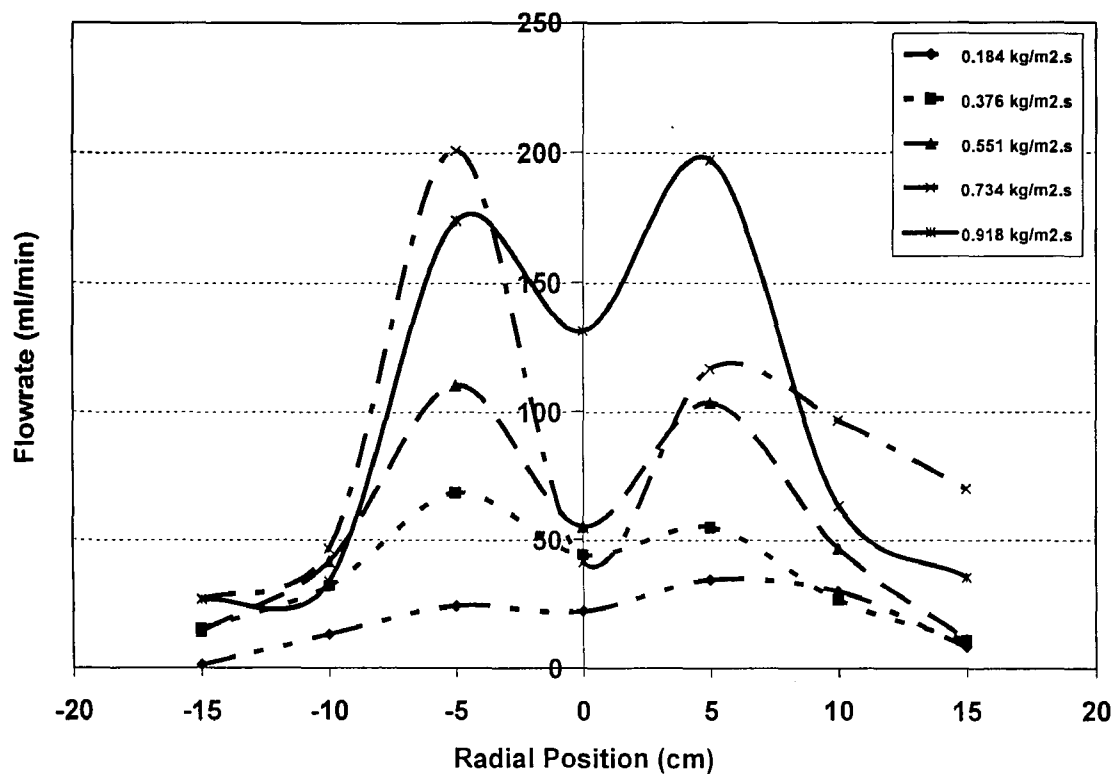
Figure A.1: Effect of liquid flow rate on liquid distribution profile at the 1.4 m bed height using a single point distributor
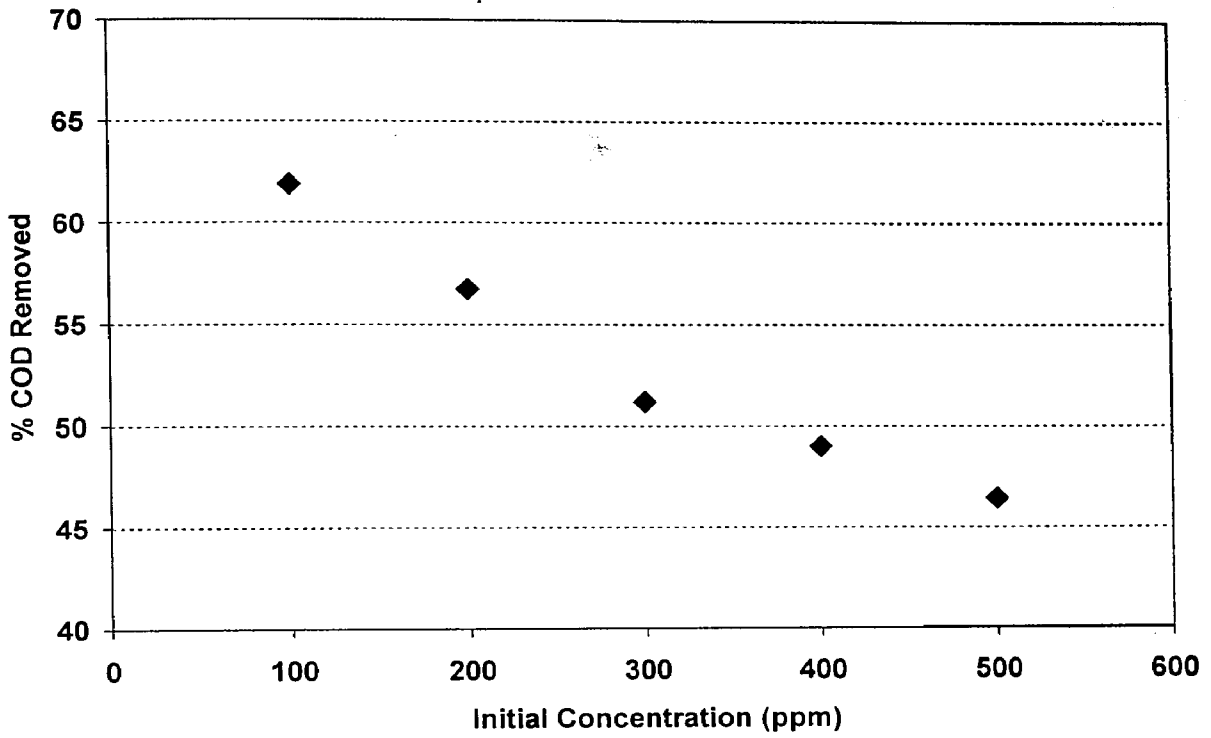
Figure A.2: Effect of initial concentration of the PGME on the percentage COD removal after 72 hours of treatment at liquid flow rate of 0.551 kg/m^2.s with e multipoint delivery distributor.
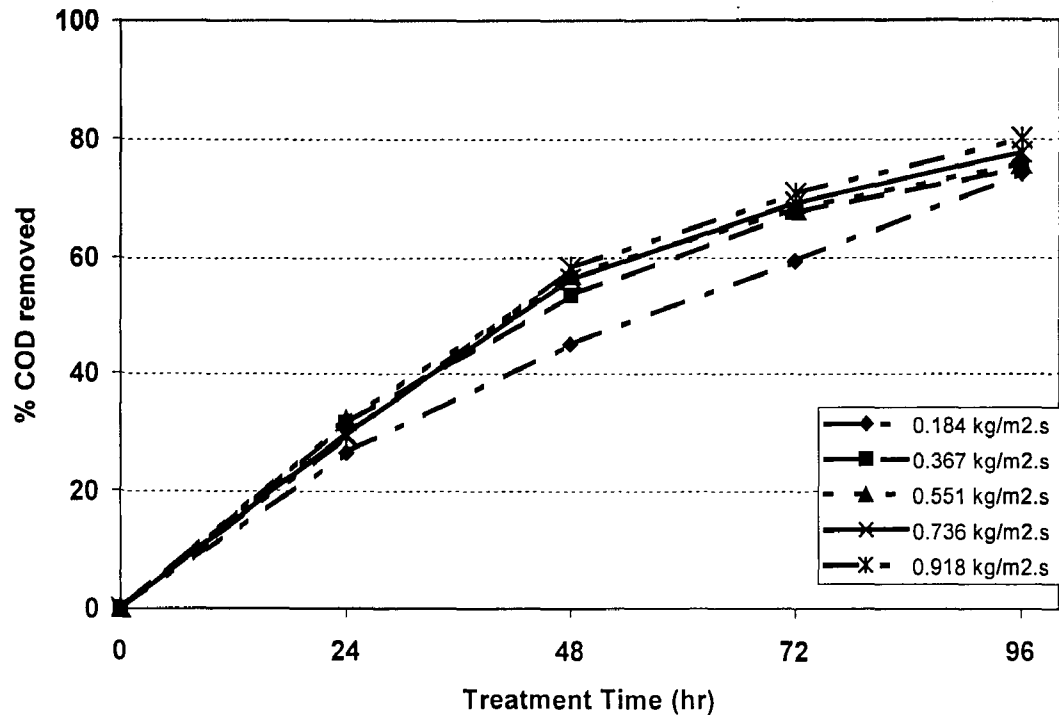
Figure A.3: Effect of the liquid flow rate on the COD removal. The data is obtained after 96 hours of treatment with [PGME] o=300ppm using multipoint delivery distributor
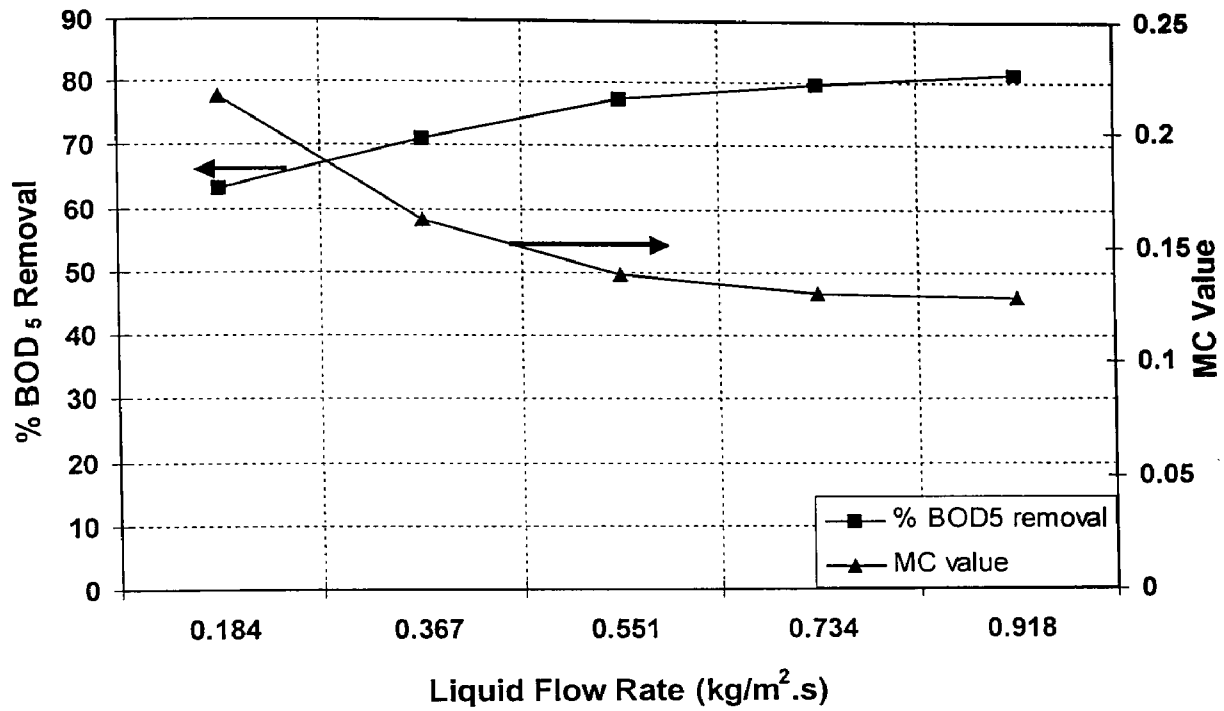
Figure A.4: Percentage BOD$_5$ removal and maldistribution coefficient versus liquid flow rate at the bed height of 0.7 m with the use of multipoint distributor

Appendix B

The uncertainty associated with calculated quantities such as BOD_5 and dynamic liquid hold up were estimated according to the method for the calculation of uncertainty in a function of several variables [111].

B.1.Uncertainty in liquid flow rate

The liquid flowing out of each cell of the liquid collector, V_l was collected and measured in a graduated cylinder over time t. Then the liquid flow rate was calculated by the following equation:

$$Q = \frac{V_l}{t}$$

The uncertainty in the volume of the liquid was based on the graduation of the graduated cylinder used. The smallest graduations of the 10, 25, 50 and 200 ml graduated cylinders were 0.2 ml (2%), 0.5 ml (2%), 2 ml (4%) and 2 ml (1%) respectively. The sample calculation is for 58 ml sample collected over 60 min at liquid flow rate of 0.734 kg/m^2.s.

$$\delta V_l = 58 \times 0.01 = \pm 0.58 \, ml$$

The uncertainty associated in measuring the time, t was based on the smallest graduation of the timer used. The timer had uncertainty of 1 second. The uncertainty associated in measuring time was the combination of the uncertainty in starting time and stopping time. The resulting error in time measurement was determined by a root-mean-square calculation:

$$\delta t = \sqrt{(1)^2 + (1)^2} = \sqrt{2} = \pm 1.4 \, sec$$

Then, the uncertainty in the liquid flow rate was calculated based on all of the above uncertainties:

$$\frac{\delta Q}{Q} = \sqrt{\left(\frac{\delta V_l}{V_l}\right)^2 + \left(\frac{\delta t}{t}\right)^2}$$

$$= \sqrt{\left(\frac{0.58}{58}\right)^2 + \left(\frac{1.4}{60}\right)^2} = 0.025$$

$$\delta Q = 58 \times 0.025 = \pm 1.47 \, ml$$

B.2 Uncertainty in average liquid flow rate

The average liquid flow rate of three paths is calculated by following expression:

$$Q_{ave} = \frac{1}{3}\left(Q_{p1} + Q_{p2} + Q_{p3}\right)$$

To determine the uncertainty in the average flow rate, the above equation was differentiated according to [111]. The sample calculation is for three samples collected at +10 cm radial position from three paths at the flow rate of 0.734 kg/m^2.s:

$$\delta Q_{ave} = \left(\frac{1}{3}\right)\sqrt{\left(\delta Q_{p1}\right)^2 + \left(\delta Q_{p2}\right)^2 + \left(\delta Q_{p3}\right)^2}$$

$$= \left(\frac{1}{3}\right)\sqrt{(0.74)^2 + (1.67)^2 + (1.9)^2}$$

$$\delta Q_{ave} = \pm 0.88 \, (ml/\min)$$

B.3 Uncertainty in maldistribution coefficient value

The uncertainty associated in maldistribution coefficient value was the calculated based on the calculation of uncertainty in a function of several variables [111]. The maldistibution coefficient is given by the filoowing equation:

$$MC = \frac{1}{x}\sqrt{\sum_{i=1}^{x}\left(\frac{Q_i - Q_{av}}{Q_{av}}\right)^2}$$

This equation was differentiated to determined uncertainty in maldistribution coefficient.

$$\frac{\delta MC}{MC} = \sqrt{\left(\frac{\partial MC}{\partial Q_1}\delta Q_1\right)^2 + \left(\frac{\partial MC}{\partial Q_2}\delta Q_2\right)^2 + \ldots\ldots + \left(\frac{\partial MC}{\partial Q_{37}}\delta Q_{37}\right)^2 + \left(\frac{\partial MC}{\partial Q_{av}}\delta Q_{av}\right)^2}$$

$$\frac{\partial MC}{\partial Q_1} = \frac{1}{37}\times\frac{1}{2}\left[\sum_{i=1}^{37}\left(\frac{Q_i - Q_{av}}{Q_{av}}\right)^2\right]^{-0.5}\left[2\frac{Q_1 - Q_{av}}{Q_{av}}\right]$$

$$\cdot$$
$$\cdot$$
$$\cdot$$

$$\frac{\partial MC}{\partial Q_{37}} = \frac{1}{37}\times\frac{1}{2}\left[\sum_{i=1}^{37}\left(\frac{Q_i - Q_{av}}{Q_{av}}\right)^2\right]^{-0.5}\left[2\frac{Q_{37} - Q_{av}}{Q_{av}}\right]$$

$$\frac{\partial MC}{\partial Q_{av}} = \frac{1}{37}\times\frac{1}{2}\left[\sum_{i=1}^{37}\left(\frac{Q_i - Q_{av}}{Q_{av}}\right)^2\right]^{-0.5}\left[-2\sum_{i=1}^{37}\left(\frac{Q_i(Q_i - Q_{an})}{Q_{av}^3}\right)\right]$$

$$\frac{\delta MC}{MC} = \left(\frac{1}{37}\left[\sum_{i=1}^{37}\left(\frac{Q_i - Q_{av}}{Q_{av}}\right)^2\right]^{-0.5}\right)\left[\sum_{i=1}^{37}\left(\left(\frac{Q_i - Q_{av}}{Q_{av}}\right)\delta Q_i\right)^2 - \left(\left(\sum\frac{Q_i(Q_i - Q_{av})}{Q_{av}^3}\right)\delta Q_{av}\right)^2\right]^{0.5}$$

Based on above equations, the sample calculation was done for the case of multipoint distributor at liquid flow rate of 0.918 kg/m2.s and bed height of 1.4 m.

$$\partial MC = \pm 0.0052$$

B.4 Uncertainty in dynamic liquid hold-up

The dynamic liquid hold up, h, is given by the following expression:

$$h_d = \frac{V_d}{V_r}$$

1. Uncertainty in the volume of drained liquid, V_d was based a 1000 ml Erlenmeyer flask used to measure it. The flask had an uncertainty of ± 5% or ± 50 ml. Therefore:

$$\delta_{V_d} = V_d \times 0.005$$

The sample calculation of the liquid hold up measured for the bed height of 0.7 m with the presence of biomass at a liquid flow rate of 0.184 kg/m^2.s is shown below:

$$\delta_{V_d} = \left(6 \times 10^{-4}\right) \times 0.005$$
$$= 3 \times 10^{-5} m^3$$
$$V_d = 0.0006 \pm 3 \times 10^{-5} m^3$$

2. the uncertainty in the bed volume , V_r was based on the graduations of the measuring tape used. The smaller graduation was 1 mm. The uncertainty in the V_r for the bed height of 0.7 m calculated as a relative uncertainty [111]:

$$V_r = \frac{\pi}{4} D_T^2 . H$$

$$\frac{\delta V_r}{V_r} = \sqrt{\left(2\frac{0.1}{30}100\right)^2 + \left(\frac{0.1}{70}100\right)^2} = 0.68\%$$

$$\delta V_r = 0.007\left(\frac{\pi}{4}(30)^2 .70\right) = 340 \ cm^3 = \pm 3.4 \times 10^{-4} m^3$$

Based on all of the above uncertainties the uncertainty in the dynamic liquid hold up was calculated:

$$\frac{\delta h_d}{h_d} = \sqrt{\left(\frac{\delta V_d}{V_d}\right)^2 + \left(\frac{\delta V_r}{V_r}\right)}$$

$$= \sqrt{\left(\frac{3\times10^{-5}}{6\times10^{-4}}100\right)^2 + \left(\frac{3.4\times10^{-4}}{4.9\times10^{-2}}100\right)} = 5.05\%$$

$$\delta h_d = 0.05\left(\frac{6\times10^{-4}}{4.9\times10^{-2}}\right) = \pm 6\times10^{-4}$$

B.5 Uncertainty in 5-day BOD

The uncertainty associated with dissolved oxygen measurements water calculated from the manufacture's (YSI, Inc.) instructions.

The individual sources of error are:

1. Instrument accuracy = ± 0.1% plus least significant figure

2. Probe background current error = background factor x *(1-a/b)* c, where *a* is the calibration value, *b* is the solubility of oxygen in fresh water at 760 mm Hg and at the measured temperature, and *c* is the measured DO value. The background factor at 20°C is 1 %.

3. Probe nonlinearity = ± 0.3%of reading

4. The variation from nominal response to sample temperature is ± 0.2% of DO reading per degree C of the temperature difference between temperature of sample and the temperature at with the probe was calibrated.

The resulting errors were estimated by calculating the root-mean- squared sum of these individual uncertainties. The sample calculation is for the initial DO measurement at $t=0$ for Run 13, 4 ml sample.

Description	Calculation	Error (mg/l)
Instrument accuracy	$\pm 0.001 \times 8.6 + 0.01$	± 0.0186
Probe background	$\pm 0.01 \times (1 - 8.6/9.07) \times 8.10$	± 0.004
Probe nonlinearity	$\pm 0.003 \times 8.10$	± 0.024
Temperature compensation	$\pm (22.5 - 19.8) \times 0.002 \times 8.10$	± 0.044

$$RMS\ error = \sqrt{0.0184^2 + 0.004^2 + 0.024^2 + 0.044^2} = \pm 0.055 \ mg/l$$

The 5-day BOD for a seeded wastewater sample is given by the following expression:

$$BOD_5 = \frac{(DO_1 - DO_2) - (B_1 - B_2) \cdot f}{P}$$

The uncertainty associated in measuring the volume of seed and sample, and the uncertainty in the volume of the BOD bottle were assumed to be negligible in comparison to the errors associated with the DO_1, DO_2, B_1 and B_2. The value of f for al biological runs was 1.0. The uncertainty in 5- day BOD was estimated according to the method of calculation of uncertainty in a function of several variables[82 Robert].The sample calculation is for Run13, 4 ml sample at $t=0$.

$$\delta BOD_s = \sqrt{\left(\frac{\partial BOD}{\partial DO_1} \cdot \delta DO_1\right)^2 + \left(\frac{\partial BOD}{\partial DO_2} \cdot \delta DO_2\right)^2 + \left(\frac{\partial BOD}{\partial B_1} \cdot \delta B_1\right)^2 + \left(\frac{\partial BOD}{\partial B_2} \cdot \delta B_2\right)^2}$$

$$= \sqrt{\left(P^{-1} \cdot \delta DO_1\right)^2 + \left(-P^{-1} \cdot \delta DO_2\right)^2 + \left(-P^{-1} \cdot \delta B_1\right)^2 + \left(P^{-1} \cdot \delta B_2\right)^2}$$

$$= \frac{300}{4} \cdot \sqrt{(0.24)^2 + (-0.1)^2 + (-0.32)^2 + (0.14)^2}$$

$$= \pm 32.5 \; mg/l$$

B.6 Uncertainty in apparent reaction rate constant

The uncertainty in apparent reaction rate constant, k_{app} is based statistical principles for determining the uncertainty associated with the slope and intercept of a least squares straight line [111]. The uncertainty for the slope was calculated from the following:

$$\delta k_{app} = \delta y \sqrt{\frac{N}{\Delta}}$$

where

$$\delta y = \sqrt{\frac{1}{N-2} \sum_{i=1}^{N} (y_i - A - Bx_i)^2}$$

and

$$\Delta = N\left(\sum x_i^2\right) - \left(\sum x_i\right)^2$$

where N is the number of pairs of data, A is the intercept, B is the slope, and y_i is the calculated value of the dependent variable based on the least square regression line at corresponding x_i. The sample calculation is for Run 8.

$$\delta k = \pm 0.00031 \, (1/\text{hr})$$